Self/tumor-reactive CD8 T cells enter a memory-like TCF1+ PD1- dysfunctional state

By

Jessica Jean Roetman

Dissertation

Submitted to the Faculty of the

Graduate School of Vanderbilt University

in partial fulfillment of the requirements

for the degree of

DOCTOR OF PHILOSOPHY

in

Cancer Biology

August 11, 2023

Nashville, Tennessee

Approved:

Fiona Yull, D.Phil. (Chair)

Justin Balko, Pharm. D., Ph.D.

Jin Chen, M.D., Ph.D.

W. Kimryn Rathmell, M.D., Ph.D.

Christopher Williams, M.D., Ph.D.

Mary Philip, MD., Ph.D. (Advisor)

DEDICATION

To my mom, Susan, whose two fights against cancer inspired my interest in cancer biology

ACKNOWLEDGEMENTS

This work would not have been possible without the support and guidance of many individuals during my graduate career. First and foremost, I would like to thank my mentor Mary Philip without whom the direction and story of my thesis work would be significantly less impactful. Thank you for teaching me how to think scientifically and helping me grow and mature. I would also like to thank my thesis committee members Drs. Fiona Yull, Justin Balko, Jin Chen, Kim Rathmell, and Chris Williams. Thank you for your constant support, uplifting comments, and guidance of this project as it developed.

To the members of the Philip laboratory past and present: Gulnara Anzarova, Minna Apostolova, Carlos Detrés-Román, Megan Erwin, Michael Rudloff, Natalie Favret, and Kristen Murray. Thank you for making the lab a joy with conversations, brainstorming sessions, and trips to Taco Mama. It has been an honor to work alongside every one of these brilliant scientists and learn from our experiences together. I cannot wait to see the impact they all make in their future endeavors.

I would especially like to thank my mom, Susan Roetman, who has been my cheerleader and confidant throughout both my undergraduate and graduate careers. She knew exactly what to say to support me throughout the trials and tribulations of graduate school, even from 1,000 miles away. Thank you to my sister, Jenn Roetman-Myhr, who has also supported me from afar and given excellent advice from a non-academic perspective.

Finally, this work would never have been completed without the support system found here at Vanderbilt through fellow members of my first-year cohort: Jacky Lu, Laura Teal, Jonah Zarrow, and Kaitlyn Schaaf. They have all provided shoulders to cry on and weekly game nights to look forward to during a difficult week. They celebrated every accomplishment, no matter how small. I never would have finished graduate school without them. In particular, my loving partner Laura Teal has taught me so much about myself both personally and professionally as we navigated grad school together, and she has unfailingly been at my side and made the hard days better.

Thank you.

TABLE OF CONTENTS

Page

LIST OF TABLES

Table Page

LIST OF FIGURES

Figure Page

LIST OF ABBREVIATIONS

2B4	Natural Killer Cell Receptor
AIRE	Autoimmune regulator transcription factor
Alb-GAG	Albumin-GAG mouse model
ALCL	Anaplastic large cell lymphoma
ALK	Anaplastic lymphoma kinase
ANOVA	Analysis of variance
APC	Antigen presenting cell
AST	Albumin-Stop-Large T Antigen
ATF3	Activating Transcription Factor 3
ATP	Adenosine Triphosphate
B2M	B_2-microglobulin
BCL-2	B-cell lymphoma 2
BILF1	EBV lytic phase protein
BIM	Bcl-2 Interacting Mediator of cell death
BNLF2a	BamHI-N leftward frame 2a
BRAF	Serine/threonine protein kinase
CCL	Chemokine (C-C motif) ligands
CD101	Immunoglobulin superfamily, member 2, fixed dysfunction marker
CD274	PD-L1-encoding gene
CD28	T cell co-stimulatory glycoprotein
CD38	Cyclic ADP ribose hydrolase, fixed dysfunction marker
CD39	Ectonucleoside triphosphate diphosphohydrolase-1
CD4	T-Cell surface glycoprotein CD4
CD44	Hematopoietic cell E- and L-selectin ligand
CD62L	L-selectin
CD8	T-Cell surface glycoprotein CD8
CD80	APC ligand for CD28 and CTLA-4, providing T cell signals
CD86	APC ligand for CD28 and CTLA-4, providing T cell signals
CDK	Cyclin dependent kinase
CFSE	CarboxyFluoroscein Succinimidyl Ester
COX-2	Prostaglandin-endoperoxide synthase 2
CTL	Cytotoxic T lymphocyte
CTLA4	Cytotoxic T-lymphocyte-associated protein 4
CXCL	Chemokine XC Ligand
DAMP	Damage associated molecular patterns
DAPI	4′,6-diamidino-2-phenylindole
DC	Dendritic cell
DMEM	Dulbecco's Modified Eagle Medium
DN	Double negative developing thymocytes
DP	Double positive developing thymocytes
EBF1	EBF Transcription Factor 1
EBNA2	Epstein–Barr virus nuclear antigen 2
EBV	Epstein-Barr Virus
EGFR	Epithelial growth factor receptor
EPHA2	Ephrin type-A receptor 2

ER	Endoplasmic reticulum
ERK	Extracellular signal-regulated kinase
FCS	Fetal calf serum
FMLuV	Friend murine leukemia virus
Fos	Fos transcription factor, part of AP-1 complex
GAG	Group specific antigen
GM-CSF	granulocyte-macrophage colony-stimulating factor
Gp33	LCMV glycoprotein 33
GPCR	G-protein coupled receptor
GVHD	Graft versus host disease
HBV	Hepatitis B Virus
HCV	Hepatitis C Virus
HER2	Human epidermal growth factor receptor-2
HIV	Human immunodeficiency virus
HLA	Human leukocytes antigen
HPV	Human Papilloma Virus
HTLV-1	Human T-lymphotropic Virus-1
IACUC	Institutional Animal Care and Use Committee
ICB	Immune checkpoint blockade
ICD	Immunogenic cell death
IFNyR1	Interferon gamma receptor 1
IFNγ	Interferon gamma
IL-2	Interleukin 2
IrAE	Immune-related adverse event
JAK	Janus tyrosine kinase
Jun	Jun transcription factor, part of AP-1 complex
Ki67	Marker of proliferation
KSHV	Kaposi sarcoma-associated Herpesvirus
LAG3	Lymphocyte Activating 3
LCMV	Lymphocytic choriomeningitis virus
LM	*Listeria monocytogenes*
LOH	Loss of heterozygosity
MAPK	Mitogen activated protein kinase
MCPyV	Merkel cell polyomavirus
MDSC	Myeloid-derived suppressor cells
MEK1	Mitogen-activated protein kinase kinase
MHC	Major histocompatibility complex
MHC-I	Major histocompatibility complex class I
MHC-II	Major histocompatibility complex class II
MK2	Mitogen-activated protein kinase
mTOR	Mammalian target of rapamycin
MYC	Oncogene named from Avian virus Myelocytomatosis
NFAT	Nuclear factor of activated T cells
NF-κB	Nuclear factor kappa-light-chain-enhancer of activated B cells
NK	Natural killer cell
NKT	Natural killer T cell
NOTCH	Highly conserved cell signaling pathway
OIS	Oncogene-induced senescence

P14	T cell receptor specific for LCMV gp33
p53	Tumor suppressor gene
PD1	Programmed death-1
PD-L1	Programmed death ligand-1
PGE2	Prostaglandin E_2
PI3K	Phosphatidylinositol 3-kinase
pMHC	Peptide-Major histocompatibility complex
pRB	Retinoblastoma protein
PRR	Pattern recognition receptors
PTEN	Phosphatase and tensin homolog
Ptgs2	Gene encoding COX-2
RAS	Small GTPase, named for rat sarcoma virus
ROCK	Rho-associated protein kinase
RPMI	Roswell Park Memorial Institute 1640 Medium
S1P	Sphingosine-1-phosphate
S1PR	Sphingosine-1-phosphate receptor 1
SASP	Senescence-associated secretory phenotype
SLO	Secondary lymphoid organ
SMAD4	Mothers against decapentaplegic homolog 4, transcription factor
SP	Single positive developing thymocytes with either CD4 or CD8
SSA	Sefl/shared antigen
SST	Self/shared-antigen-specific T cell
STAT1	Signal Transducer and Activator of Transcription 1
SV40	Simian virus 40
TAG	Large T antigen
T-ALL	T-cell acute lymphoblastic leukemia
TAM	Tamoxifen
TAP	Transporter associated with antigen processing
TCF1	T cell factor-1, stem-like transcription factor
TCGA	The Cancer Genome Atlas
TCR	T cell receptor
TCR_{GAG}	T cell receptor specific for GAG antigen
TCR_{TAG}	T cell receptor specific for TAG antigen
TEC	Thymic epithelial cells
TGFβ	Transforming growth factor beta
TIM3	T cell immunoglobulin and mucin domain-containing protein 3
TNFα	Tumor necrosis factor alpha
TOX	Thymocyte selection-associated high mobility group box protein
TP53	Gene encoding p53
Treg	Regulatory T cell
TSA	Tumor-specific antigen
TST	Tumor-specific T cell
TTP	Tristetraprolin

ORIGINAL PUBLICATIONS

1. **Jessica J. Roetman,** Megan M. Erwin, Michael W. Rudloff, Natalie R. Favret, Carlos R. Detrés Román, Minna K. I. Apostolova, Kristen Murray, Ting-Fang Lee, Youngmin A. Lee, Mary Philip. (**2023**), “Self/tumor-reactive CD8 T cells enter a memory-like TCF1+ PD1- dysfunctional cell state,” Accepted in Cancer Immunology Research
2. Michael W. Rudloff, Paul Zumbo, Natalie R. Favret, **Jessica J. Roetman**, Carlos R. Detrés Román, Megan M. Erwin, Sriya T. Jonnakuti, Friederike Dündar, Doron Betel, Mary Philip. (**2023**), “Epigenetic encoding of T cell dysfunction is enacted within hours of tumor antigen encounter prior to cell division,” Accepted in Nature Immunology
3. Eben Negasi, **Jessica J. Roetman**, Mary Philip. (**2023**). “Evaluating the Affinity of Tumor-Specific and Self-Specific CD8+ T Cells in a Liver Cancer Mouse Model,” Young Scientists Journal
4. **Jessica J. Roetman**, Minna K. I. Apostolova, Mary Philip. (**2022**), “Viral and cellular oncogenes promote immune evasion,” Oncogene

CHAPTER 1
INTRODUCTION

This chapter is adapted from “Viral and cellular oncogenes promote immune evasion” published in Oncogene and has been reproduced in line with publisher policies.
Roetman JJ, Apostolova MKI, Philip M. Viral and cellular oncogenes promote immune evasion. Oncogene. 2022 Feb 41;7:921-929. doi: 10.1038/s41388-021-02145-1. Epub 2022 Jan 13. PMID: 35022539; PMCID: PMC8851748.

OVERVIEW

The power of T cells to detect and eliminate cancers has long been appreciated. Immune checkpoint therapy, which harnesses patient tumor-reactive T cells, is now part of the standard of care treatment for multiple cancer types, providing another line of therapy for cancers that are resistant to chemotherapy (Twomey and Zhang *AAPS J* 2021). Unfortunately, only a small subset of patients responds to immune checkpoint therapy (Haslam, Gill, and Prasad *JAMA Netw Open* 2020). CD8 T cells specific for mutated proteins expressed by cancer cells can be found in many tumors; however, in most patients these tumor-specific T cells (TST) are dysfunctional and do not eliminate cancer cells (Philip and Schietinger *Nat Rev Immunol* 2021). Therefore, to improve immunotherapy efficacy, we need to determine how TST become dysfunctional.

CD8 T cells can recognize and respond to tumor antigens arising from the aberrant expression of non-mutated genes (self/shared-antigens (SSA)); these antigens may also be expressed on non-cancerous/normal cells (reviewed in (Schietinger, Philip, and Schreiber *Semin Immunol* 2008; Leko and Rosenberg *Cancer Cell* 2020)). In addition to SSA, cancer cells often express tumor-specific antigens (TSA) caused by mutations unique to the tumor and not expressed on normal tissue. T cell responses to SSA may differ in tumors versus normal tissue as SSA might be distinctly regulated or presented in cancer cells. ICB can unleash anti-tumor T cell responses but also initiate immune related adverse effects (IrAE), mediated by self-reactive T cells (Postow, Sidlow, and Hellmann *N Engl J Med* 2018; Johnson et al. *Nat Rev Clin Oncol* 2022).

TST dysfunction was long thought to arise late during carcinogenesis due to the immunosuppressive tumor microenvironment. Recent studies have demonstrated that TST rapidly differentiate to a dysfunctional state, long before the emergence of a pathologically defined tumor (Schietinger et al. *Immunity* 2016; Philip et al. *Nature* 2017). Bystander non-tumor specific T cells activated in the premalignant liver remain functional effector cells; thus, the tumor microenvironment is not the primary driver of TST dysfunction (Schietinger et al. *Immunity* 2016). Blocking TST expression of multiple inhibitory receptors (e.g. PD1, LAG3, 2B4) fails to prevent dysfunction (Scott et al. *Nature* 2019a).

These observations suggest that TST dysfunction might be driven by signals from the transformed cells themselves. There is growing awareness that oncogenes not only promote cancer cell proliferation and survival but also have immunomodulatory effects. Currently, little is known about the early cell-intrinsic and cell-extrinsic immunomodulatory effects downstream of oncogene activation and their impact on TST differentiation.

Additionally, the rapid onset of dysfunction before a tumor microenvironment has been established leads to the question of whether these T cells are undergoing a tolerance program upon activation toward cognate antigen. The relationship of tolerance and dysfunction is not well known, except that the end result is T cell hypofunction. Thus, if there are different mechanisms and phenotypes associated with both states, there may be additional or alternative therapeutics required to reactivate T cell function in tumors.

Thus, investigating how T cell responses to self and tumor antigens is a key aspect of deepening the current understanding of T cell biology and methods to harness the power of CD8 T cells to destroy cancer cells. This dissertation will primarily focus on the impact of oncogene activation on

T cell responses, the characterization of a novel mouse liver model to study both self- and tumor-reactive T cell responses, and the identification of a novel subset of self-reactive T cells.

OVERVIEW OF CD8 T CELL FUNCTION AND DYSFUNCTION

CD8 T cell development and function

CD8 T cells contain enormous power to protect the host from intracellular pathogens. The development of CD8 T cells begins in the bone marrow as hematopoietic cells that then migrate to the thymus for further maturation. T cell maturation stages are named for the expression of glycoproteins CD8 and CD4. The first stage is known as the double negative (DN) stage, where first the β chain of the TCR undergoes somatic DNA rearrangement followed by proliferation and DNA rearrangement of the α chain (Hwang et al. *Exp Mol Med* 2020). The rearrangement of the β and α chains occurs through a process known as V(D)J recombination. During formation of the β chain, segments of the V-gene, D-gene, and J-gene located within the beta gene locus are randomly chosen, and the intervening, non-chosen DNA segments form hairpin loops that are then ligated out of the locus (Russell et al. *Elife* 2022). The alpha chain is formed similarly at the TCR alpha locus, except without a D-gene segment (Russell et al. *Elife* 2022). Another T cell subset known as γδ T cells also form through V(D)J recombination at the gamma and delta locus (Legut, Cole, and Sewell *Cell Mol Immunol* 2015). γδ T cells are not the focus of this dissertation and constitute <5% of all T cells in humans, but they represent an important component of immunity that are still understudied (Fonseca et al. *Cells* 2020).

Once the TCR chains are formed, T cells enter a double positive (DP) stage by expressing both CD4 and CD8 glycoproteins (Kumar, Connors, and Farber *Immunity* 2018). DP T cells are exposed to a variety of antigens by thymic epithelial cells expressing peptide on the major histocompatibility complex (MHC) as a peptide-MHC (pMHC) complex. DP cells that bind too strongly to self-antigen undergo negative selection via apoptosis to avoid self-reactivity (central

tolerance, described below) (Xing and Hogquist *Cold Spring Harb Perspect Biol* 2012). Those that bind appropriately to foreign antigen undergo positive selection and further differentiate into mature T cells. After DP cells undergo this selection, they undergo MHC restriction where those that bind to MHC-I lose CD4 expression and retain CD8 while cells that bind MHC-II retain CD4 and lose CD8 expression (Kumar, Connors, and Farber *Immunity* 2018).

These mature SP T cells must finally acquire the ability to egress from the thymus and enter the periphery to enact their cytotoxic capabilities upon antigen counter. Chemokine receptor expression as well as other surface markers denote cells in the final maturation stage. CCR4+CCR7-CCR9+ with CD69+CD62L- expression has been revealed as the expression pattern in newly generated SP cells (James, Jenkinson, and Anderson *J Leukoc Biol* 2018). SP T cells that have further matured to leave the thymus subsequently invert this expression pattern, becoming CCR4-CCR7+CCR9-CD69-CD62L+. Cells expressing this phenotypic second stage also express the sphingosine-1-phosphate receptor 1 (S1PR) (James, Jenkinson, and Anderson *J Leukoc Biol* 2018). Mature T cells use S1PR to follow an increasing gradient of sphingosine-1-phosphate (S1P), which is expressed by endothelial cells in blood vessels (Aoki et al. *Mediators Inflamm* 2016), to leave the thymus as a fully mature, naïve T cell.

Once in the periphery, T cells circulate through secondary lymphoid organs (SLO). Antigen presenting cells (APC), especially dendritic cells (DC), will enter SLO upon taking up an antigen and present antigen to T cells that migrate through the organ (Krummel, Bartumeus, and Gerard *Nat Rev Immunol* 2016). These T cells will scan the presented antigens, and if the TCR and the CD8 co-receptor binds to the pMHC complex, the T cell begins an activation signaling cascade to migrate and respond to its cognate antigen.

Antigen recognition initiates a complex signaling cascade that activates the MAPK pathway and Ras/Erk signaling pathways (Courtney, Lo, and Weiss *Trends Biochem Sci* 2018). TCR signaling also causes calcium influx from stores in the endoplasmic reticulum (ER) and from outside the cell. Co-receptors such as CD28 recognize CD80/CD86 on APC or cytokines from helper CD4 T cells provide a secondary signal for CD8 T cell activation and initiates more signaling through mTOR and NF-κB pathways. These signaling pathways activate a variety of transcription factors such as NFAT (calcium signaling), Fos (calcium and MAPK signaling), Jun (MAPK), and NF-κB (Courtney, Lo, and Weiss *Trends Biochem Sci* 2018) (**Fig 1.1**). Each transcription factor plays a role in T cell differentiation to an effector state.

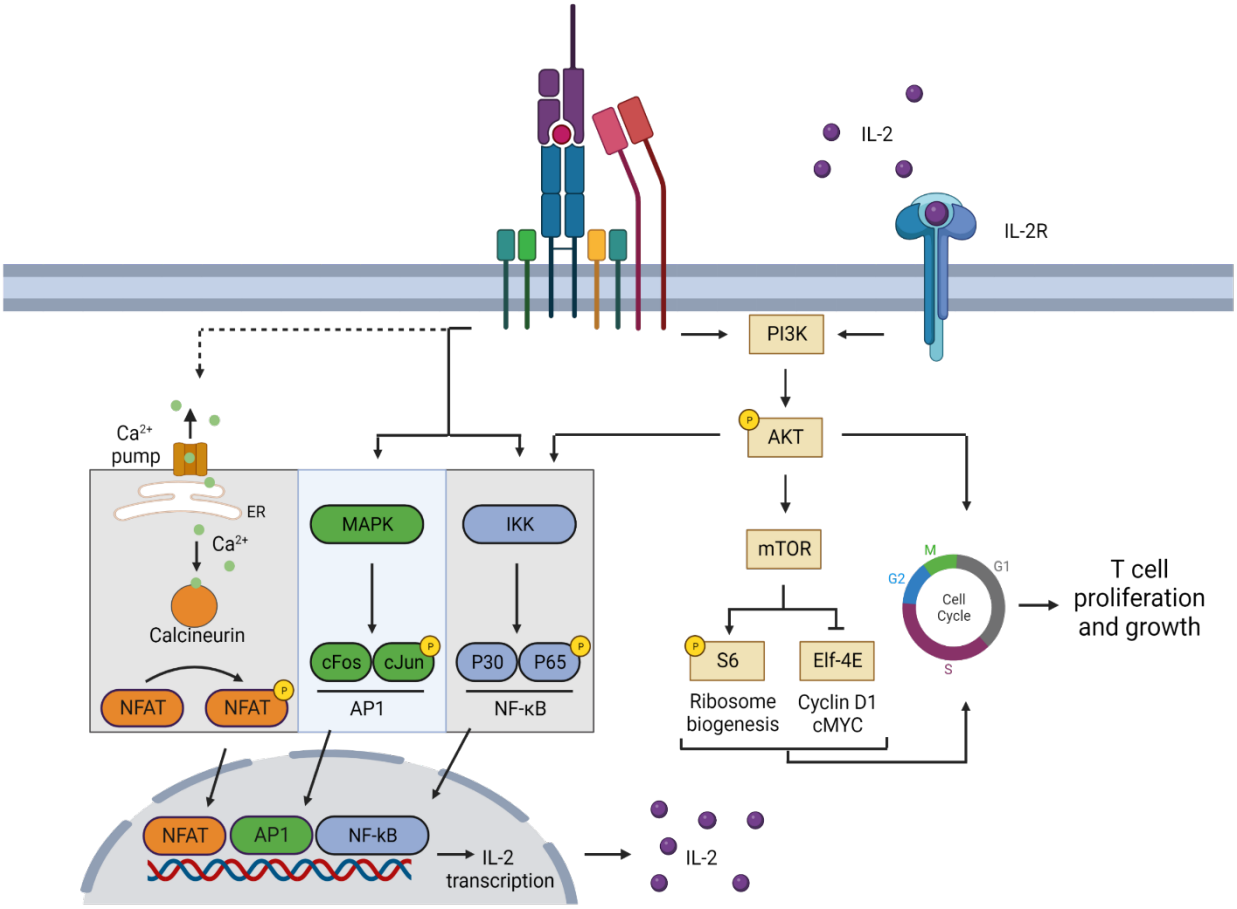

Figure 1.1| Schematic of T cell receptor signaling. Activation signals from TCR upon pMHC encounter activates multiple downstream signaling pathways in T cells with (1) NFAT, (2) NF-κB, (3) MAPK and (4) mTOR pathways. These pathways lead to nuclear translocation of NFAT, NF-κB and AP1 transcription factors and IL-2 transcription. IL-2 binds to its receptor on the cell surface and initiates mTOR pathway. TCR activating signals induce the expression of *Nlrp12* that consequently inhibits NF-κB and MAPK signaling pathways, which suppress IL-2 production.

Adapted from Gharagozloo et al. 2018 (Gharagozloo et al. *Cells* 2018), created in BioRender.

Once a T cell is activated, it utilizes multiple routes to lyse and kill its target cell. Perforin is released into the immunological synapse and forms a lytic pore in the target cell (Trapani and Smyth *Nat Rev Immunol* 2002; Voskoboinik, Whisstock, and Trapani *Nat Rev Immunol* 2015). Granzymes, also released into the synapse, enter the cell through these pores and activate apoptosis pathways by cleaving proteins at the same sites that activated caspases can cleave (Voskoboinik, Whisstock, and Trapani *Nat Rev Immunol* 2015). Granzymes also cleave pro-caspases to induce caspase activity (Li et al. *J Immunol* 2014). The gold standard for assessing CD8 function is the release of effector cytokines IFNγ and TNFα upon stimulation with cognate antigen. IFNγ can induce apoptosis in target cells through a yet-undefined mechanism (Jorgovanovic et al. *Biomark Res* 2020), and also acts on T cells themselves to improve activation, differentiation, and proliferation (Bhat et al. *Cell Death Dis* 2017). IFNγ binding to the receptor IFNγR1 also stimulates increased expression of both MHC-I and MHC-II to enhance T cell recognition of target cells (Tau and Rothman *Allergy* 1999). TNFα binds to TNFα Receptor 1 (TNFR1), which includes a death domain that drives apoptosis upon activation (Schievella et al. *J Biol Chem* 1997). Thus, with a wide variety of routes to kill target cells, CD8 T cells represent a powerful arm of the adaptive immune system that can directly respond to both foreign and tumor antigens presented on MHC-I.

Tumor-specific CD8 T cell dysfunction

Tumor specific CD8 T cells (TST) have an enormous power to detect and destroy transformed cells. However, despite being found in tumors, CD8 T cells fail to respond to and kill the cancerous cells. This loss of CD8 T cell function in tumors contributes to immune escape and allows for progression of disease. Recent studies on CD8 T cells' role in tumors and chronic viral infections have begun to unravel T cell exhaustion and dysfunction mechanisms and differentiation states (Philip and Schietinger *Nat Rev Immunol* 2021). There is currently debate on the language regarding exhaustion versus dysfunction – this dissertation will define exhaustion as T cell

nonfunction (i.e. the inability to produce effector cytokines IFNγ and TNFα upon restimulation) in the context of chronic viral infection while dysfunction will be defined as T cell nonfunction in tumor settings.

T cell activation and trafficking in tumor-bearing hosts is different from activation when the host is infected by a pathogen/virus. Cancer cells can cause abnormal vascularization and can compromise vascular integrity, leading to compromised trafficking to the site of the tumor (Nagy et al. *Br J Cancer* 2009). In addition, cancer cells secrete a wide variety of chemokines that can prevent T cells from trafficking to the site of the tumor. Chemokine CXC ligand (CXCL) 9 and 10 are prominent chemokines involved in promoting T cell trafficking to the site of infection or tumor. VEGF secreted by cancer cells can prevent the induction of CXCL9 and CXCL10 (Huang et al. *FASEB J* 2015). Regulatory T cells (T regs) recruited to the tumor can secrete IL35, which prevents TST recruitment (Pylayeva-Gupta et al. *Cancer Discov* 2016).

If TST do make it into an established tumor, they will encounter a tumor microenvironment filled with suppressive factors and immune suppressive cells such as T regs and myeloid derived suppressor cells (MDSC) (McLane, Abdel-Hakeem, and Wherry *Annu Rev Immunol* 2019) that are often upregulated or trafficked to the tumor by signaling provided by an oncogene (further explained in the following section).

T cell inhibitory receptors, including PD1, CTLA4, LAG3, TIM3, 2B4, CD38, CD39, and CD101 (Philip et al. *Nature* 2017; Schietinger et al. *Immunity* 2016), are often found on TST. These receptors dampen T cell activation by blocking ligation or signaling of CD28, CTLA4 (Krummel and Allison *J Exp Med* 1995) and PD1 (Hui et al. *Science* 2017) respectively, or decreasing immediate TCR signaling via LAG3 (Guy et al. *Nat Immunol* 2022). The past decade has seen a major increase in the use of checkpoint blockade to stimulate nonfunctional T cells in tumors,

especially using anti-CTLA-4 or anti-PD1/PDL1 antibodies to block T cell inhibitory receptors from inhibiting T cell activity (Twomey and Zhang *AAPS J* 2021). The popular thought regarding this mechanism of action has been that the blockade of these inhibitory signals can reinvigorate already exhausted or dysfunctional T cells (Lee et al. *For Immunopathol Dis Therap* 2015; Viramontes et al. *Front Immunol* 2022). However, recent studies have suggested that inhibitory blockade merely acts on naïve, still-functional T cells that have recently entered the tumor environment (Kurtulus et al. *Immunity* 2019; Sade-Feldman et al. *Cell* 2018), coinciding with the massive epigenetic changes seen in fixed, profoundly dysfunctional, antigen-experienced T cells.

Studies on dysfunctional T cells by our group have shown that T cells rapidly undergo dysfunction within the first few hours to days of encountering cognate tumor antigen (Schietinger et al. *Immunity* 2016; Philip et al. *Nature* 2017). This dysfunction is characterized by massive epigenetic remodeling that is initially plastic and can be reversed by ICB, but between 7-14 days in the tumor, another wave of epigenetic remodeling occurs, setting T cells into a fixed, non-reversable state in which T cells remain in the tumor but without the ability to produce effector cytokines TNFα or IFNγ or granzyme and perforin (Philip et al. *Nature* 2017).

It is likely that TCR signaling following recognition of a tumor antigen plays a role in driving T cell dysfunction, especially early in antigen encounter before the formation of a suppressive tumor microenvironment. Our group has shown that the initiation of dysfunctional states requires TCR signaling, and bystander T cells are still able to function, even though they have been exposed to the tumor environment (Schietinger et al. *Immunity* 2016; Mognol et al. *Proc Natl Acad Sci U S A* 2017). A study using subcutaneous tumors injected into MHC-I knockout mice showed that tumors can directly activate CD8 T cells, and their activation does not solely rely on APC in the spleen or other lymphoid tissues (Thompson et al. *J Exp Med* 2010). Thus, in pre-malignant lesions, it is

possible that TST are undergoing a form of self-tolerance toward tumor antigen, explaining why we see such early T cell dysfunction despite the absence of an immunosuppressive environment.

Self-specific CD8 T cells and tolerance

During T cell development, T cell receptors can arrange to recognize an enormous variety of both foreign antigens (expressed on pathogens) and self-antigens (expressed normally in the host's tissues). These self-specific T cells, if allowed to leave the thymus as mature, functional T cells, have the potential to cause damage to tissues, known as autoimmunity. The first line of defense against self-reactive T cells is central tolerance, which occurs in the thymus during development. Peripheral tolerance acts as a second line of defense once a self-specific T cell has developed and enters circulation.

Central tolerance initiates when single positive (SP) T cells developing in the thymus begin to undergo testing of their newly arranged TCR (Kumar, Connors, and Farber *Immunity* 2018). Thymic epithelial cells (TEC) express a variety of self-antigens due to the autoimmune regulator (AIRE) transcription factor, and they present these self-antigens to developing T cells. If a T cell can bind MHC with a foreign or mutated peptide, it will pass positive selection by receiving survival signals; however, if a T cell binds both MHC and self-antigen presented on MHC, it will receive signals to undergo apoptosis to remove it from the T cell repertoire, a process known as negative selection (Xing and Hogquist *Cold Spring Harb Perspect Biol* 2012). T cells that successfully pass this testing selection migrate out of the thymus and enter circulation to secondary lymphoid organs as mature, naïve T cells (Xing and Hogquist *Cold Spring Harb Perspect Biol* 2012).

Central tolerance only eliminates about 70% of self-reactive T cells, due to variations in TCR affinity as well as the incomplete presentation of every self-antigen in the body (ElTanbouly and Noelle *Nat Rev Immunol* 2020). Peripheral tolerance mechanisms curb self-specific T cell

responses in mature T cells after egress from the thymus. Self-reactive T cells undergo peripheral tolerance in several forms. Ignorance occurs when the affinity of TCR to cognate pMHC is too low to initiate activation signaling, essentially keeping the T cell naïve (Mueller *Nat Immunol* 2010). Anergy is a state in which T cell becomes unresponsive in the periphery without the capacity to respond to cognate antigen and arises due to the lack of costimulation upon TCR activation, preventing the activation of the MAPK signaling pathway to fully activate effector responses (Macian et al. *Cell* 2002). Anergy is thought to be reversible; however, massive epigenetic remodeling does occur in this state, and several studies have shown anergic T cells cannot be permanently rescued (ElTanbouly and Noelle *Nat Rev Immunol* 2020; Schietinger et al. *Science* 2012). Finally, deletional tolerance causes the T cell to undergo apoptosis and remove it from the T cell repertoire (Redmond and Sherman *Immunity* 2005). Deletional tolerance is often mediated by the upregulation of pro-apoptotic Bcl-2 Interacting Mediator of cell death (BIM) (Mueller *Nat Immunol* 2010). The signals leading to anergy versus deletional tolerance are unclear but are thought to involve the balance between BIM and anti-apoptotic protein BCL-2 (ElTanbouly and Noelle *Nat Rev Immunol* 2020). It has been difficult to study deletional tolerance mechanisms due to the rapid death and clearance of T cells undergoing this program.

While tolerance mechanisms are important for the prevention of autoimmunity, they also hinder immunotherapeutic efforts to activate T cells in the context of cancer. Cancers express both tumor neoantigens as well as self-antigens, leading to the prevention of self-reactive T cell activation. While it is important to reinvigorate T cells to fight cancer, scientists must also keep in mind the potential of activated T cells to cause immune released adverse effects (IrAE), in which activated self-reactive T cells cause autoimmune damage to healthy tissues. Thus, the development of T cell therapies that mitigate IrAE has been challenging.

Liver mouse models of peripheral tolerance

Several different mouse models of liver self-antigen have been utilized to study self-reactive T cells, especially in the context of graph versus host disease (GVHD) or chronic viral liver infections. This dissertation focuses on the Albumin-GAG (Alb-GAG) model, and this section will discuss known observations in this model as well as other liver tolerance models.

Alb-GAG mice contain the Friend murine leukemia virus (FMLuV) GAG antigen under the albumin promoter, expressing GAG as a liver-specific self-antigen expressed from birth. Previous work with the Alb-GAG model examined GAG-specific CD8 T cells (TCR_{GAG}) that escaped central tolerance. The self-specific T cells (TCR_{GAG}/SST) in this model reacquire function when transferred into a lymphopenic host; however, they reestablish tolerance quickly and do not respond to acute *Listeria* infection (Schietinger A *Science* 2012). There is likely an epigenetic signature that keeps TCR_{GAG} in a tolerized state. Another study has shown that tolerant TCR_{GAG} can be stimulated by pMHC on hepatocytes without the need for Kupffer cells or other APC in the liver to cross-present GAG antigen (Morimoto et al. *J Immunol* 2007). Finally, TCR_{GAG} crossed with P14 T cells, which are specific for the lymphocytic choriomeningitis virus antigen gp33, expressed both TCR types (dual TCR T cells) and displayed a nonfunctional tolerant phenotype and proximal TCR signaling defects only when stimulated by the GAG self-antigen, while stimulation with viral gp33 allowed for functional responses (Teague et al. *Immunity* 2008). Stimulation of dual TCR T cells with tolerizing GAG antigen followed by viral gp33 rescued T cell function, but only temporarily (Teague et al. *Immunity* 2008), indicating that some antigens may confer tolerogenic signals and that tolerance is imprinted and cannot be permanently reversed.

Other models looking at T cell tolerance in the liver have shown that self-specific T cells were generated via cross-presentation in secondary lymphoid tissues but became hyporesponsive. One study found that the level of hepatocyte-expressed antigen is a dominant parameter in

determining long-term CD8 T-cell functional outcome (Tay et al. *Proc Natl Acad Sci U S A* 2014). When primed by HBV protein-expressing hepatocytes, T cells proliferated but differentiated into a dysfunctional phenotype (Benechet et al. *Nature* 2019). Another study found that T cells activated in the liver undergo tolerance differentiation while those activated in the lymph nodes differentiate into functional effectors (Bowen et al. *J Clin Invest* 2004). However, T cells activated by HCV-expressing hepatocytes responded with proliferation and functional cytokines (Wuensch, Pierce, and Crispe *J Immunol* 2006). Thus, the hyporesponsiveness of liver-specific T cells can be influenced by antigen level or antigen presenting cell; however, what signals are needed or what parameter is dominant in this differentiation is unknown.

ONCOGENE INFLUENCE ON THE IMMUNE SYSTEM

Overview

Over a century ago Peyton Rous identified that viruses could cause cancer (Rous *J Exp Med* 1911), and since then, seven human cancer-causing viruses have been identified: Epstein-Barr Virus (EBV), Human Papilloma Virus (HPV), Kaposi sarcoma-associated Herpesvirus (KSHV), Hepatitis B Virus (HBV), Hepatitis C Virus (HCV), Human T-lymphotropic Virus-1 (HTLV-1), and Merkel cell polyomavirus (MCPyV) (Krump and You *Nat Rev Microbiol* 2018). While many of these viruses are widely endemic in humans, relatively few infected individuals go on to develop cancer, indicating that other factors in addition to viral infection are required for cancer induction. Nevertheless, virus-associated cancers account for a significant fraction (13%) of the global cancer burden worldwide, particularly in the developing world (de Martel et al. *Lancet Glob Health* 2020). Viral oncoproteins such as the Simian Virus 40 (SV40) Large T Antigen (TAG) are also used in tumor models to understand oncogene functions and cancer progression. This dissertation utilizes the TAG oncoprotein as well as the viral GAG protein from the Friend murine leukemia virus (FMLuV); thus, it is important to consider the effects of both human cellular oncoproteins and viral oncoproteins in immune modulation.

Initially, it was thought that viral oncoproteins served mainly to bypass cell cycle checkpoints such as p53 and pRB, driving host cell proliferation to facilitate viral genome replication and leading to eventual cancer in some cases (Gaglia and Munger *Curr Opin Virol* 2018). However, oncogenic viral replication and transmission does not require host cell transformation, evidenced by the fact that most people infected with oncogenic viruses do not develop virus-associated cancers (Pandey *Virusdisease* 2020). If oncogenic viruses do not need to cause cancer to replicate, the question arises why human tumor viruses encode viral oncogenes? Our growing knowledge of anti-viral immunology suggests an alternative explanation, elegantly put forward by Drs. Patrick Moore and Yuan Chang: viral oncogenes prevent innate immune-induced cell death or cell cycle arrest (Moore and Chang *Nat Rev Cancer* 2010).

The adaptive immune system is critical to control viral infection, including infection by oncogenic viruses, evidenced by the increased incidence of viral-associated cancers in immunocompromised individuals (Arroyo Muhr et al. *Int J Cancer* 2017). On first infection, T and B cells specific for a particular virus take several days to emerge, expand, eliminate infected cells, and neutralize virus; a subset of these virus-specific T and B cells differentiate into memory cells that can then respond more rapidly and robustly to viral re-challenge. The ability of adaptive cells to form memory has motivated efforts to develop vaccines against oncogenic viruses. Successful vaccines have been developed against HPV and HBV, significantly decreasing the incidence of HPV- and HBV-associated cancers (Stanley *Philos Trans R Soc Lond B Biol Sci* 2017).

It is becoming increasingly clear that TP53 coordinates responses to multiple cellular stresses, including viral infection (Rivas, Aaronson, and Munoz-Fontela *Viruses* 2010). Thus, viral oncoproteins, by inhibiting critical cell regulators such as p53 and pRB, may serve to prevent virus-trigged innate immune signaling and cell cycle arrest or apoptosis, allowing viral persistence

and/or latency. It is long-term persistence that is crucial for viral replication. One hypothesis is that larger DNA viruses, which rely on high-fidelity cellular replication machinery, cannot use antigenic drift to evade immune responses but must rather become latent in hosts, re-activating periodically to allow infection of naïve hosts from generation to generation (Pandey *Virusdisease* 2020). Given that orthologs of *TP53* exist in organisms in which cancers do not occur (Lu and Abrams *Cell Death Differ* 2006), *TP53* likely initially evolved not primarily to prevent cancers, but to respond to cellular stresses such as viral infection (Munoz-Fontela et al. *Nat Rev Immunol* 2016; Rivas, Aaronson, and Munoz-Fontela *Viruses* 2010).

This section discusses several major pathways of viral and non-viral cancer immune evasion with the goal of using selected viral and cellular oncogenes to illustrate specific mechanisms and further describe the immune modulatory effects cancer cells and oncoproteins can exert. Similar to viral oncoproteins, several oncogenes mutated in non-viral cancers not only function to drive proliferation and cell survival but also enhance immune evasion. With the growing clinical use of cancer immunotherapies such as immune checkpoint blockade (ICB), understanding immune evasion strategies in both viral and non-viral cancers will provide important insights into immunotherapy resistance.

Preventing immune cell recruitment: oncogenes alter cytokine/chemokine production

Upon viral infection, infected cells and their surrounding cells release inflammatory cytokines and chemokines (**Fig 1.2)**. Chemokines induce immune cell migration to sites of infection, while cytokines regulate immune cell differentiation and activity. Thus, viruses have evolved several mechanisms to alter cytokine/chemokine production to evade both the innate and adaptive immune response.

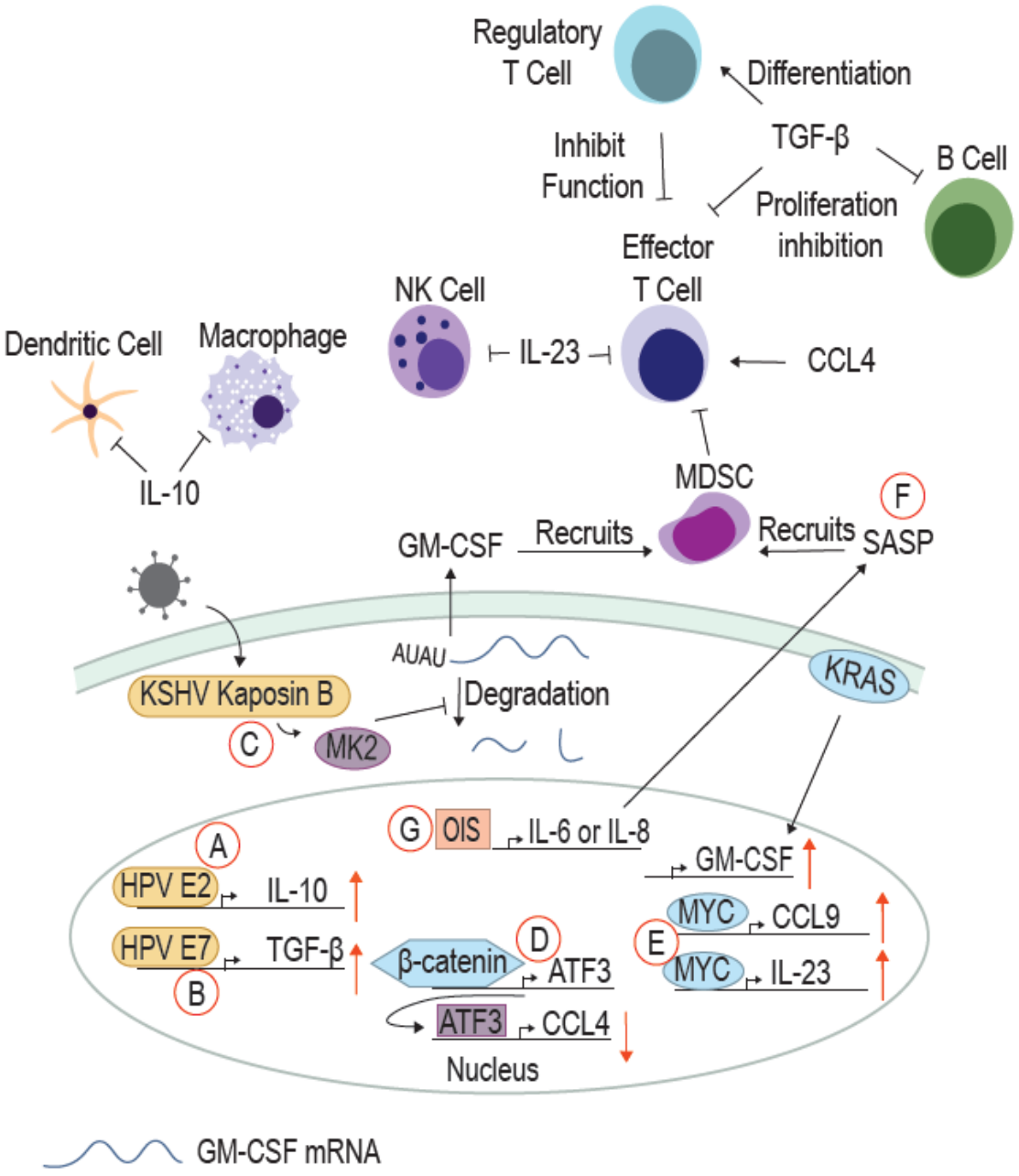

Figure 1.2| Viral and cellular oncoproteins modulate cytokine production to change the immune landscape. A) HPV E2 upregulates IL-10 to inhibit DCs and macrophages. B) E7 upregulates TGF-β to inhibit B cells and effector T cells and promote regulatory T cell infiltration. C) KSHV Kaposin B activates MK2, which inhibits proteins that promote the degradation of cytokine RNAs such as GM-CSF that recruits MDSC. D) β-catenin upregulates ATF3 that acts as a negative regulator for CCL4. E) MYC upregulates both CCL9 and IL-23, cytokines that inhibit T cells and NK cells. F) KRAS promotes GM-CSF production. G) Oncogene-induced senescence (OIS) induces the upregulation of IL-6 or IL-8, which promotes SASP. (Reviewed in Roetman et al 2022 Oncogene).

Kaposi's sarcoma-associated herpesvirus (KSHV) is primarily known for causing Kaposi Sarcoma but also causes primary effusion lymphoma and multicentric Castleman's disease, both B-cell malignancies (Schneider and Dittmer *Am J Clin Dermatol* 2017). Transmission occurs primarily through repeated exchange of saliva or sexual contact. KSHV-associated malignancies are most frequently observed in patients infected with human immunodeficiency virus (HIV) and patients on immunosuppression after organ transplant, indicating that KSHV transformation is prevented by the immune system. The KSHV protein Kaposin B promotes pro-tumorigenic angiogenesis by partnering with MYC to inhibit expression of anti-angiogenic miRNAs (Chang et al. *BMC Syst Biol* 2016). In addition, Kaposin B activates the kinase MK2, which phosphorylates and deactivates AU-rich-binding proteins that normally degrade cytokine mRNAs such as granulocyte-macrophage colony-stimulating factor (GM-CSF) (McCormick and Ganem *Science* 2005) (**Fig 1.2C**). GM-CSF attracts myeloid-derived suppressor cells (MDSC), which in turn induces T cell dysfunction/exhaustion through engagement of inhibitory receptors (described below) and production of inhibitory cytokines such as transforming growth factor-β (TGFβ) (Pylayeva-Gupta et al. *Cancer Cell* 2012). TGFβ inhibits proliferation of activated B cells, prevents T cell function through inhibition of both IL-2-induced proliferation and production of cytotoxic molecule perforin, and promotes regulatory T cell differentiation, which further suppress effector T cell function (Li et al. *Annu Rev Immunol* 2006).

The HPV E2 protein is expressed early during HPV infection. E2 binds to E2-binding sites to drive transcription of viral genes and as well as several cellular genes. E2 transactivates expression of interleukin-10 (IL-10), an anti-inflammatory cytokine that can suppress the function of both macrophages and dendritic cells (Couper, Blount, and Riley *J Immunol* 2008; Bermudez-Morales et al. *Mol Med Rep* 2011) (**Fig 1.2A**). E6 and E7 have also been shown to upregulate TGFβ expression (Alcocer-Gonzalez et al. *Viral Immunol* 2006) (**Fig 1.2B**).

In non-viral cancers, oncogenes have also been shown to alter cellular cytokine production. EPHA2 works through the SMAD4/TGFβ signaling pathway to exert immune inhibitory effects in the tumor microenvironment. In a model of pancreatic ductal adenocarcinoma, expression of EPHA2 and SMAD4 increases the expression of TGFβ as well as *Ptgs2,* encoding COX-2, which increases the levels of PGE2, a proinflammatory prostaglandin. TGFβ and *Ptgs2* in turn act as a positive regulator for EPHA2 and SMAD4 expression, further driving PGE2 expression and inhibiting T cell response in the tumor microenvironment (Markosyan et al. *J Clin Invest* 2019).

β-catenin plays a dual role in driving proliferation and immune evasion. Increased β-catenin in human melanomas correlates with a decrease in tumor-infiltrating T cells, and activated β-catenin in a mouse model of melanoma induces expression of the transcriptional repressor ATF3 (Spranger, Bao, and Gajewski *Nature* 2015). ATF3 suppresses chemokine (C-C motif) ligand 4 (CCL4) expression, a cytokine that recruits dendritic cells (DC) and is required for T cell infiltration and elimination of melanomas (Spranger, Bao, and Gajewski *Nature* 2015) (**Fig 1.2D**).

In a $KRAS^{G12D}$-driven model of lung adenocarcinoma, MYC activation drives expression of CCL9, a chemokine that recruits macrophages and plays a role in programmed death ligand-1 (PD-L1) upregulation (Kortlever et al. *Cell* 2017). In the same model, co-expression of KRAS and MYC upregulated interleukin-23 (IL-23), which suppresses innate immune cells such as natural killer (NK) cells and reduces CTL infiltration (Kortlever et al. *Cell* 2017; Langowski et al. *Nature* 2006) (**Fig 1.2E**). In pancreatic ductal epithelial cells, $KRAS^{G12D}$ drives production of GM-CSF (Pylayeva-Gupta et al. *Cancer Cell* 2012) (**Fig 1.2F**).

A critical determinant of immune cell recruitment to tumors is the manner in which cancer cells die and release antigens. Cells undergoing immunogenic cell death (ICD) release potent immune-stimulatory factors such as DAMPs and antigens, which can robustly activate the adaptive

immune response (Galluzzi et al. *J Immunother Cancer* 2020). On the other side of the spectrum is tolerogenic cell death, which prevents dying cells from eliciting an unwanted immune response (i.e. autoimmunity or organ-damaging inflammation in an immune-privileged site). Early on, the main recognized forms of cell death were apoptosis, considered a form of tolerogenic cell death, and necrosis, an ICD mechanism, but since then many other cell death pathways have been described (Galluzzi et al. *Cell Death Differ* 2018). For further discussion of immunogenic and tolerogenic cell death, see (Green et al. *Nat Rev Immunol* 2009).

Given that ICD is a powerful activator of immune responses, it is perhaps not surprising that oncogenes have been found to inhibit ICD. Anaplastic lymphoma kinase (ALK) is one such oncogene (Wang et al. *Genes Dis* 2018), and ALK promotes survival and proliferation of anaplastic large cell lymphoma (ALCL) by signaling through several major downstream pathways, including phosphatidylinositol 3-kinase (PI3K), extracellular signal-regulated kinase (ERK), and signal transducer and activator of transcription (STAT) pathways (Petrazzuolo et al. *Cell Death Dis* 2021). In a mouse model of ALCL, inhibition of ALK induces ICD, and pharmacologic inhibition of downstream ALK pathways, particularly PI3K, also induces ICD (Petrazzuolo et al. *Cell Death Dis* 2021).

While ICD is an inflammatory cell death, oncogene-induced senescence (OIS) prevents death of cells harboring oncogenic mutations through cell cycle arrest. OIS can induce IL-6 and IL-8 production, cytokine components of the senescence-associated secretory phenotype (SASP). SASP can be anti-tumorigenic through anti-tumor immune cell recruitment or pro-tumorigenic through promotion of inflammation-driven carcinogenesis (Eggert et al. *Cancer Cell* 2016). In a model of radiation-induced tumorigenesis, IL-6 promoted NKT cell infiltration and inflammation, and IL-6 knockout mice had accelerated development of osteosarcoma (Kansara et al. *J Clin Invest* 2013). In a hepatocellular carcinoma model driven by $NRAS^{G12V}$, NOTCH1 drove malignant

hepatocytes to secrete TGFβ, suppressing the SASP response and causing decreased T cell recruitment and proliferation (Hoare et al. *Nat Cell Biol* 2016). In contrast, mice with *Pten*$^{-/-}$ prostate cancer exhibited constitutively active JAK2/STAT3 signaling and upregulated SASP, leading to MDSC recruitment and decreased T cell infiltration (Toso et al. *Cell Reports* 2014) (**Fig 1.2G**). Clearly, the impact of SASP on cancer development is complex and context dependent, and further studies using different *in vitro* and *in vivo* models of oncogene activation are needed to dissect the cell-intrinsic and cell-extrinsic impact of SASP on cancer development and immune responses.

Evading adaptive immunity: oncogenes inhibit MHC Class I antigen presentation

While the innate immune system provides the first line of defense for both oncogenic viral infection and cancer induction, adaptive immune cells subsequently mount antigen-specific responses and form long-lasting memory immunity. Thus, both viral and cellular cancers have evolved mechanisms to avoid the activation of the adaptive immune response.

Cytotoxic CD8 T lymphocytes (CTL) recognize and kill virally infected cells through recognition of viral peptides presented on major histocompatibility complex class I (MHC-I), found on all nucleated cells. Oncogenic viruses frequently evade CTL responses through MHC-I downregulation. Viral proteins in the cytosol are processed by proteasomes to generate short peptides that are then transported into the endoplasmic reticulum by the transporter associated with antigen processing (TAP; **Fig 1.3**). These viral peptides are loaded onto MHC-I, and the peptide/MHC-I (pMHC-I) complex is transported to the plasma membrane for presentation to T cells. CTL with T cell receptors specific for the viral pMHC-I become activated, proliferate, and directly lyse infected cells and secrete cytotoxic cytokines (Hansen and Bouvier *Nat Rev Immunol* 2009).

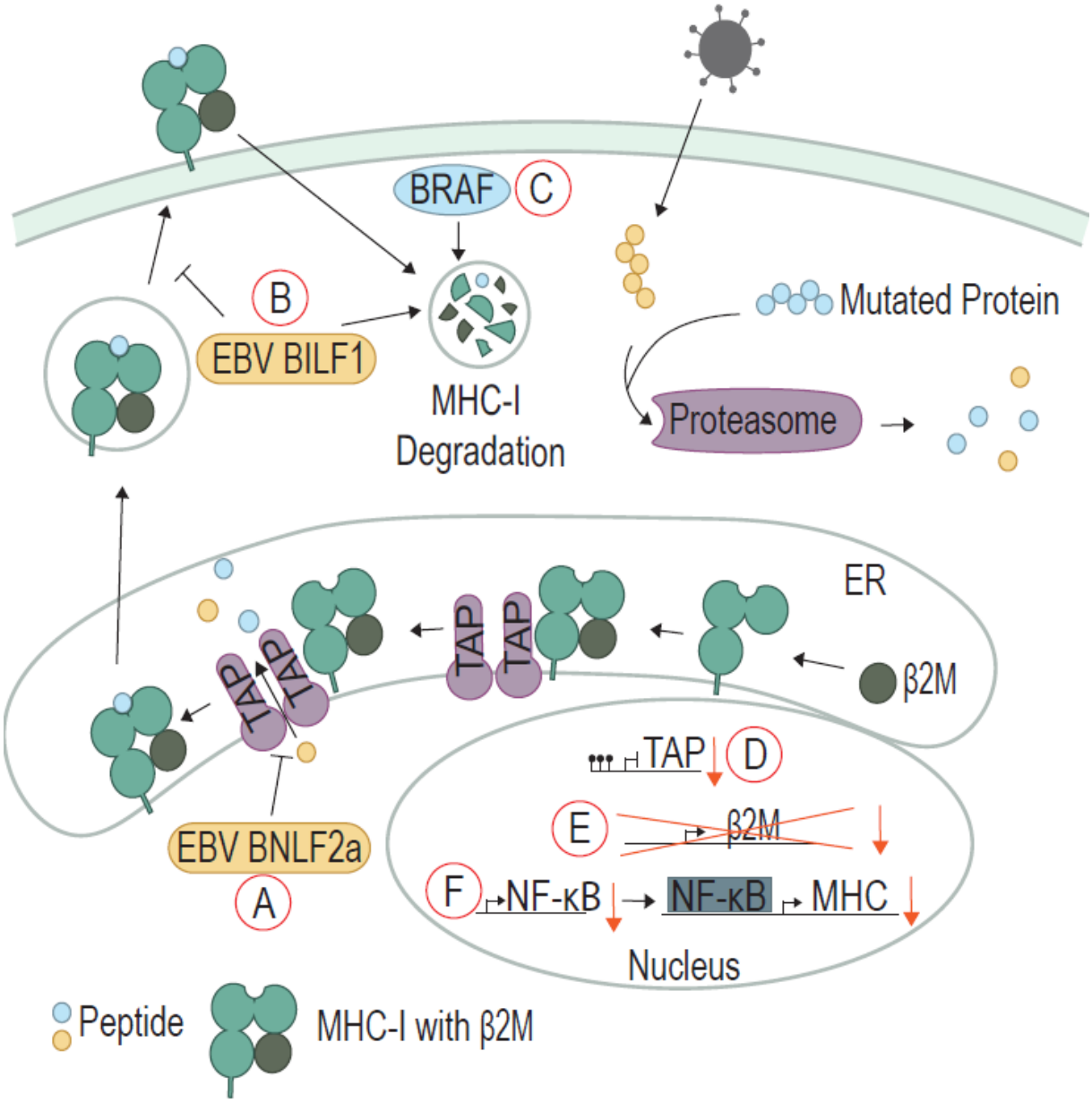

Figure 1.3| Viral and cellular oncoproteins inhibit MHC class I and antigen processing/presentation. A) EBV BNFL2a binds to TAP and inhibits the transport of peptides into the ER. B) EBV BILF1 promotes the degradation of surface MHC-I and can also prevent MHC-I from reaching the cell surface. C) Mutated BRAF can promote degradation of surface MHC-I. Non-viral cancers D) exhibit methylation of the promoter of TAP to prevent expression, E) LOH of β2-microglobulin (β2M), and F) downregulate NF-kB to lower the expression of MHC-I. (Reviewed in Roetman et al 2022 Oncogene).

Epstein-Barr Virus (EBV), the first human oncogenic virus discovered in 1964, is a large DNA herpesvirus that is nearly ubiquitous in humans (Young, Yap, and Murray *Nat Rev Cancer* 2016). EBV is transmitted through contact with bodily fluids and infects both epithelial and lymphoid cells, establishing latency most commonly in B cells. While EBV infection is generally asymptomatic, it has been linked to epithelial and lymphoid cancers, including gastric cancer, nasopharyngeal cancer, Burkitt lymphoma, and Hodgkin lymphoma, with these 4 cancer types responsible for about 17% of global cancer deaths each year (Khan et al. *BMJ Open* 2020). EBV undergoes several different latent stages as well as a lytic phase in which it actively replicates and packages its genome into virions to infect other cells (Tsurumi, Fujita, and Kudoh *Rev Med Virol* 2005). Because actively replicating EBV results in host cell lysis, EBV-driven malignancies mainly occur in latently-infected cells (Paulsen et al. *J Virol* 2005).

The presentation of viral peptides on MHC-I is a critical signal to the adaptive immune system as to whether a cell is healthy or has been virally infected. Melanoma cells were transduced to express the EBV protein BamHI-N leftward frame 2a (BNLF2a) (Strong et al. *J Virol* 2015), resulting in T cells failing to recognize and lyse BNLF2a-expressing cells (Hislop et al. *J Exp Med* 2007). BNLF2a's cytosolic domain associates with TAP to inhibit ATP and peptide binding and prevent viral peptide transport into the ER (Strong et al. *J Virol* 2015; Hislop et al. *J Exp Med* 2007) (**Fig 1.3A**).

Even during EBV infection stages when BNLF2a is not expressed, T cell recognition of EBV-infected cells is poor, indicating that other proteins may be involved in immune evasion during EBV infection (Croft et al. *PLoS Pathog* 2009). BILF1, an EBV lytic phase protein, functions as a constitutively-active G-protein coupled receptor (GPCR) and oncogene (Paulsen et al. *J Virol* 2005). Independent of its GPCR activity, BILF1 associates with MHC-I molecules at the cell surface and rapidly enhances MHC-I internalization and degradation (Zuo et al. *PLoS Pathog*

2009). In addition, BILF1 can divert MHC-I molecules from being transported to the plasma membrane, further inhibiting viral peptide presentation on MHC-I to T cells (Zuo et al. *J Virol* 2011) (**Fig 1.3B**). Thus, the lack of viral peptides on MHC-I prevents CD8 T cells from recognizing the EBV-infected cell.

Many non-viral cancers also employ the strategy of downregulating MHC-I presentation of neoepitopes generated from mutated proteins. An estimated 40-90% of human tumors present with MHC-I downregulation (Cornel, Mimpen, and Nierkens *Cancers (Basel)* 2020). BRAF, a serine/threonine protein kinase, is mutated in 50% of melanoma patients and induces downstream mitogen-activated protein kinase (MAPK) signaling to activate the cell cycle. More recent studies have shown that $BRAF^{V600E}$ has a secondary function: driving internalization and sequestration of MHC-I into endocytic compartments (Bradley et al. *Cancer Immunol Res* 2015) (**Fig 1.3C**). Treatment with the BRAF inhibitor vemurafenib increased MHC-I expression on the cell surface and led to increased T cell recognition (Bradley et al. *Cancer Immunol Res* 2015; Sapkota, Hill, and Pollack *Oncoimmunology* 2013). Expression of the breast cancer oncoprotein HER2, an upstream receptor in the MAPK pathway, is inversely correlated with MHC-I expression (Inoue et al. *Oncoimmunology* 2012). While the mechanism of HER2 and $BRAF^{V600E}$ internalization of MHC-I is not yet known, a screening study showed that other components of the MAPK pathway, namely MAP kinase/ERK kinase 1 (MEK1) and epithelial growth factor receptor (EGFR), negatively regulate MHC-I expression in a mesothelioma cell line (Brea et al. *Cancer Immunol Res* 2016).

Non-viral cancer cells can also block T cell pMHC-I recognition by interfering with peptide processing and presentation. A subset of primary triple-negative breast cancer cells exhibits TAP downregulation along with MHC-I downregulation, and this phenotype is strongly associated with poor clinical outcome (Pedersen et al. *Oncoimmunology* 2017). In addition, some cervical cancers

exhibit promoter methylation and downregulated expression of multiple genes encoding antigen presentation proteins, including TAP (Hasim et al. *PLoS ONE* 2012) (**Fig 1.3D**). The inflammation-induced transcription factor NF-κB directly binds to the *HLA* gene promoters (encoding MHC-I in humans) to induce MHC-I expression (Forloni et al. *Cancer Res* 2010). In neuroblastoma tumors, downregulation of the NF-κB subunit p65 occurs frequently, reducing MHC-I expression (Forloni et al. *Cancer Res* 2010) (**Fig 1.3E**). Patients with metastatic melanoma often undergo loss of heterozygosity (LOH) in the locus encoding β_2-microglobulin (*B2M*). β_2-microglobulin is an essential subunit of MHC-I molecule; therefore, loss of β_2-microglobulin prevents pMHC-I complex formation (del Campo et al. *Int J Cancer* 2014) (**Fig 1.3F**).

Studies have also uncovered MHC-I downregulation as a common response in ICB resistance. Metastatic melanoma patients with *B2M* LOH had reduced response to ICB and worse overall survival (Sade-Feldman et al. *Nat Commun* 2017). Additionally, *B2M* LOH was found in lung tumor samples from patients that had acquired resistance to checkpoint immunotherapies (Gettinger et al. *Cancer Discov* 2017). Thus, more research into the restoration of MHC-I is needed to boost the immune response and for effective ICB treatment.

Dampening T cell responses: oncogenes upregulate checkpoint molecules

Immune checkpoint molecules, such as programmed death-1 (PD-1) and cytotoxic T-lymphocyte associated protein 4 (CTLA-4), are expressed on T lymphocytes and other immune cells and negatively regulate TCR and immune receptor-driven signaling. As mentioned above, inhibitory receptors are a hallmark of T cell dysfunction/exhaustion. Inhibitory ligands such as PD-L1 are expressed on immunosuppressive cells, including regulatory T cells as well as on non-immune tissues in response to inflammatory cytokines such as interferon gamma (IFNγ) (Mandai et al. *Clin Cancer Res* 2016). Immune checkpoints are an essential dampening mechanism that prevent autoimmune disease or excessive immunopathology during chronic viral inflammation (Havel,

Chowell, and Chan *Nat Rev Cancer* 2019). However, these inhibitory mechanisms can prevent effective anti-cancer immune responses, prompting intense interest in immune checkpoint blockade (ICB) therapy (reviewed in (Havel, Chowell, and Chan *Nat Rev Cancer* 2019)).

Patients with chronic HBV infection have been shown to have higher percentages of PD-1+ T cells in peripheral blood, and infected cells have lower levels of *CD274* (encoding PD-L1) methylation (Jiao et al. *J Gene Med* 2020). There is evidence that a higher EBV load correlates with an increase in PD-L1 expression in gastric carcinomas and non-small cell lung cancer (Nakayama et al. *PLoS ONE* 2019; Sugiyama et al. *Sci Immunol* 2020). One of the first proteins expressed in EBV infection is Epstein-Barr virus nuclear antigen 2 (EBNA2), which is capable of immortalizing B cells (Zimber-Strobl et al. *Curr Top Microbiol Immunol* 1999). In Burkitt lymphoma cells, EBNA2 forms a complex with Early B-cell Factor 1 (EBF1), a transcription factor important in B cell signal transduction and differentiation (Anastasiadou et al. *Leukemia* 2019). The EBNA2-EBF1 complex binds to the microRNA *mir-34a* promoter and downregulates its expression. miR-34a binds to the 3'UTR of the *CD274* mRNA, preventing PD-L1 translation (Wang et al. *Cell Signal* 2015). Thus, EBNA2 inhibition of miR-34a leads to high PD-L1 expression and T cell inhibition (Anastasiadou et al. *Leukemia* 2019) (**Fig 1.4A**).

Non-viral cancers make use of several mechanisms to upregulate PD-L1. An inverse correlation between miR-34a and PD-L1 expression has been found in Acute Myeloid Leukemia (AML), and downregulation of miR-34a is associated with poor clinical outcomes (Wang et al. *Cell Signal* 2015). The highest response rate to PD-1/PD-L1 ICB occurs in patients with Hodgkin Lymphoma (HL) (Ansell et al. *N Engl J Med* 2015). HL cases often have a copy number gain of chromosome 9p, containing *CD274* (Roemer et al. *J Clin Oncol* 2016; Green et al. *Blood* 2010), which leads to increased PD-L1 expression (**Fig 1.4B**). The gene encoding Janus kinase 2 (*JAK2*) is also located on 9p, and increased JAK2 signaling was shown to drive further upregulation of PD-L1 (Green et

al. *Blood* 2010). Additionally, dysregulation of other pathways such as κB (NF-κB), JAK/STAT, and PI3K may also contribute to the upregulation of inhibitory molecules (Wienand et al. *Blood Adv* 2019) within malignant cells.

Several oncogenes have been shown to regulate PD-L1 expression. Lung cancers with mutated EGFR exhibit increased PD-L1 as compared to EGFR wild-type lung cancers. EGFR inhibition abrogated the increased PD-L1, indicating that mutant EGFR signals through a yet-unknown mechanism to contribute to the immunosuppressive environment of lung cancer, in addition to its role in driving growth and proliferation (Akbay et al. *Cancer Discov* 2013). Oncogenic MYC can bind directly to the *CD274* promoter to drive PD-L1 expression in T cell acute lymphoblastic leukemia (T-ALL; **Fig 1.4C**). MYC inhibition in T-ALL cells lowered PD-L1 expression and improved T cell responses against these cancers (Casey et al. *Science* 2016). FGFR amplification or mutation in colorectal cancer causes downstream proliferation and transformation through the activation of the MAPK and PI3K pathways. In addition, FGFR signals through the JAK/STAT pathway, which causes upregulation of PD-L1 expression (Li et al. *J Immunol* 2019).

Analyses of lung and colon adenocarcinomas in TCGA suggest an association between RAS activation and PD-L1 upregulation (Coelho et al. *Immunity* 2017). Studies in a human epithelial cell model with inducible RAS^{G12V} expression showed that RAS regulates PD-L1 expression through tristetraprolin (TTP), an RNA-binding protein that binds to AU-rich elements. PD-L1 mRNA contains AU-rich regions, and TTP binding causes degradation of PD-L1 mRNA. However, aberrant RAS signaling activates the kinase MAPK-activated protein kinase 2 (MK2), which directly phosphorylates and inhibits TTP, stabilizing PD-L1 mRNA, increasing PD-L1 expression, and inhibiting T cell responses (Coelho et al. *Immunity* 2017) (**Fig 1.4D**).

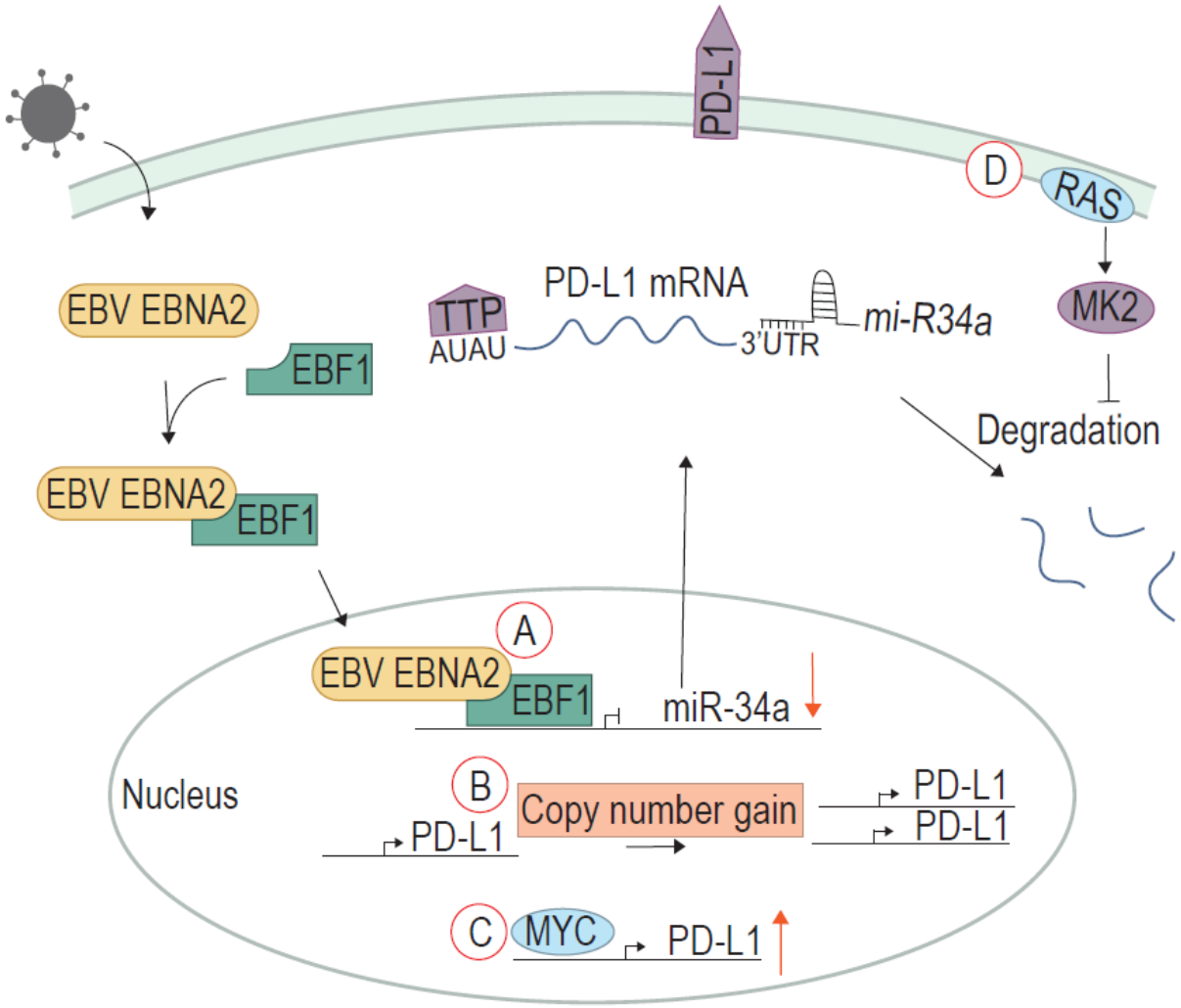

Figure 1.4| Viral and cellular oncoproteins upregulate checkpoint molecules such as PD-L1. A) EBV EBNA2 stabilizes PD-L1 mRNA by forming a complex with EBF1 to downregulation miR-34a, a microRNA that promotes the degradation of PD-L1 mRNA. Some non-viral cancers have B) copy number gains in the PD-L1 gene. C) Oncogenic MYC drives upregulation of PD-L1. D) Mutated RAS activates MK2, which promotes the phosphorylation of TTP to inhibit the degradation of PD-L1 mRNA. (Reviewed in Roetman *et al* 2022 Oncogene).

Clinically, ICB has been a substantial advancement in cancer treatment. However, primary non-responsiveness to ICB therapies as well as secondary resistance (reviewed in (Schoenfeld and Hellmann *Cancer Cell* 2020)) in patients who initially respond remains a significant clinical obstacle. We are just beginning to understand the mechanisms for ICB treatment failures, paving a clear direction for future research. By studying mechanisms of resistance in both viral and non-viral cancers, we can develop strategies to make ICB therapy effective in more patients.

Clinical therapeutics: oncoprotein inhibitors enhance the immune response

While the effects of oncoproteins on the immune system described above prevent efficient activation of the immune system, therapeutic oncoprotein inhibition can not only lead to slowed cancer cell growth and death but can boost immune responses by bypassing or counteracting the oncogene-induced immune evasion strategies discussed above.

Inhibitors of cell surface growth factor receptors have been part of cancer therapy for well over a decade. For example, lapatinib inhibits both EGFR and HER2 intracellular tyrosine kinase domains. This inhibition prevents downstream signaling while also preventing the ubiquitination and downregulation and HER2. The accumulation of HER2 promotes antibody-dependent cellular cytotoxicity, which increases cancer cell lysis, typically by NK cells. Lapatinib also promotes infiltration of T cells and their subsequent production of IFNγ through a STAT1-dependent expression of T-cell chemotactic cytokines, including CXCL9, CXCL10, and CXCL11 (Griguolo et al. *J Immunother Cancer* 2019; Hannesdottir et al. *Eur J Immunol* 2013).

CDK4/6 inhibitors used to treat breast cancers have been shown in both mice and humans to recruit T cells to otherwise immunologically cold tumors. Inhibitors palbociclib, ribociclib, and abemaciclib all enhance the production of CCL5, CXCL9, and CXCL10, cytokines that attract T cells (Uzhachenko et al. *Cell Rep* 2021). When treated with only CDK4 or CDK6 inhibitors, this

effect was abrogated, suggesting that both cyclins need to be inhibited to produce these cytokines. Patients with these cytokines present have also shown better prognoses than those without (Uzhachenko et al. *Cell Rep* 2021). Further improving our understanding of how oncogenes alter immune responses will allow clinicians and researchers to design synergistic combinations of oncogene-targeted therapies and immunomodulatory agents.

The study of oncogenic viruses historically provided many valuable insights and paved the way for our understanding of cellular oncogenes and tumor suppressor genes. In 2000, Hanahan and Weinberg described six hallmark pathways altered in cells that lead to carcinogenesis, including many pathways first identified through the study of viral oncogenes such as evading apoptosis and growth factor-independent proliferation. In the years since then, the critical role of the immune system in carcinogenesis has become clear, and in 2011, Hanahan and Weinberg added a new hallmark pathway: evasion of the immune system (Hanahan and Weinberg *Cell* 2011). As we have learned more about how oncogenes alter key hallmark pathways in cells to cause cancer, it has become clear that oncogenes can impact several pathways at once.

Oncogene	Role in Immune Evasion	References
ALK	Inhibits immunogenic cell death	(Wang et al. *Genes Dis* 2018; Petrazzuolo et al. *Cell Death Dis* 2021)
β-catenin	Represses the expression of CCL4, which recruits DCs and T cells	(Spranger, Bao, and Gajewski *Nature* 2015)
BRAF	Drives internalization and sequestration of MHC-I	(Bradley et al. *Cancer Immunol Res* 2015; Sapkota, Hill, and Pollack *Oncoimmunology* 2013)
EGFR	Contributes to increased PD-L1 expression	(Brea et al. *Cancer Immunol Res* 2016; Akbay et al. *Cancer Discov* 2013)
EPHA2	Increases TGFB signaling and COX-2 expression, causing increased proinflammatory PGE2	(Markosyan et al. *J Clin Invest* 2019)
FGFR	Drives PD-L1 expression	(Li et al. *J Immunol* 2019)
HER2	Binds to STING to prevent immune sensing Internalization of MHC-I	(Moasser *Oncogene* 2007; Wu et al. *Nat Cell Biol* 2019; Inoue et al. *Oncoimmunology* 2012)
MYC	Induces expression of CCL9 to recruited macrophages Acts with KRAS to upregulate IL-23 to suppress innate immune cells and reduce CTL infiltration Drives PD-L1 expression Inhibits immunogenic cell death	(Kortlever et al. *Cell* 2017; Langowski et al. *Nature* 2006; Chang et al. *BMC Syst Biol* 2016; Casey et al. *Science* 2016)
NOTCH	Suppresses SASP, causing decreased T cell recruitment	(Hoare et al. *Nat Cell Biol* 2016)
RAS	Drives OIS and SASP expression	(Pylayeva-Gupta et al. *Cancer Cell* 2012; Kortlever et al. *Cell* 2017; Langowski et al. *Nature* 2006; Coelho et al. *Immunity* 2017)
SMAD4	Drives TGFB signaling, which inhibits adaptive immune response	(Markosyan et al. *J Clin Invest* 2019)

Table 1. Role of cellular oncogenes in immune evasion.

SUMMARY AND STUDY DESIGN

Tumor-specific CD8 T cell dysfunction has been well-characterized through analyses of protein and RNA expression as well as epigenic landscapes. However, analyses of self-specific T cells recognizing antigens overexpressed by tumors but also shared as normal, “self” antigen in other parts of the body are not well understood in the tumor context. This dissertation will present findings that will address some of the current gaps in knowledge pertaining to CD8 T cell dysfunction/exhaustion, with particular focus on persistence of self-specific T cells recognizing self-antigen on oncogene-transformed hepatocytes. To accomplish this work, a novel mouse model combining liver tumor neoantigen expression with liver self-antigen expression was created. Chapter II will detail the research methods used.

Tumors express both tumor-specific antigens (TSA) and self/shared-antigen antigens (SSA). It is unknown whether T cells that respond to these antigens undergo the same signals to become functionally unresponsive. Chapter III will highlight the creation of liver ductal organoids and attempts to differentiate stem cells in liver ducts into hepatocytes to create a liver cancer organoid model that could be used to dissect direct interactions of oncogenic neoantigens on CD8 T cell differentiation. Chapter IV will discuss the characterization of self- vs tumor-specific T cell responses to liver cancer in a novel mouse model in which hepatocytes express both self and tumor antigens as well as a novel self-specific T cell subset that is phenotypically memory-like but do not function upon secondary stimulation or ICB. Chapter V will include further probes into the mechanism by which CD8 T cell fail to persist and leave cell cycle prematurely after recognition of self/shared antigen. Finally, Chapter VI will discuss implications and future directions of this work.

CHAPTER II

MATERIALS AND METHODS

Mice. All mice were bred and maintained in a specific pathogen free barrier facility at Vanderbilt University Medical Center. Experiments were performed in compliance with the Institutional Animal Care and Use Committee regulations. Mice were age- and sex-matched, between 6 and 12 weeks old when used for experiments and assigned randomly to experimental groups. Both female and male mice were used. TCR_{GAG} transgenic mice and Albumin-GAG (Alb-GAG) mice have been previously described (Ohlen et al. *J Exp Med* 2002; Ohlen et al. *J Immunol* 2001). TCR_{TAG} transgenic mice (Stock No 005236), Cre-ER^{T2} (Stock No 008463), and C57BL/6J Thy1.1 mice (Stock No. 000406) mice were purchased from The Jackson Laboratory. TCR_{TAG} and TCR_{GAG} mice were crossed to Thy1.1 mice to generate TCR_{TAG};Thy1.1 and TCR_{GAG};Thy1.1 mice, respectively. AST (AlbuminfloxStop-SV40 large T antigen (TAG)) (Stahl et al. *Immunol Lett* 2009) were crossed to Cre-ER^{T2} mice to generate AST;Cre-ER^{T2}. Alb-GAG mice were crossed to Cre-ER^{T2} to generate Alb-GAG;Cre-ER^{T2} mice, which were then crossed with AST mice to generate Alb-GAG;AST;Cre-ER^{T2} mice.

Liver ductal cell isolation. Livers were manually minced, and the resulting supernatant and liver pieces were then transferred to a 50 mL conical tube containing a dissociation cocktail consisting of collagenase IV, dispase, and DMEM/F-12 with 15 mM HEPES (StemCell) and incubated for 20 minutes at 37°C. The supernatant was discarded, and additional dissociation media was added and incubated at 37°C 3 times. The resulting supernatant was then passed through a 70 μm cell strainer and then through a 37 μm cell strainer. The strainer was then reversed and passed with DMEM/F-12 into a pre-wetted tube to prevent ductal cells from adhering to tube.

Organoid initiation. Isolated ductal cells were resuspended in 50 µl of cold Matrigel® and plated in a bubble on a warm 24-well plate. After allowing Matrigel to solidify, HepatiCult™ (STEMCELL Technologies) was added and incubated at 37°C with 5% CO_2. Organoids were split every 3 days.

Organoid differentiation. Organoid expansion media was replaced with two different differentiation medias for 15 days with media replenished every 2-3 days. One media contained Williams E, 1% pen/strep, 1% GlutaMAX, 1% NEAA, 2% B27 supplement, 1% N2 supplement, noggin-conditioned medium, 0.2% normocin, 3 uM ChIR99021, 1.25 mM N-acetylcysteine, 10 mM nicotinamide, 25 ng/mL recombinant EGF, 50 ng/mL recombinant human HGF, 100 ng/mL TNFa, 1 uM A83-01, and 10 uM Y-27632 (Peng et al. *Cell* 2018). The second media contained Advanced DMEM/F-12, 1% B27 supplement, 1% N2 supplement, 10 nM recombinant gastrin, 50 ng/mL recombinant EGF, 100 ng/mL recombinant human FGF19, 25 ng/mL recombinant human HGF, 500 nM A83-01, 10 uM DAPT, 25 ng/mL BMP7, and 30 uM dexamethasone (Huch et al. *Cell* 2015).

Organoid imaging. Matrigel domes were formed on glass wells and allowed to form overnight. CellTracker Orange-labelled TCR_{TAG} splenocytes were then added to surrounding media and incubated for 3 days at 37°C with 5% CO_2. This culture was then live imaged using an LSM 710 confocal microscope at the Vanderbilt Cell Imaging Shared Resource.

RNA extraction. For liver RNA, liver sections were placed in ceramic bead tubes with TRIzol™ reagent and vigorously shaken. Using Phasemaker™ tubes (Thermo-Fisher), chloroform was then added to isolate the RNA. The PureLink® RNA Mini Kit (Thermo-Fisher) was then used to purify the RNA extraction according to manufacturer instructions. For organoid RNA, organoids were first dissociated with DMEM/F-12 and spun down. RNA was then extracted and purified using the RNeasy kit (Qiagen).

RT-qPCR. RNA from the organoids and cell lines were reverse transcribed into cDNA using the SuperScript™ IV kit (Invitrogen) and diluted in range of the standard curve. PowerUp™ SyBR® Green Master Mix was used according to manufacturer instructions, and 18S, Alb, Sox9, and Krt19 genes were amplified using QuantStudio 3 (Applied Biosciences). Fold change was then calculated using ΔCt values and the Pfaffl method (Pfaffl *Nucleic Acids Res* 2001).

Antibodies and reagents. Fluorochrome-conjugated antibodies were purchased from BD Biosciences, eBioscience, Biolegend, Tonbo Biosciences, and Cell Signaling Technology (**Table 2 and 3**). Tamoxifen (Sigma) solution was prepared by warming tamoxifen at 50°C for 1 h in sterile corn oil with 5% absolute ethanol. Tamoxifen (1 mg) was administered i.p. into AST;Cre-ER^{T2} or Alb-GAG;AST;Cre-ER^{T2} mice.

Cell isolation. Spleens were mechanically disrupted to a single-cell suspension with the back of a 3 mL syringe plunger, passed through a 70 μm strainer, and lysed with ammonium chloride potassium (ACK) buffer. Cells were washed once with cold RPMI 1640 media supplemented with 10% FCS. Livers were mechanically disrupted to a single-cell suspension using a glass pestle against a 150 μ metal mesh in cold PBS containing 2% FCS (FCS/PBS) and filtered through a 100 μm strainer. The liver homogenate was spun down at 400g for 5 min at 4°C, and the pellet was resuspended in 15 mL FCS/PBS, 500 U heparin, and 10 mL PBS Buffered Percoll (GE), mixed by inversion, and spun at 500g for 10 min at 4°C. Pellets were lysed with ACK buffer, and cells were resuspended in RPMI 1640 containing 10% FCS for downstream analysis.

Antibody	Fluorophore	Clone	Dilution	Source	Identifier
Anti-BCL-2	PE-Cy7	BCL/10C4	1:200	BioLegend	Cat# 633512
Anti-BIM	AF488	C34C5	1:200	Cell Signaling Technology	Cat# 94805S
Anti-CD8a	BV605	53-6.7	1:250	BioLegend	Cat# 100744
Anti-CD8a	PE-Cy7	53-6.7	1:800	BioLegend	Cat# 100722
Anti-CD38	PcP-Cy5.5	90	1:200	BioLegend	Cat# 102721
Anti-CD39	PcP-eF710	242DMS1	1:200	Invitrogen	Cat# 46-0391-80
Anti-CD44	PcP-Cy5.5	IM7	1:200	Tonbo	Cat# 65-0441
Anti-CD44	FITC	IM7	1:200	BioLegend	Cat# 103006
Anti-CD44	APC	IM7	1:200	Tonbo	Cat# 20-0441
Anti-CD62L	BV785	MEL-14	1:300	BioLegend	Cat# 104440
Anti-CD90.1	BV421	OX-7	1:800	BioLegend	Cat# 202529
Anti-CD90.1	BV510	OX-7	1:600	BioLegend	Cat# 202535
Anti-CD90.1	PcP-Cy5.5	HIS51	1:800	eBioscience	Cat# 45-0900-80
Anti-CD90.1	APC	HIS51	1:800	eBioscience	Cat# 17-0900-82
Anti-CD90.1	APC-eF780	HIS51	1:800	eBioscience	Cat #47-0900-82
Anti-CD90.2	BV421	53-2.1	1:800	BioLegend	Cat# 140327
Anti-CD127	PE-Cy7	A7R34	1:200	BioLegend	Cat# 135013
Anti-IFNγ	APC	XMG.12	1:1600	BioLegend	Cat# 505810
Anti-Ki67	FITC	SolA15	1:300	eBioscience	Cat# 11-5698-80
Anti-Ki67	PcP-Cy5.5	16A8	1:200	BioLegend	Cat# 652423
Anti-Ki67	AF700	16A8	1:400	BioLegend	Cat# 652419
Anti-PD1	PcP-eF710	RMP1-30	1:200	eBioscience	Cat# 46-9981-80
Anti-PD1	APC	RMP1-30	1:200	BioLegend	Cat# 109112
Anti-TCF1	AF647	C63D9	1:400	Cell Signaling Technology	Cat# 6709S
Anti-TCR Vα7	FITC	TR310	1:100	BioLegend	Cat# 118305
Anti-TCR Vβ12	PE	MR11-1	1:100	BioLegend	Cat# 139703
Anti-TNFα	PE	MP6-XT22	1:800	Life	Cat# 12-7321-82
Anti-TOX	PE	REA473	1:400	Miltenyl Biotec	Cat# 130-120-716

Table 2. Flow cytometry antibodies.

Dye Name	Dilution/Concentration	Source	Identifier
Annexin V-PE	1:200	BioLegend	Cat# 640908
CFSE	5 μM	Tonbo	Cat# 13-0850
DAPI	50 ng/mL	BioLegend	Cat# 422801
Ghost Dye Violet 450 Viability Dye	1:1000	Tonbo	Cat# 13-0863
Ghost Dye Violet 780 Viability Dye	1:2000	Tonbo	Cat# 13-0865

Table 3. Flow cytometry cell dyes.

Intracellular cytokine staining. T cells were mixed with $2x10^6$ congenically marked splenocytes and incubated in RPMI 1640 containing 10% FCS for 4 h at 37°C in the presence of GolgiPlug (brefeldin A) and peptide at the following concentrations: GAG peptide (1.5 μM), TAG peptide (0.5 μM). Cells were stained for surface molecules and then fixed and permeabilized using the FoxP3 Transcription Factor Fix/Perm (Tonbo Biosciences) per the manufacturer's instructions before staining for intracellular molecules.

Flow cytometric analysis. Flow cytometric analysis was performed using an Attune NxT Acoustic Focusing Cytometer (ThermoFisher). Flow data were analyzed with FlowJo v.10 software (Tree Star Inc.).

Listeria infection. The *Listeria monocytogenes* (*Lm*) ΔactA ΔinlB strain expressing the GAG epitope (CCLCLTVFL, FMuLV GAG_{75-83}) or Tag-I epitope (SAINNYAQKL, SV40 large T $antigen_{206–215}$) were generated by Genscript and stored at −80°C. Mice were infected with $3x10^7$ c.f.u. *Lm*GAG and $5x10^6$ c.f.u. of *Lm*TAG via i.v. injection.

Adoptive T cell transfer. To transfer naive TCR_{GAG} T cells into Alb-GAG and Alb-GAG;AST;Cre-ER^{T2} mice or naïve TCR_{TAG} T cells into AST;Cre-ER^{T2} or Alb-GAG;AST;Cre-ER^{T2}, $2x10^6$ CD8+ splenocytes from TCR_{GAG};Thy1.1 or TCR_{TAG};Thy1.1 transgenic mice were adoptively transferred via retroorbital i.v. injection. For the generation of effector and memory TCR_{GAG} CD8+ T cells or TCR_{TAG};Thy1.1 CD8+ T cells, $5x10^5$ CD8+ splenocytes from TCR_{GAG};Thy1.1 or TCR_{TAG};Thy1.1 transgenic mice were adoptively transferred into B6 (Thy1.2) mice. Mice were infected the following day with *Listeria* as described above. TCR_{GAG} or TCR_{TAG} CD8+ T cells were isolated from the spleens of B6 host mice and analyzed 5 days after *Listeria* immunization for effector T cells and at least 21 days after *Listeria* immunization for memory T cells.

CFSE labeling. To assess cellular proliferation, splenocytes were incubated with 5 μM CFSE at 37ºC. Remaining extracellular dye was quenched with cold FCS, and cells were washed twice with serum-free RPMI before transfer into hosts.

Cell cycle analysis. T cells were stained for surface and intracellular markers as described above. Samples were suspended in FoxP3 Fix/Perm buffer (Tonbo Biosciences), and DAPI was added to sample immediately prior to flow cytometric analysis.

Immune checkpoint blockade. Anti-PD1 (clone RMP1-14) and anti-PDL1 (clone 10.F.9G2) antibodies or isotype control (clone LTA-2) were purchased from BioXcell. Antibodies were injected intraperitoneally five times, every other day, at 200 μg per antibody per mouse.

***In vitro* hepatocyte culture.** ASTxGAG and C57BL/6 mice were perfused under anesthesia with liver perfusion medium (Gibco) and liver digestion medium (Gibco). Primary hepatocytes were isolated using Percoll gradient purification (GE) at low grade centrifugations (50g) and incubated on collagen I-precoated plates (Gibco) as previously described (Dijkstra et al. *Cell* 2018). Hepatocytes were incubated in low-glucose DMEM (Gibco) supplemented with 5% fetal bovine serum and 1% penicillin/streptomycin at 37ºC with 5% CO_2. The following day, splenocytes from TCR_{GAG};Thy1.1 or TCR_{TAG};Thy1.1 transgenic mice were labeled with CFSE as described above, and 100,000 CD8+ T cells were added to hepatocyte culture for 3 days.

Gene set enrichment analysis. Previously published microarray data (Schietinger et al. *Science* 2012; Schietinger et al. *Immunity* 2016) were analyzed using Broad Institute's Gene Set Enrichment Analysis software (GSEA; http://www.broadinstitute.org/gsea) to determine whether predefined gene sets showed enrichment in T cell sample groups "GAG" versus "TAG." Statistical significance was determined by permutation testing and normalized enrichment score (NES).

Statistics. GraphPad Prism V9 was used for all statistical analyses. Unless otherwise stated, a one-way ANOVA was performed followed by a Tukey's test to correct for multiple comparisons. The significance level was set at 0.05. Equal variances were verified by the Brown-Forsythe Test.

CHAPTER III

IN VITRO ORGANOID MODEL TO STUDY T CELL RESPONSES TO ONCOGENICALLY TRANSFORMED HEPATOCYTES

OVERVIEW

Not only do oncogenes provide signals to a transformed cell to proliferate and survive, but they can also exert immune modulatory effects. These modulatory effects can recruit or inhibit certain types of immune cells, release cytokines to exert signaling alterations, or stimulate the transformed cell to express ligands of inhibitory receptors expressed on immune cells. (For more detail, see Chapter I). A wide variety of oncogenes have immunomodulatory effects, and both viral and cellular oncogenes have been observed to promote immune modulation. Previous studies have shown that CD8 T cells that enter a tumor environment very rapidly undergo loss of function and enter a dysfunctional state characterized by the lack of effector cytokines IFNγ and TNFα. This dysfunction is not only seen in an established tumor with a complex microenvironment but also in premalignant lesions in which cells have only recently transformed and a tumor microenvironment has not yet formed (Schietinger et al. *Immunity* 2016; Philip et al. *Nature* 2017). Without a tumor microenvironment, we hypothesized that the oncogene itself was exerting an immune modulatory effect on the CD8 T cells and rendering them dysfunctional.

$Lgr5^+$ liver stem cells were first thought to be a valuable source of regenerative cells that could form organoids via the stimulation of Wnt-signaling through a Rspo-1 agonist (Huch et al. *Nature* 2013). Based on these findings, Broutier, *et. al*., 2016 suggested that ductal cell-derived cells could be isolated, expanded in Matrigel, and differentiated under favorable conditions to form hepatocyte-like organoids that upregulated hepatocyte markers such as *Alb* (Broutier et al. *Nat Protoc* 2016), and we aimed to adapt this protocol to generate liver organoids with an inducible oncogene.

We used our AST;Cre-ER^{T2} (Albumin-Stop-Large T Antigen) mouse model in which the viral SV40 large T antigen (TAG) is induced by Tamoxifen (TAM) and acts as a potent oncogene by inhibiting both p53 and pRB and promoting cell proliferation under a liver-specific promoter (**Fig. 3.1**). Because it is difficult to ascertain whether a component of the tumor microenvironment or the transformed cell itself is the culprit of immune modulation, we turned to the new organoid technology to create an *in vitro* environment in which a pseudo-liver with transformed cells could interact with TAG-specific CD8 T cells (TCR_{TAG}). Thus, we could determine if and how the TAG oncogene was responsible for CD8 T cell dysfunction, or we could add in components of the tumor microenvironment to determine what was necessary to act on the T cells.

RESULTS

2D culture system to assess T cell culture with transformed hepatocytes

To determine whether the TAG oncogene is responsible for the differentiation of CD8 T cells to dysfunction, we wanted to generate liver organoids using our AST;Cre-ER^{T2} TAM-inducible model. We would generate these organoids from uninduced livers to propagate, and then treat organoids at a specific time to turn on TAG oncogene expression. We could then co-culture these organoids with TCR_{TAG} T cells to assess their function after contact with the organoids.

To first assess the validity of these experiments, I generated a cell line derived from AST;Cre-ER^{T2} mice by disrupting a liver from one of these mice and culturing the resulting slurry in cell culture medium. The cells that grew out were named ACE1825 and provided us with a liver cell line as a 2D culture (**Fig 3.2A**). ACE1825 were TAG positive and expressed H-2Kb, the MHC-I in which TAG is restricted to (**Fig 3.2B).** I then co-cultured ACE1825 with TCR_{TAG} T cells for 3,

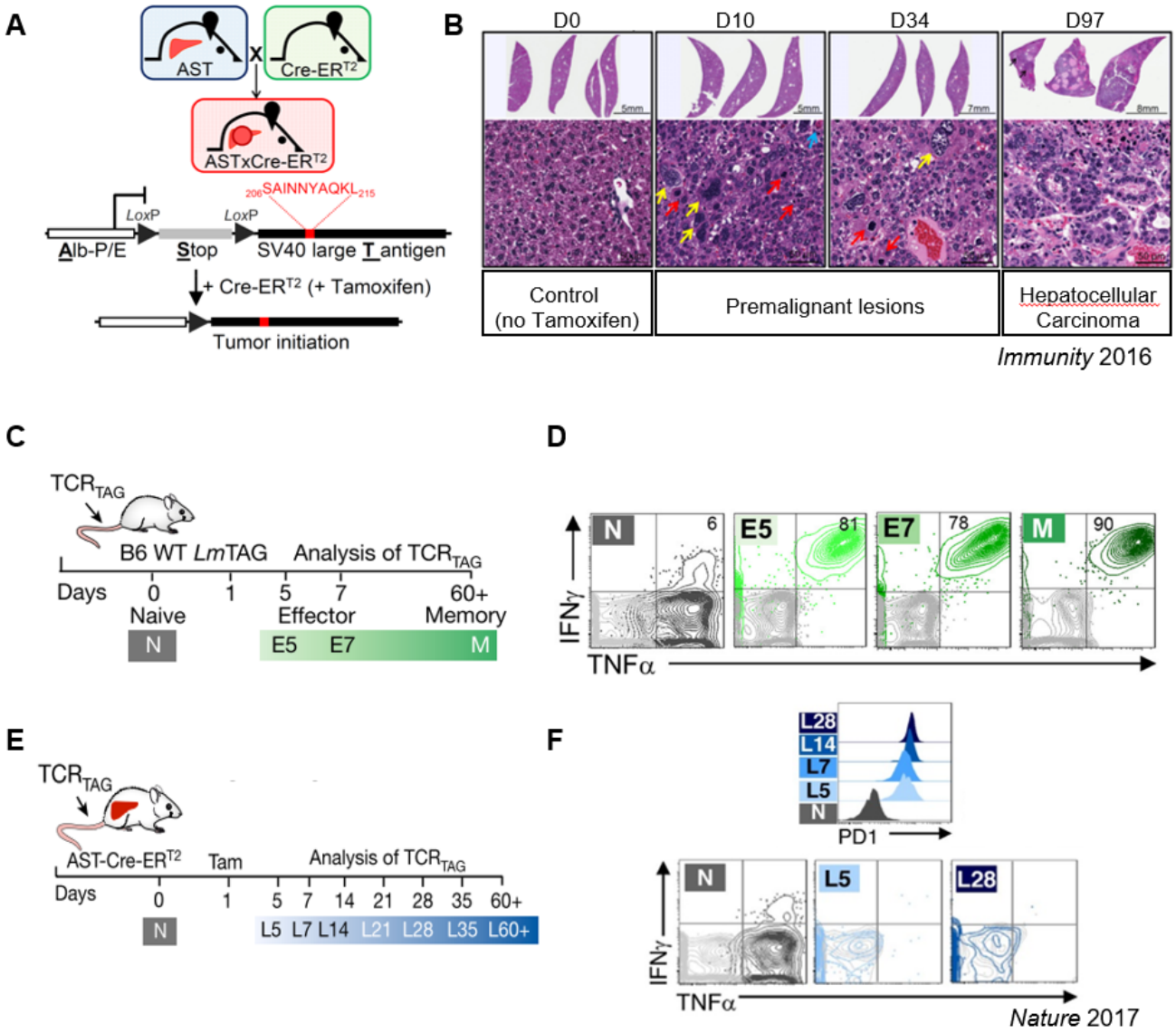

Figure 3.1| A. Inducible AST;Cre-ER^{T2} HCC model induces CD8 T cell dysfunction. CD8 T cell TAG epitope shown in red. **B.** H&E staining of liver sections from AST;Cre-ER^{T2}. **C.** Naïve TCR$_{TAG}$ (N) were transferred into B6 mice and inoculated with *Lm*TAG one day later to model infection. **D.** Transferred TCR$_{TAG}$ were reisolated from the spleen at different time points. Flow analysis shows efficient production of effector cytokines (assessed by intracellular cytokine staining after 4-hour *ex vivo* TAG peptide stimulation). **E.** Naïve TCR$_{TAG}$ (N) were transferred into ASTxCre-ER^{T2} mice, and Cre activated by TAM one day later to induce liver carcinogenesis. **F.** Transferred TCR$_{TAG}$ were reisolated from the liver at different time points (L5-60). Flow analysis shows rapid PD1 upregulation (top) and loss of effector cytokine production (bottom; assessed by intracellular cytokine staining after 4-hour *ex vivo* TAG peptide stimulation).

From Schietinger *2016 Immunity* and Philip *2017 Nature.*

5, and 7 days and assessed inhibitory receptor expression as well as effector cytokine production. The longer T cells remained cultured with ACE1825, the higher the expression levels of both PD-1 and LAG3 (**Fig 3.2C**). Already by day 3 in culture, T cells could no longer produce TNFα and INFγ, replicating what we see *in vivo* with the AST;Cre-ER^{T2} model (**Fig 3.2D**).

Liver organoid generation

To generate the liver organoid system, we turned to a series of recently published papers from the Hans Clevers lab in which the authors generated organoids from liver stem cells (Huch et al. *Nature* 2013; Huch et al. *Cell* 2015) and commercialized through STEMCELL Technologies. These stem cells are found primarily in the ductal cells of the liver. Thus, to isolate these ductal cells we followed the paper and manufacturer protocols to digest an AST;Cre-ER^{T2} mouse liver and dissociate pieces into ductal cells. These ducts were then cultured in Matrigel domes (**Fig 3.3**).

To determine if T cells could access the Matrigel dome to contact the liver organoids, we peptide-pulsed ductal organoids with TAG peptide and embedded these cells in Matrigel, allowing them to re-form their spheroid structure overnight. I then added CellTracker Orange-labelled TCR$_{TAG}$ splenocytes to the media surrounding the Matrigel dome. Confocal microscopy revealed that the T cells had migrated into the Matrigel domes and contacted the ductal organoid cells (**Fig 3.4**).

Differentiation of liver ductal cells to hepatocytes

The cells that made up these organoids were liver ductal cells filled with stem cells that do not express albumin, the promoter in which our TAG-oncogene is under, but mature hepatocytes

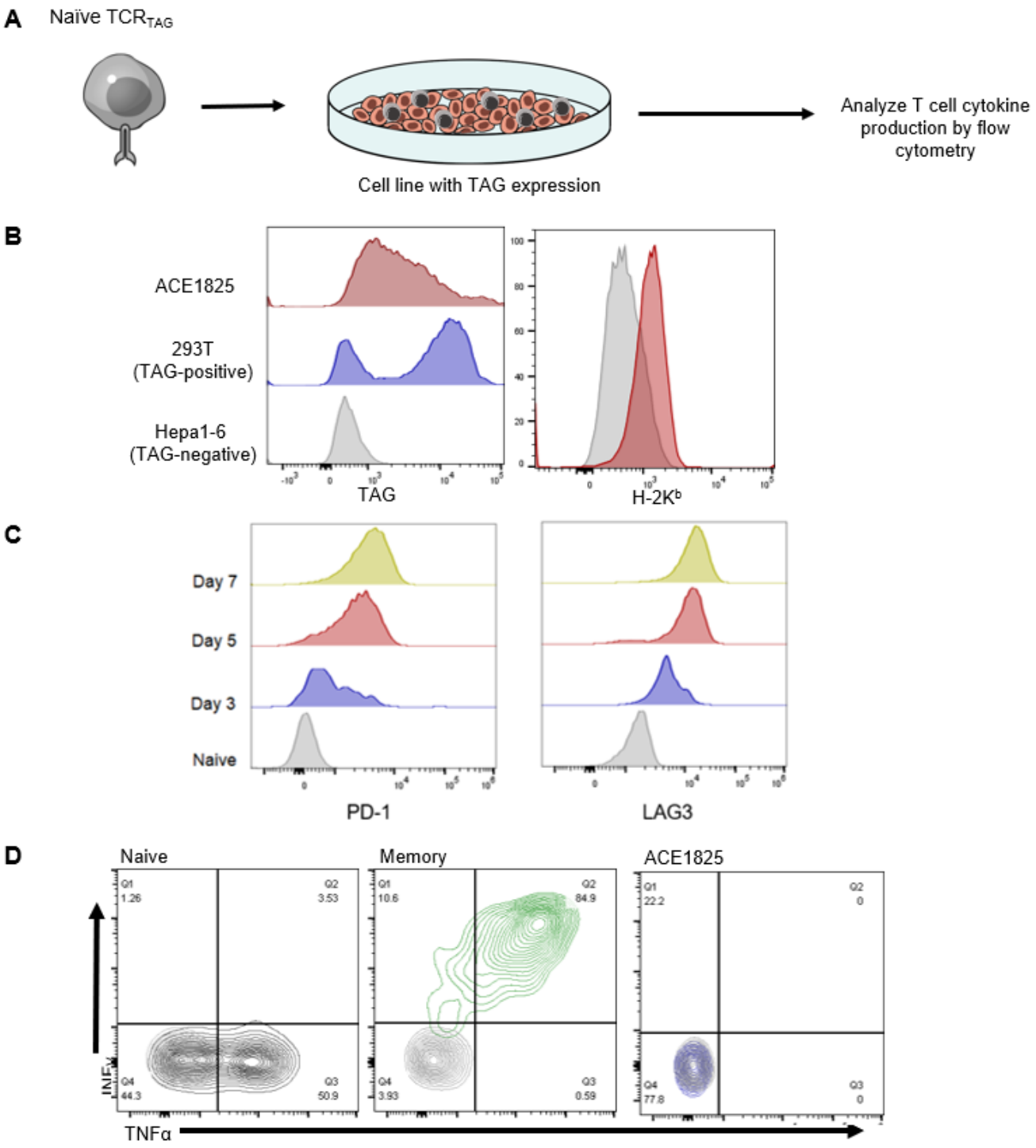

Figure 3.2| HCC mouse cell line to study *in vitro* CD8 T cell responses. A. Experimental scheme. **B.** ACE1825, a cell line derived from AST;Cre-ER^{T2} tumors, expresses TAG and MHC class I H-2K^b (MHC polymorphism on which TAG is presented) as compared to 293T and Hepa1-6 cell lines. **C, D.** TCR$_{TAG}$ co-cultured with ACE1825 upregulate inhibitory receptors PD1 and LAG 3 (**C**) and lose effector cytokine production (**D**) assessed by intracellular cytokine staining after 4-hour *ex vivo* TAG peptide stimulation).

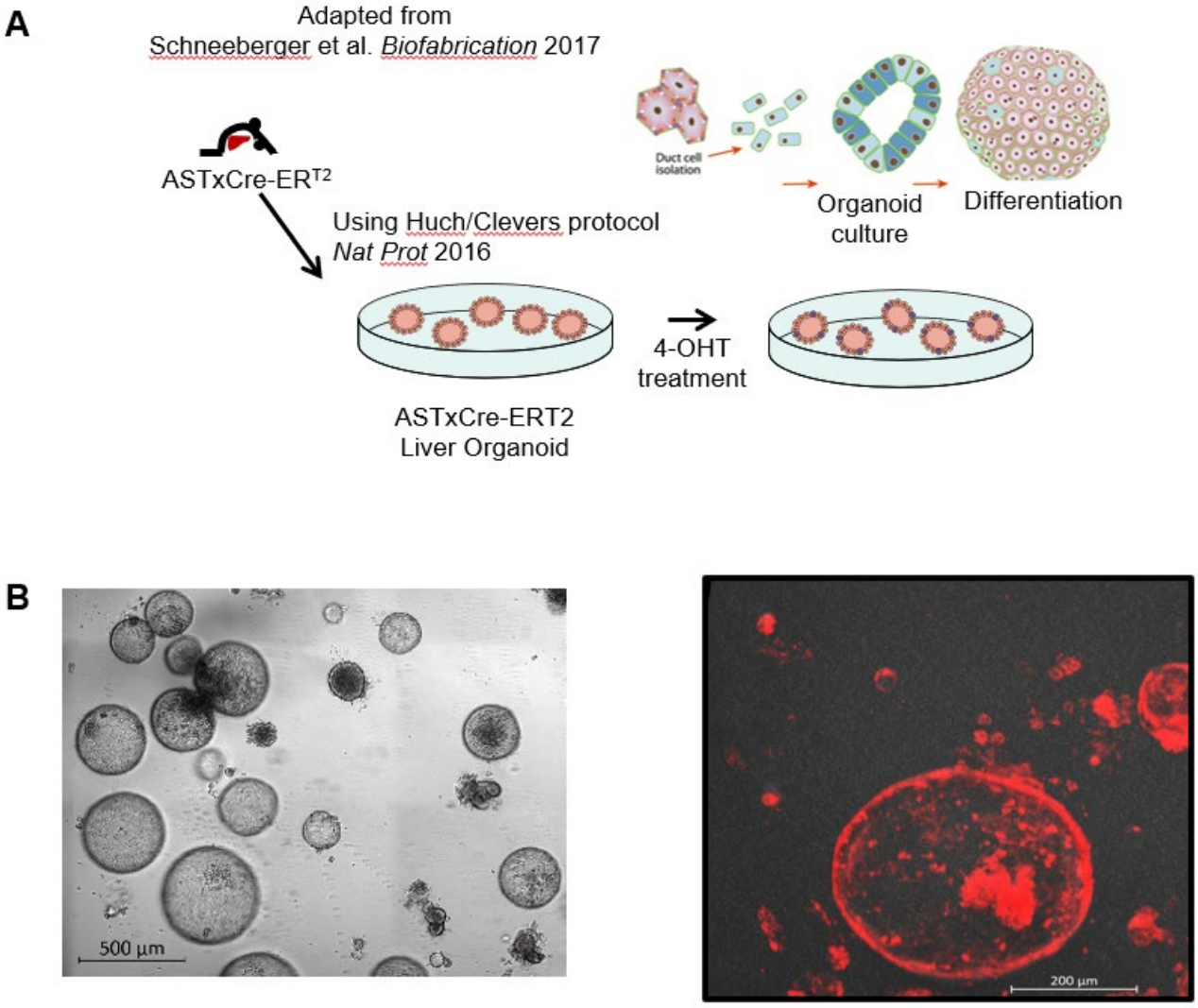

Figure 3.3| Liver organoids can be derived from liver ductal stem cells and then differentiated into functional hepatocytes. A. Methods from *Biofabrication* and *Nature Protocols* provide a way to culture liver primary cells. Organoids derived from the AST;Cre-ER^{T2} model can then be treated with TAM to induce TAG expression. **B**. Left, brightfield microscopy of liver ductal organoids. Right, confocal microscopy of liver ductal organoids expressing mTomato.

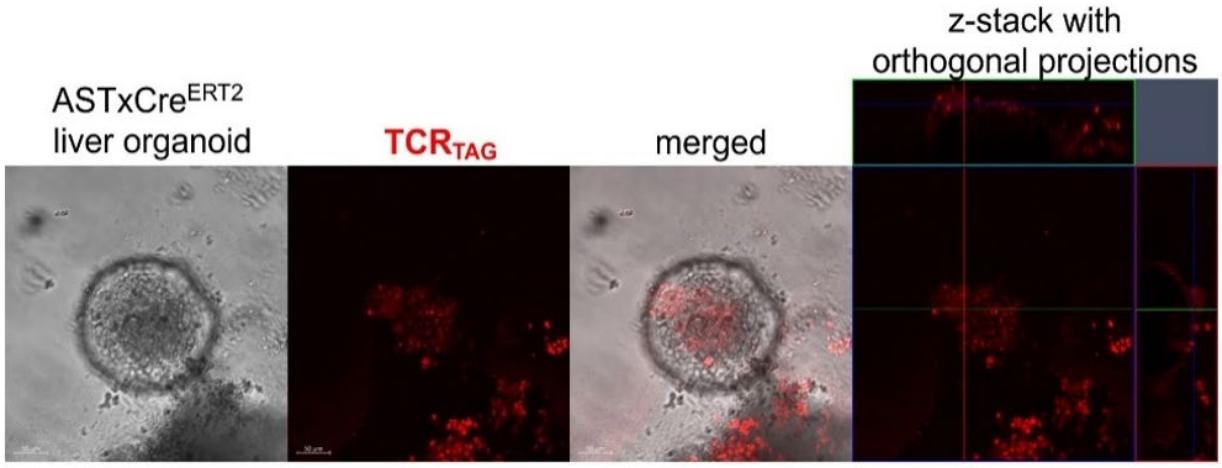

Figure 3.4| T cells can migrate into organoid Matrigel domes and contact liver cells. Confocal imaging of TAG peptide-pulsed AST;Cre-ER^{T2} organoids cultured with CellTracker Orange-labeled naïve TCR_{TAG} CD8 T cells. The rightmost panel shows z-stack with orthogonal projections showing that TCR_{TAG} in contact with cells on the exterior surface of the organoids. Scale bar (50μ).

should express albumin. In addition, we wanted to replicate our AST;Cre-ER^{T2} hepatocellular carcinoma model as closely as possible in the dish. Thus, we next sought to differentiate the stem cells within the liver ducts to hepatocytes to generate a mini-liver organoid.

The Clevers lab published the components they used in differentiating the ductal cells to hepatocytes (Huch et al. *Nature* 2013). Another group (Nusse) found that the use of TNFα improved the long-term expansion of hepatocellular organoids (Peng et al. *Cell* 2018). According to published protocol, we swapped out the basal medium with differentiation medium from either group for 15 days (**Table 4**). We then isolated RNA from these organoids to determine albumin expression for cell maturity and possible TAG expression by RT-qPCR. We also included RNA from a WT C57/BL6 liver and hepatocyte cell lines Hepa1-6 and ACE1825. Albumin expression in the two cell lines had approximately a log lower baseline albumin expression than a WT liver, suggesting that cultured cells may intrinsically express lower levels of albumin (**Fig 3.5**). However, organoids that had been cultured with or without the differentiation medium showed significantly lower albumin expression and showed no increase in albumin expression after culture with differentiation medium (**Fig 3.5**). Thus, in our hands, liver ductal stem cells could not be differentiated into albumin-expressing hepatocytes.

CONCLUSIONS

The ability to simplify the study of a tissue down to the most crucial components has been a huge advantage of organoid technology for research into the biology of the cells and tissue. Organoids provide a 3D aspect that traditional 2D culture cannot provide; for example, intestinal organoids can form crypts and villi as well as produce mucus, providing an invaluable *in vitro* model of the organ (Hofer and Lutolf *Nat Rev Mater* 2021).

We utilized this premise to create a liver organoid model using cells derived from our TAM-inducible liver cancer mouse model driven by the TAG oncogene. Since we have previously seen that TAG-specific T cells rapidly become dysfunctional *in vivo* before the establishment of a tumor microenvironment, we wanted to co-culture inducible liver cancer organoids with TAG-specific T cells to determine if recognizing an oncogene alone could drive CD8 T cell dysfunction, and if not, what components of the premalignant microenvironment were needed to push these T cells into dysfunction.

One of the key components of establishing liver organoids is the differentiation of the ductal stem cells to functional hepatocytes. We required the derivation of functional hepatocytes to 1) accurately model hepatocellular carcinoma in a dish and 2) drive the expression of the TAG oncogene, which is under the hepatocyte-specific Albumin promoter. This endeavor, however, proved difficult. We undertook several different methods to differentiate the ductal stem cells to hepatocytes, but we never observed an increase in albumin expression as compared to undifferentiated organoids and hepatocyte cell lines. Because the focus of our studies was intended to study the function and dysfunction of CD8 T cells, we turned to the lab's *in vivo* mouse models to ask whether the early T dysfunction is a form of self-tolerance.

Components	Role in media or differentiation	Hep-Medium Expansion (Peng et al. *Cell* 2018)	Hep-Differentiation (Broutier et al. *Nature Protocols* 2016)
Williams E	Base medium	+	-
Advanced DMEM/F-12	Base medium	-	+
1% penicillin/streptomycin	Culture antibiotics	+	
1% GlutaMAX	L-glutamine alternative, prevents ammonia generation	+	-
1% NEAA	Increase cell growth/viability	+	-
10 mM HEPES	Cell culture buffer	-	-
B27 supplement	Serum-free supplement	2%	1%
N2 supplement	Serum-free supplement	1%	1%
Noggin-conditioned medium	Bone Morphogenetic Proteins (BMP) signalling inhibitor	50 ng/mL (after 2nd passage)	-
Normocin	Culture antibiotics	0.2%	-
ChIR99021	Wnt activator	3 uM	-
N-acetylcysteine	anti-oxidant, prevents apoptosis	1.25 mM	-
nicotinamide	PARP inhibitor	10 mM	-
recombinant gastrin	CCK2 receptor agonist	-	10 nM
recombinant EGF	Activator of RAS, PKC pathways	25 ng/mL	50 ng/ml
recombinant human FGF7	Induction of MAPK, PI3K signaling	-	-
recombinant human FGF10	Induction of Ras-ERK, MAPK, PI3K, PKC signaling	-	-
recombinant human FGF19	activates mTOR, inhibits GSK3α/β	-	100 ng/ml
recombinant human HGF	Induction of Ras-ERK, PI3K signaling	50 ng/mL	25 ng/ml
TNFa	Activator of NF-kB	100 ng/mL	
A83-01	TGFβ inhibitor	1 μM	500 nM
DAPT	NOTCH inhibitor	-	10 uM
dexamethasone	Apoptosis inhibitor	-	30 uM
Y-27632	ROCK inhibitor	10 μM	-
BMP7	Activates BMP and Smad pathways	-	25 ng/ml

Table 4. Media components for ductal organoid differentiation to liver hepatocyte organoids

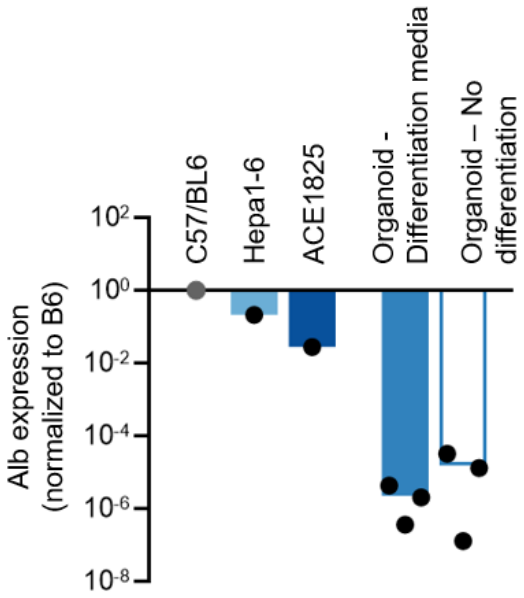

Figure 3.5| Organoids cultured in differentiation media do not express albumin. RT-qPCR of Albumin expression in Hepa 1-6 liver cancer cell line, ACE1825 AST;Cre-ER^{T2} cell line, organoids incubated in differentiation media, and organoids not incubated in differentiation media. Albumin expression is normalized to WT C57/BL6 liver expression.

CHAPTER IV

SELF-REACTIVE T CELLS STOP PROLIFERATING PREMATURELY AND ENTER A MEMORY-LIKE TCF1+ DYSFUNCTIONAL STATE

This chapter is adapted from “Self/tumor-reactive CD8 T cells enter a memory-like TCF1+ PD1- dysfunctional cell state” accepted in Cancer Immunology Research and has been reproduced in line with publisher policies.
Jessica J. Roetman**,** Megan M. Erwin, Michael W. Rudloff, Natalie R. Favret, Carlos R. Detrés Román, Minna K. I. Apostolova, Kristen Murray, Ting-Fang Lee, Youngmin A. Lee, Mary Philip. (2023), “Self/tumor-reactive CD8 T cells enter a memory-like TCF1+ PD1- dysfunctional cell state,” Accepted in Cancer Immunology Research

SUMMARY

T cells recognize several types of antigens in tumors, including aberrantly expressed, non-mutated proteins (self/shared-antigens; SSA) and mutated proteins or oncogenic viral proteins (tumor-specific antigens; TSA). Immunotherapies such as immune checkpoint blockade (ICB) can activate T cell responses against TSA, leading to tumor control, but also against SSA, causing immune related adverse events (IrAE). To improve anti-TSA immunity while limiting anti-SSA autoreactivity, we need to understand how tumor-specific CD8 T cells (TST) and SSA-specific CD8 T (SST) cells differentiate in response to cognate antigens during tumorigenesis. Therefore, we developed a novel genetic cancer mouse model in which we can track TST and SST differentiation longitudinally as liver cancers develop. We found that both TST and SST lost effector function, but while TST persisted long term and had a dysfunctional/exhausted phenotype (including expression of PD1, CD39, and TOX), SST exited cell cycle prematurely and disappeared from liver lesions. Interestingly, SST persisted in spleens in a TCF1+ PD1- state. Memory-like SST were not only unable to produce effector cytokines, but surprisingly, these TCF1+ SST failed to proliferate in response to anti-PD1/anti-PDL1 immune checkpoint blockade (ICB). Our studies identify a novel dysfunctional T cell state occupied by self/tumor-reactive T cells: a TCF1+ PD1- state lacking in effector function, demonstrating that the type/specificity of tumor antigen may determine tumor-reactive T cell differentiation.

INTRODUCTION

CD8 T cells can recognize and respond to tumor antigens arising from the aberrant expression of non-mutated genes (self/shared-antigens (SSA)); these antigens may also be expressed on non-cancerous/normal cells (reviewed in (Schietinger, Philip, and Schreiber *Semin Immunol* 2008; Leko and Rosenberg *Cancer Cell* 2020)). In addition to SSA, cancer cells often express tumor-specific antigens (TSA) caused by mutations unique to the tumor and not expressed on normal tissue. ICB can unleash anti-tumor T cell responses but also initiate immune related adverse effects (IrAE), mediated by self-reactive T cells (Postow, Sidlow, and Hellmann *N Engl J Med* 2018; Johnson et al. *Nat Rev Clin Oncol* 2022). Patients who experience ICB-induced IrAE have been shown to have better anti-tumor responses and survival (Petrelli et al. *J Immunother* 2020). Interestingly, the target tissue of IrAE can correlate with the cancer tissue origin, suggesting that T cells reacting against SSA in tumors also cause IrAE. For example, patients with melanoma are more likely to develop vitiligo (Rosenberg and White *J Immunother Emphasis Tumor Immunol* 1996; Byrne and Fisher *Cancer* 2017), while patients with lung cancer treated with ICB are more likely to develop pneumonitis (Nishino et al. *JAMA Oncol* 2016), likely due to T cell recognition of SSA expressed in normal and malignant lung tissue (Berner et al. *Sci Immunol* 2022).

Much of our understanding of the differentiation, fate, and molecular regulation of tumor-reactive T cells has come from studying preclinical cancer mouse models of CD8 T cell responses against TSA (reviewed in (Philip and Schietinger *Nat Rev Immunol* 2022)). Tumor-specific T cells (TST) differentiate to a dysfunctional (exhausted) state, lacking effector function, expressing multiple inhibitory receptors such as PD1 and CD39 (Thommen et al. *Cancer Immunol Res* 2015; Schietinger et al. *Immunity* 2016), and harboring characteristic transcriptional and epigenetic programs (Baitsch et al. *J Clin Invest* 2011; Philip et al. *Nature* 2017; Li et al. *Cell* 2019). In contrast, the fate of CD8 T cells reactive against self-antigens varies widely (reviewed in (Redmond and Sherman *Immunity* 2005; Schietinger and Greenberg *Trends Immunol* 2014;

Nussing, Trapani, and Parish *Front Immunol* 2020)). SSA-reactive T cells (SST) can remain ignorant of cognate antigen, undergo peripheral deletion, or be rendered anergic/self-tolerant, depending on antigen affinity, abundance/persistence, or tissue expression patterns (Redmond, Marincek, and Sherman *J Immunol* 2005; Schietinger et al. *Science* 2012; Bettini et al. *J Immunol* 2014; Smith et al. *J Immunol* 2014). Moreover, T cell responses to SSA may differ in tumors versus normal tissue as SSA might be distinctly regulated or presented in cancer cells. In addition, oncogenic transformation not only transforms cells but impacts inflammatory/immune signaling by transformed cells and surrounding stromal cells (reviewed in (Roetman, Apostolova, and Philip *Oncogene* 2022)). The unique tumor microenvironment, as compared to normal tissue, can impact CD8 T cell differentiation (Anderson, Stromnes, and Greenberg *Cancer Cell* 2017).

The dysfunctional TST population in tumor-bearing hosts is spatially heterogeneous, with progenitor/stem-like TST expressing the naive/memory-associated transcription factor TCF1 localizing to secondary lymphoid organs and tertiary lymphoid structures within tumors, and terminally-differentiated TCF1- dysfunctional/exhausted TST in the tumor parenchyma (reviewed in (Philip and Schietinger *Curr Opin Immunol* 2019; Tooley, Escobar, and Anderson *Trends Cancer* 2022)). In contrast, less is known about how SST differentiate in tumor-bearing hosts over time and in different tissues. Therefore, we developed a preclinical mouse model in which we could assess CD8 T cell responses to SSA and TSA in parallel in an autochthonous liver cancer model, in which tumors develop slowly over weeks to months. We found that both SST and TST lost effector function rapidly upon antigen encounter in hosts with progressing liver lesions. However, while TST persisted within progressing liver lesions, SST did not persist, in large part due to premature cell cycle exit. Unexpectedly, we found a population of persisting TCF1+ PD1- memory-like SST in the spleen, which were nevertheless unable to proliferate or produce effector cytokines even after ICB treatment. T cell dysfunction has mainly been associated with TCF1- terminally-differentiated T cells in tumors and during chronic infection, but

we now identify a novel TCF1+ PD1- nonfunctional CD8 differentiation state in SST in normal tissues and tumor-bearing hosts.

RESULTS

SST and TST lack effector function but have distinct immunophenotypes and persistence patterns

We previously developed an autochthonous mouse model of liver cancer (AST;Cre-ER^{T2}), in which we can study TST differentiation and function from the initiation of carcinogenesis onward (Schietinger et al. *Immunity* 2016). After a single dose of tamoxifen (TAM), AST;Cre-ER^{T2} hepatocytes undergo Cre recombinase-mediated induction of the SV40 large T antigen (TAG), under the control of the albumin promoter/enhancer. TAG acts as both an oncogene (inhibiting tumor suppressors TP53 and RB (Comerford et al. *Oncogenesis* 2012) to drive liver carcinogenesis), and a tumor-specific antigen (TAG=TSA). By 5-7 days post-TAM, most AST;Cre-ER^{T2} hepatocytes express TAG, and features of premalignant lesions are evident during the first 30-40 days post-TAM with development of full-blown hepatocellular carcinoma by 3 months (Fig. 2 of (Schietinger et al. *Immunity* 2016)). By adoptively transferring naive TAG epitope I-specific transgenic CD8 T cells (TCR$_{TAG}$) (Staveley-O'Carroll et al. *J Immunol* 2003) into AST;Cre-ER^{T2}, we can study TST responses throughout carcinogenesis. To compare TSA- to SSA-specific responses, we turned to a model of liver self-antigen developed by Phil Greenberg's lab: the Alb-GAG mouse (Alb-GAG) (Ohlen et al. *J Immunol* 2001). Alb-GAG express the Friend murine leukemia virus *gag* gene under control of the albumin promoter/enhancer, leading to hepatocyte-specific gPr75^{gag} protein (GAG=SSA) expression from birth on. Adoptively transferring GAG-specific transgenic CD8 T cells (TCR$_{GAG}$) (Ohlen et al. *J Exp Med* 2002) into Alb-GAG allows liver SSA responses to be studied.

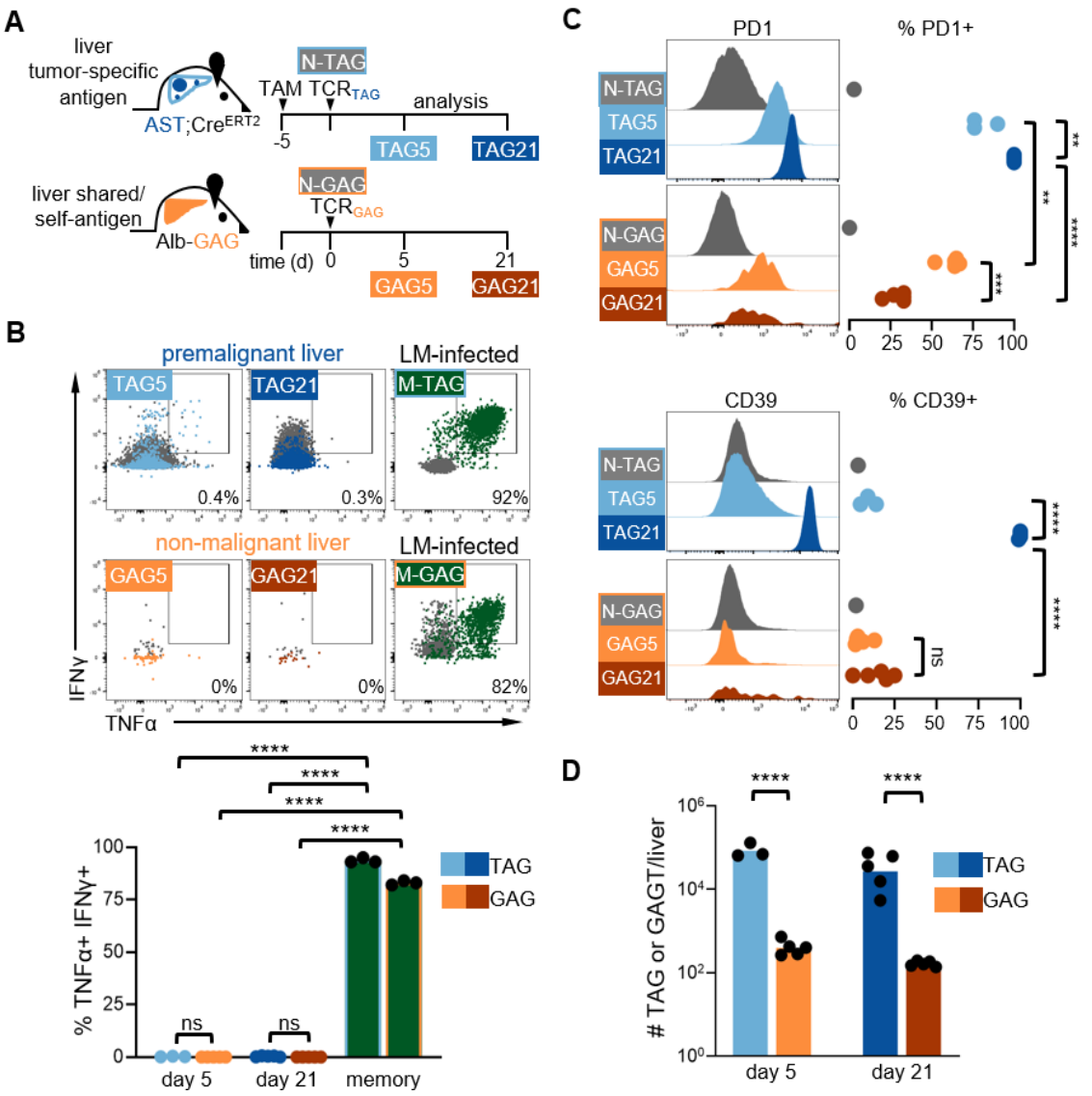

Figure 4.1| SST and TST lack effector function but have distinct immunophenotypes and persistence patterns. A. Experimental scheme: naive TCR_{TAG} (Thy1.1) were adoptively transferred into TAM-treated AST;Cre-ER^{T2} mice (Thy1.2), and naive TCR_{GAG} (Thy1.1) were adoptively transferred into Alb-GAG mice (Thy1.2). TCR_{TAG} (blue) and TCR_{GAG} (orange) were re-isolated from recipient livers 5 and 21 days later for flow cytometric analysis. **B**. Upper, TNFα and IFNγ production following 4h *ex vivo* peptide stimulation with % TNFα+ IFNγ+ shown in insets and lower graph. Memory TCR_{TAG} (M-TAG) and memory TCR_{GAG} (M-GAG) generated after *Listeria* infection (as in Fig. S1A; green) and no peptide-stimulated cells (gray) are shown for comparison. Each symbol represents an individual mouse. ns=not statistically significant, ****p<0.0001 (one-way ANOVA). **C.** Left, histograms of PD1 and CD39 expression. Right, % marker+ as compared to naive; each symbol represents an individual mouse. **p<0.01, ***p<0.001, ****p<0.0001 (one-way ANOVA). **D**. Absolute cell numbers recovered from liver. Each symbol represents an individual mouse. ****p<0.0001 (one-way ANOVA). Data is representative of three independent experiments. All flow plots are gated on live CD8+ Thy1.1+ cells, and flow data for each time point is concatenated from individual biological replicates. n=3-5 mice per group.

We adoptively transferred naive TCR_{TAG} into AST;Cre-ER^{T2} 5 days after TAM-treatment, just as premalignant lesions were beginning. In parallel, we transferred naive TCR_{GAG} into Alb-GAG and analyzed T cell numbers, cytokine production, and immunophenotype 5 and 21 days later (**Fig. 4.1A**). Both TCR_{TAG}/TST and TCR_{GAG}/SST were similarly unable to produce IFNγ and TNFα at 5 and 21 days (assessed by *ex vivo* re-stimulation with cognate peptide (TAG and GAG)) (**Fig. 4.1B**). While both TCR_{TAG}/TST and TCR_{GAG}/SST initially upregulated the activation/inhibitory marker PD1, TST continued to increase PD1 expression over time, while SST PD1 expression dropped at the later time point (**Fig. 4.1C**). By day 21 post-transfer, TST upregulated CD39, a marker of late/terminal T cell dysfunction/exhaustion (Gupta et al. *PLoS Pathog* 2015), whereas SST did not (**Fig. 4.1C**). TCR_{GAG} and TCR_{TAG} transferred into C57BL/6 mice (B6) infected with attenuated *Listeria monocytogenes* expressing either TAG (LM_{TAG}) or GAG (LM_{GAG}) epitopes (**Fig. 4.2A**) differentiated into highly functional effector and memory T cells, producing high levels of both IFNγ and TNFα (**Fig. 4.1B and 4.2B**), demonstrating that SST/TST functional deficits in AST;Cre-ER^{T2} and Alb-GAG were context-dependent. Notably, TCR_{GAG}/SST had markedly impaired persistence as previously observed (Morimoto et al. *J Immunol* 2007), with fewer SST found in non-malignant livers as compared to TST in premalignant livers at early and late timepoints (**Fig. 4.1D**).

We also carried out a peptide stimulation dose response (**Fig. 4.3**) and demonstrated that both TCR_{TAG} and TCR_{GAG} have functional avidity (EC_{50}) in the nanomolar range. The TAG EC_{50} was ~10^2 fold lower than GAG (**Fig. 4.3**). The higher functional avidity of the tumor-specific antigen TAG as compared to the SSA GAG is in line with what has been observed with human tumor antigens: a recent study found that the functional avidity of melanoma neoantigens/tumor-specific antigens was in the range of 0.1-100 nM, while self/shared antigens had EC_{50} ranging from 100 – 1000 nM (Oliveira et al. *Nature* 2021), similar to what we observed for TAG and GAG.

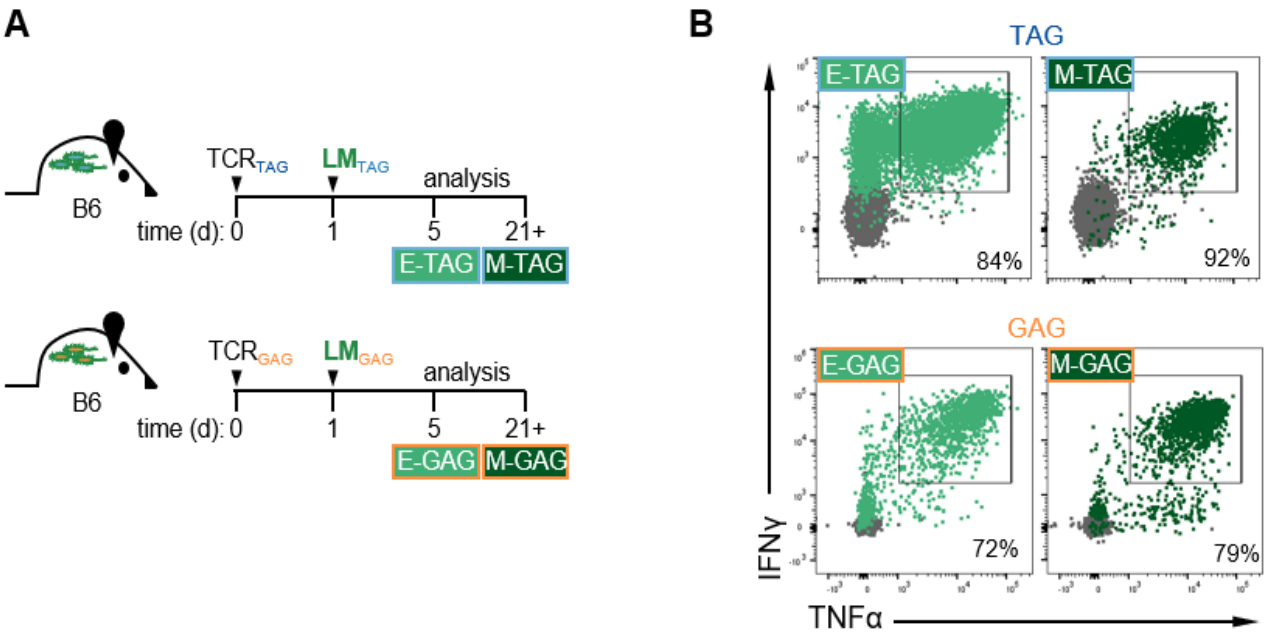

Figure 4.2| SST and TST are functional in the acute infection context. A. Experimental scheme: naive TCR_{TAG} (Thy1.1) or TCR_{GAG} (Thy1.1) were adoptively transferred into B6 immunized with *Listeria* expressing either TAG antigen (LM_{TAG}) or GAG antigen (LM_{GAG}). TCR_{TAG} and TCR_{GAG} were re-isolated from recipient spleens 5 (effector timepoint; E-TST and E-SST) and 21+ days (memory timepoint; M-TAG and M-GAG) later for flow cytometric analysis. **B**. TNFα and IFNγ production following 4h *ex vivo* peptide stimulation with % TNFα+ IFNγ+ shown in insets. No peptide-stimulated cells (gray) are shown for comparison.

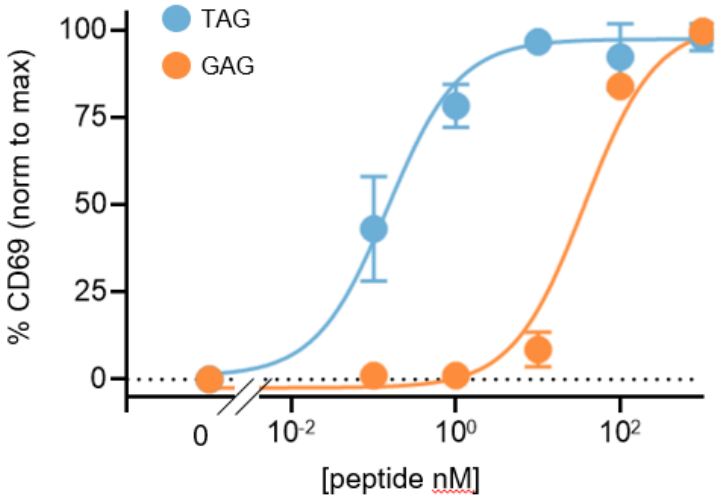

Figure 4.3| Naive TST and SST are activated in response to cognate peptide. Naive TCR_{TAG} (blue) and TCR_{GAG} (orange) splenocytes were stimulated *in vitro* for 48 hours with TAG and GAG peptide, respectively. % CD69+ in the CD8+ Thy1.1+ population is plotted versus cognate peptide concentration, normalized to min-max (non-linear regression).

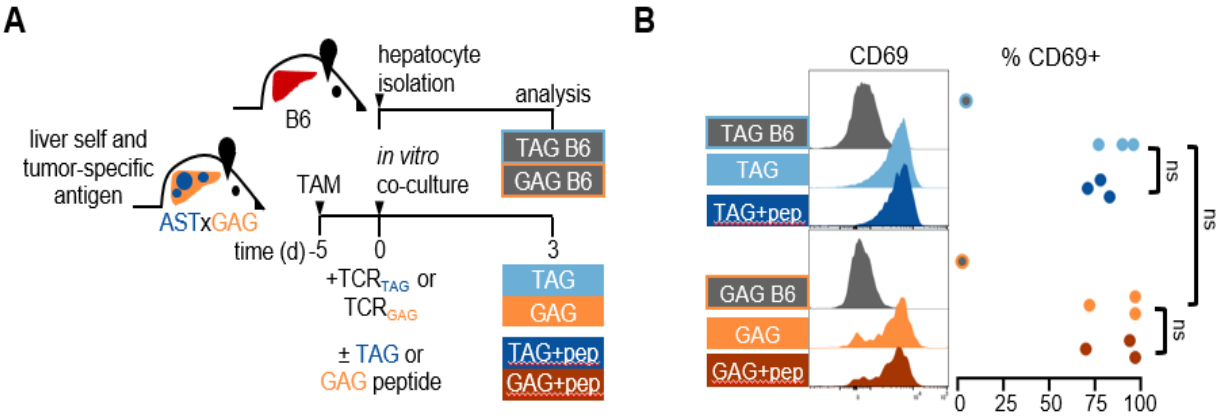

Figure 4.4| SST and TST upregulate CD69 upon co-culture with ASTxGAG hepatocytes. **A.** Experimental scheme: Hepatocytes from TAM-treated ASTxGAG or B6 were isolated, plated on collagen, and co-incubated *in vitro* with naive TCR_{TAG} (Thy1.1) or TCR_{GAG} (Thy1.1) for 3 days ± TAG and GAG peptide, respectively. TCR_{TAG} and TCR_{GAG} were analyzed by flow cytometric analysis. **B**. Left, Histograms of CD69 expression. Right, % marker+ as compared to naive; each dot represents an individual mouse, statistical testing by one-way ANOVA. Data pooled from two independent experiments. Flow plots gated on live CD8+ Thy1.1+ cells.

Oncogenic transformation does not impact SST differentiation or persistence

The improved persistence of TST in liver lesions as compared to SST in normal liver could be due to increased inflammation or other signals present in progressing tumors. To test this idea, we crossed AST;Cre-ER^{T2} to Alb-GAG to create ASTxGAG. In ASTxGAG, hepatocytes express GAG constitutively from birth and TAG only after TAM-induction. To confirm that both antigens were expressed, we isolated hepatocytes from TAM-treated ASTxGAG and B6, for control, and co-incubated them with naive TCR_{GAG} and TCR_{TAG} (**Fig. 4.4A**). Both TCR_{TAG} and TCR_{GAG} robustly upregulated CD69 in response to ASTxGAG but not B6 hepatocytes (**Fig. 4.4B**), demonstrating that TAM-treated ASTxGAG hepatocytes similarly activate TCR_{TAG} and TCR_{GAG}.

We transferred TCR_{TAG} and TCR_{GAG} into ASTxGAG (5 days post-TAM) and into B6 (antigen-free) (**Fig. 4.5A**). TCR_{TAG}/TST and TCR_{GAG}/SST rapidly lost the ability to produce effector cytokines in ASTxGAG mice (**Fig. 4.6A and B**), similar to what we observed in Alb-GAG and AST;Cre-ER^{T2} (**Fig. 4.5B**). Surprisingly, oncogene induction in ASTxGAG livers did not restore the numbers of TCR_{GAG}/SST to the level of TCR_{TAG}/TST (**Fig. 4.5B**). By day 21 post-transfer, few TCR_{GAG}/SST remained in ASTxGAG livers, though they did persist in the livers of antigen-free B6 (**Fig. 4.5B**), demonstrating that presence of the cognate GAG/SSA led to SST disappearance. TCR_{TAG}/TST expressed high levels of PD1 and TOX, a DNA-binding protein highly expressed in exhausted/dysfunctional CD8 T cells (Scott et al. *Nature* 2019b), while TCR_{GAG}/SST in the same premalignant environment only transiently expressed low levels of PD1 and TOX (**Fig. 4.5C**). In contrast, BCL2, a pro-survival/anti-apoptosis factor, was similarly downregulated at day 5 and upregulated at day 21 in both TST and SST (**Fig. 4.5D**), unexpected given the failure of TCR_{GAG}/SST to persist at day 21. However, fewer SST than TST were MKI67+ at days 5 and 14 (**Fig. 4.5D**), suggesting impaired proliferation by SST.

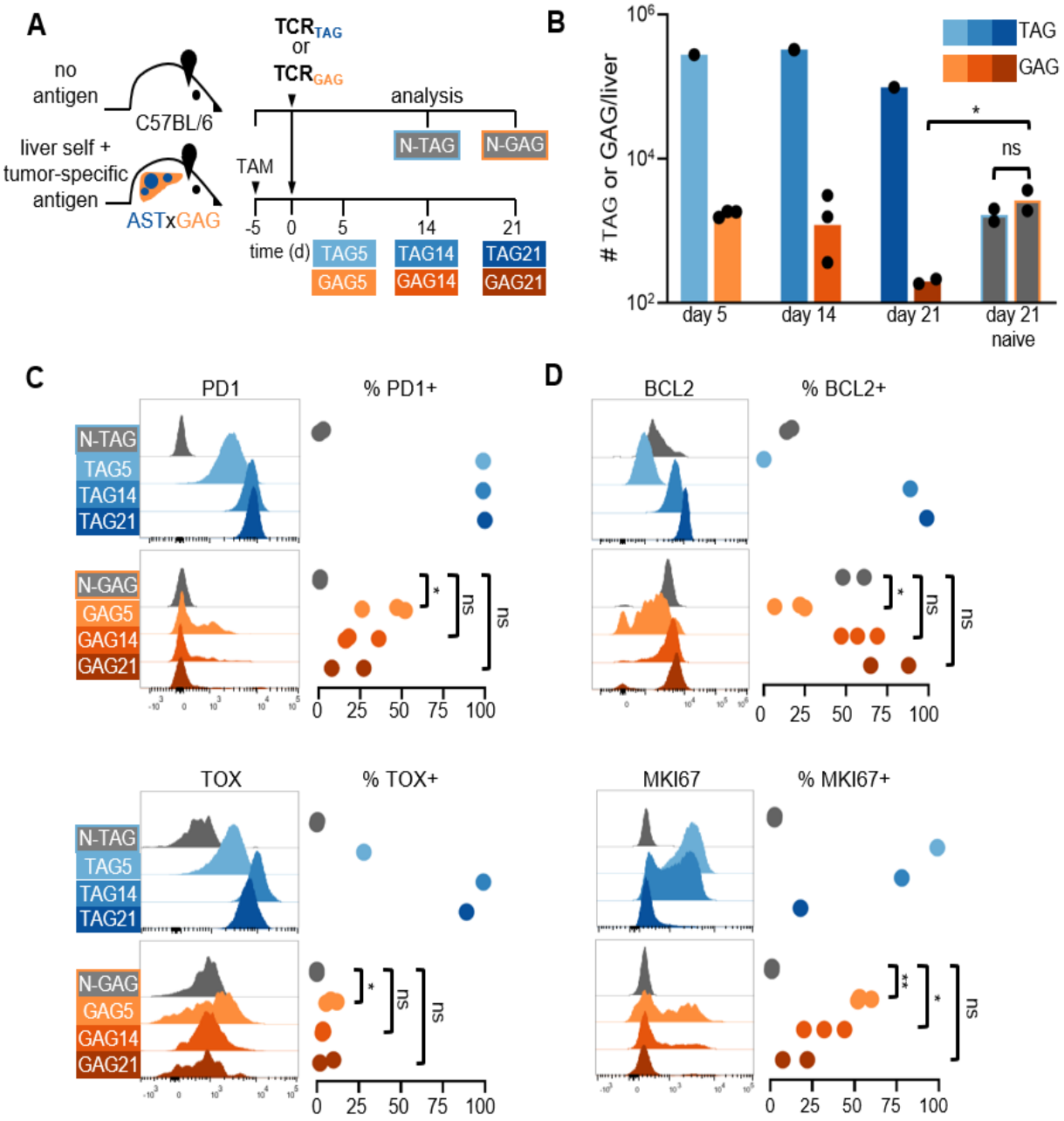

Figure 4.5| Oncogenic transformation does not impact SST differentiation or persistence. A. Experimental scheme: naive TCR_{TAG} (Thy1.1) or naive TCR_{GAG} (Thy1.1) were adoptively transferred into C57BL/6 (B6) (Thy1.2) or Alb-GAG;AST;Cre-ER^{T2} (ASTxGAG) mice (Thy1.2). TCR_{TAG} (blue) and TCR_{GAG} (orange) were re-isolated from recipient livers 5, 14, and 21 days later for flow cytometric analysis. **B**. Cell numbers recovered from livers. Each symbol represents an individual mouse. *p<0.05 (one-way ANOVA). **C**. Left, histograms of PD1 and TOX expression. Right, % marker+ as compared to naive; each symbol represents an individual mouse. *p<0.05 (one-way ANOVA). **D**. Left, histograms of BCL2 and MKI67 expression. Right, % marker+ as compared to naive; each symbol represents an individual mouse. *p<0.05, **p<0.01 (one-way ANOVA). Data representative of three independent experiments. All flow plots are gated on live CD8+ Thy1.1+ cells and flow data for each timepoint is concatenated from all biological replicates. n=1-3 mice per group.

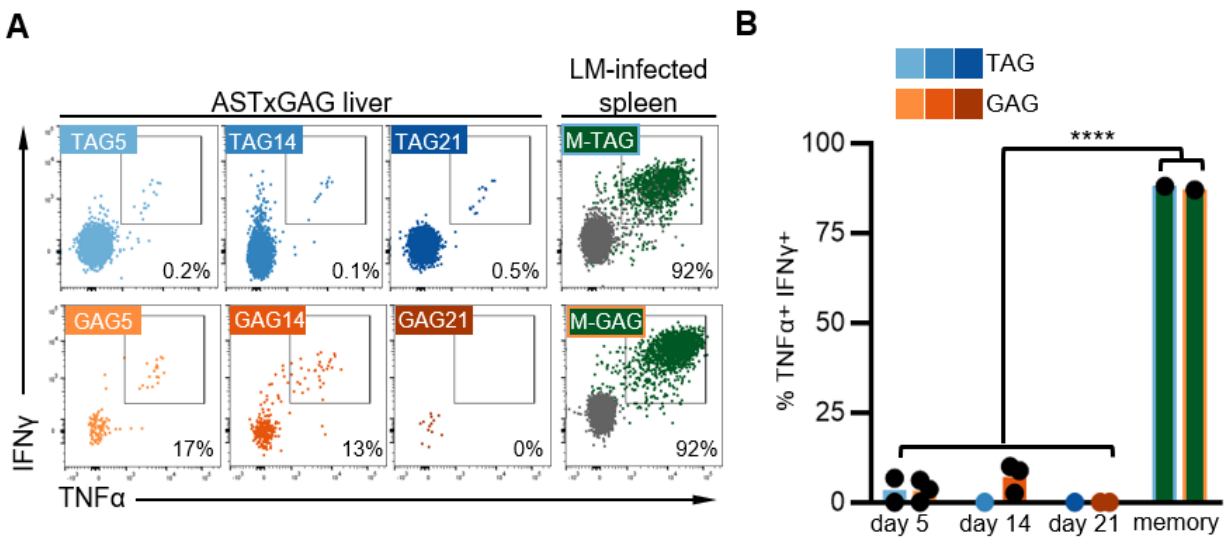

Figure 4.6| SST in ASTxGAG mice with premalignant liver lesions lose effector function. A. Naive TCR_{TAG} (Thy1.1) or naive TCR_{GAG} (Thy1.1) were adoptively transferred into B6 (Thy1.2) or Alb-GAG;AST;Cre-ER^{T2} (ASTxGAG) mice (Thy1.2) as in Fig. 2A. TCR_{TAG} (blue) and TCR_{GAG} (orange) were re-isolated from recipient livers 5, 14, and 21 days later for flow cytometric analysis. TNFα and INFγ production following 4h *ex vivo* peptide stimulation with % TNFa+ IFNg+ shown in insets. Memory TCR_{TAG} (M-TAG) and memory TCR_{GAG} (M-GAG) isolated from spleens of LM_{TAG} or LM_{GAG} infected-mice (as in Fig. S1; green) and no peptide-stimulated cells (gray) are shown for comparison. **B.** % TNFα+ IFNγ+ with each symbol representing an individual mouse. ****p<0.0001 (unpaired Student's t-test). All flow plots are gated on live CD8+ Thy1.1+ cells, and flow data for each time point is concatenated from 3 biological replicates, n=3 mice per group.

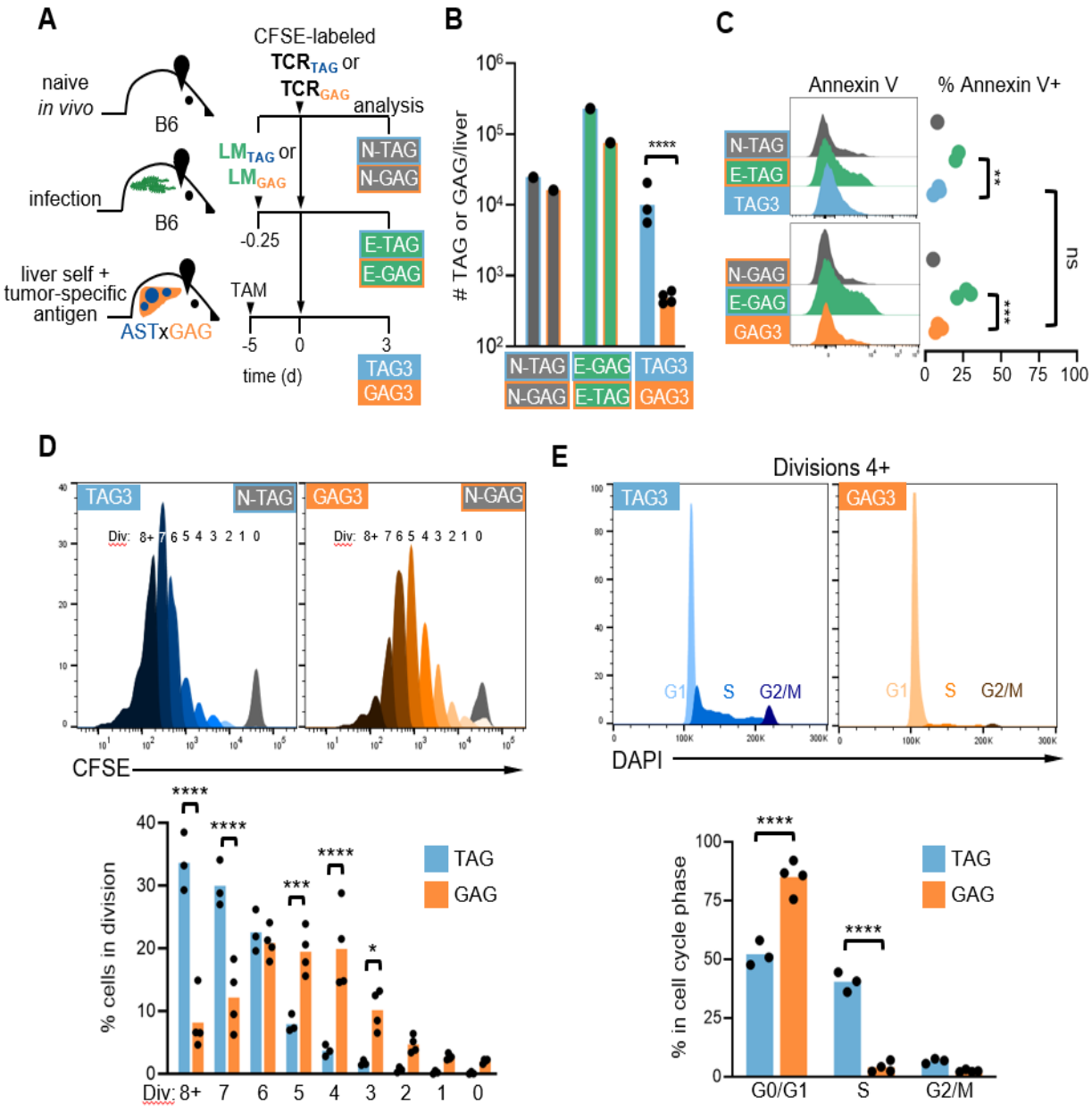

Figure 4.7| SST stop proliferating prematurely. A. Experimental scheme: naive TCR_{TAG} (Thy1.1) or naive TCR_{GAG} (Thy1.1) were adoptively transferred into *Listeria*-immunized B6 or TAM-treated ASTxGAG (Thy1.2). TCR_{TAG} (blue) and TCR_{GAG} (orange) were reisolated from recipient livers 3 days later for flow cytometric analysis. **B.** Cell numbers recovered from liver. Each symbol represents an individual mouse. ****p<0.0001 (one-way ANOVA). **C**. Left, histograms of Annexin V staining. Right, % Annexin V+ as compared to naive; each symbol represents an individual mouse. **p<0.01, ***p<0.001 (one-way ANOVA). **D**. Upper, CFSE histograms showing cell proliferation. Lower, percentage of cells by cell division. *p<0.05, ***p<0.001, ****p<0.0001 (two-way ANOVA). E. Upper, histograms of DAPI staining/DNA content in divisions 4+. Lower, % division 4+ cells in G1, S, G2 phase of cell cycle. ****p<0.0001 (two-way ANOVA). Data representative of four independent experiments. All flow plots are gated on live CD8+ Thy1.1+ cells and show data concatenated from all biological

SST stop proliferating prematurely

We next sought to determine why SST failed to persist in ASTxGAG. We labeled TCR_{TAG}/TST and TCR_{GAG}/SST with carboxyfluorescein succinimidyl ester (CFSE) and adoptively transferred CFSE-labeled T cells into untreated B6, LM_{TAG} or LM_{GAG}-infected B6, or ASTxGAG treated with TAM 5 days prior. TCR_{TAG} and TCR_{GAG} were reisolated from premalignant livers 3d post-transfer for flow cytometric analysis (**Fig. 4.7A**). Even at this early time point, fewer TCR_{GAG}/SST than TCR_{TAG}/TST were found in ASTxGAG livers (**Fig. 4.7B**). To assess cell death, we stained T cells with annexin V and DAPI and, surprisingly, found similar proportions of total apoptotic (Annexin V+), early apoptotic (Annexin V+), and late apoptotic (Annexin V+ DAPI+) SST and TST in the liver (**Fig. 4.7C and Fig. 4.8A, B**)**.** Notably, infection-activated TCR_{GAG} and TCR_{TAG} underwent apoptosis at a much higher rate than SST and TST in ASTxGAG (**Fig. 4.7C and Fig. 4.8A, B**), despite the fact that infection-activated TCR_{TAG} and TCR_{GAG} accumulated in higher numbers (**Fig. 4.7B)**. While apoptosis has been thought to be the main driver of deletional tolerance (Redmond and Sherman *Immunity* 2005), this has mainly been inferred from cell numbers (Redmond, Marincek, and Sherman *J Immunol* 2005) because quantifying apoptosis *in vivo* is challenging due to rapid clearance of apoptotic cells (Bahl et al. *J Virol* 2010).

Given the lack of correlation between apoptosis rates and persistence, we next examined proliferation by assessing CFSE dilution. TCR_{GAG}/SST were mainly found in earlier divisions (divisions 4-6), in contrast to TCR_{TAG}/TST, which accumulated in the later divisions (divisions 7-8+) (**Fig. 3D**). Given that SST failed to proliferate to the same extent as TST, we analyzed cell cycle distribution on later division TST and SST using DAPI/DNA content staining. While TST in cell divisions 4+ were actively cycling, as shown by the high proportion of TST in S and G2/M, SST were nearly all in G0/G1 (**Fig. 3E**). Thus, SST proliferated initially but stopped cycling prematurely, leading to decreased numbers of SST in the liver/tumor lesions.

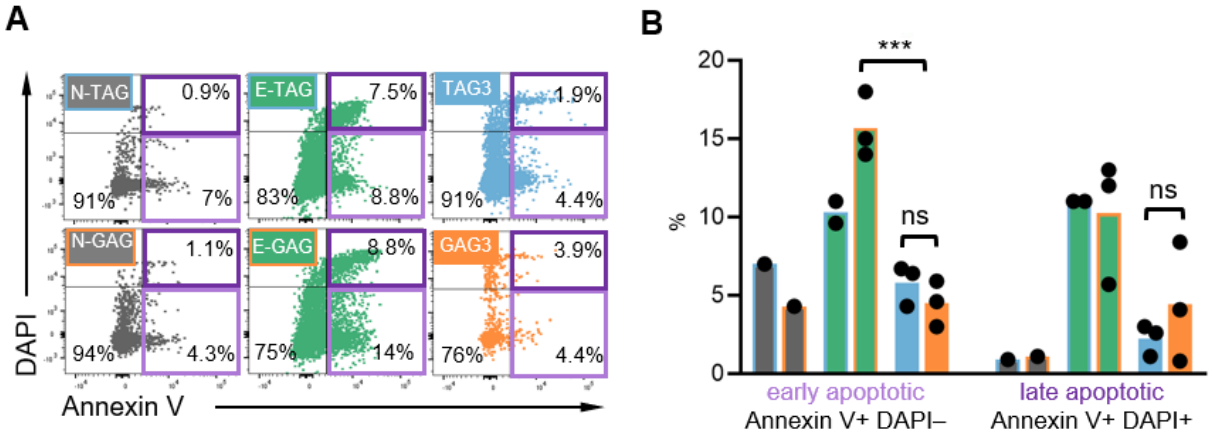

Figure 4.8| SST and TST undergo apoptosis at similar rates. A. Annexin V and DAPI staining on naive TCR_{TAG} (N-TST) and TCR_{GAG} (N-GAG) (gray), TCR_{TAG} (E-TAG) and TCR_{GAG} (E-GAG) activated during *Listeria* infection (green), TCR_{GAG} (orange) and TCR_{TAG} (blue) from ASTxGAG livers (as in Fig. 3A). **B.** % early apoptotic (Annexin V+ DAPI–) and late apoptotic (Annexin V+ DAPI+). Each symbol represents an individual mouse. ***p<0.001 (one-way ANOVA). All flow plots are gated on live CD8+ Thy1.1+ cells and data for each timepoint is concatenated from biological replicates. n=3 mice per group.

Persistent SST in the spleen are memory-like but lack effector function

Given the failure of TCR_{GAG}/SST to persist in normal and premalignant liver lesions, we next asked whether SST could home to and/or persist at other sites, including secondary lymphoid organs. We carried out adoptive transfers of TCR_{TAG}/TST and TCR_{GAG}/SST into *Listeria*-infected B6 or TAM-treated (5 days prior) ASTxGAG mice (**Fig. 4.9A**). 30 days post transfer, we recovered similar numbers of TST and SST from the spleens of ASTxGAG mice (**Fig. 4.9B**). TCR_{GAG}/SST in ASTxGAG spleens were immunophenotypically indistinguishable from memory TCR_{GAG} generated in LM_{GAG}-infected B6, having a central memory immunophenotype (CD44+ CD62L+) (**Fig. 4.10A**) with upregulation of IL7R/CD127, TCF1 (**Fig. 4.9C)**, and BCL2 (**Fig. 4.10B**), and low PD1, TOX (**Fig. 4.9C)**, and CD39 (**Fig. 4.10B**) expression. In contrast, TCR_{TAG}/TST in ASTxGAG spleens expressed high levels of PD1, TOX (**Fig. 4.9C**), and CD39 (**Fig. 4.10B)** and low levels of CD127 and TCF1 (**Fig. 4.9C**). Surprisingly, though TCR_{GAG}/SST in ASTxGAG spleens appeared memory-like, they were incapable of producing effector cytokines (**Fig. 4.9D**).

We next wanted to determine whether non-transgenic tumor-reactive CD8 T cells undergo similar differentiation as TCR_{TAG} /TST or TCR_{GAG} /SST. Given that endogenous TAG- or GAG-specific CD8 T cells are absent from ASTxGAG due to central tolerance (Ohlen et al. *J Immunol* 2001; Stahl et al. *Immunol Lett* 2009), we examined endogenous PD1+ CD8 T cells, enriched for T cells reactive to other tumor antigens (Gros et al. *J Clin Invest* 2014) arising in TAG-transformed hepatocytes. Notably, we found that endogenous PD1+ CD8 T cells were heterogeneous, including three subsets: TCF1+TOX- (similar to memory-like TCR_{GAG}/SST), TCF1+TOX1+ (similar to early TCR_{GAG}/SST or TCR_{TAG}/TST), and TCF1-TOX+ (similar to late TCR_{TAG}/TST) (**Fig. S5C, D**). These data suggest that some endogenous non-transgenic tumor-reactive PD1+ CD8 T cells also enter the TCF1+ memory-like state.

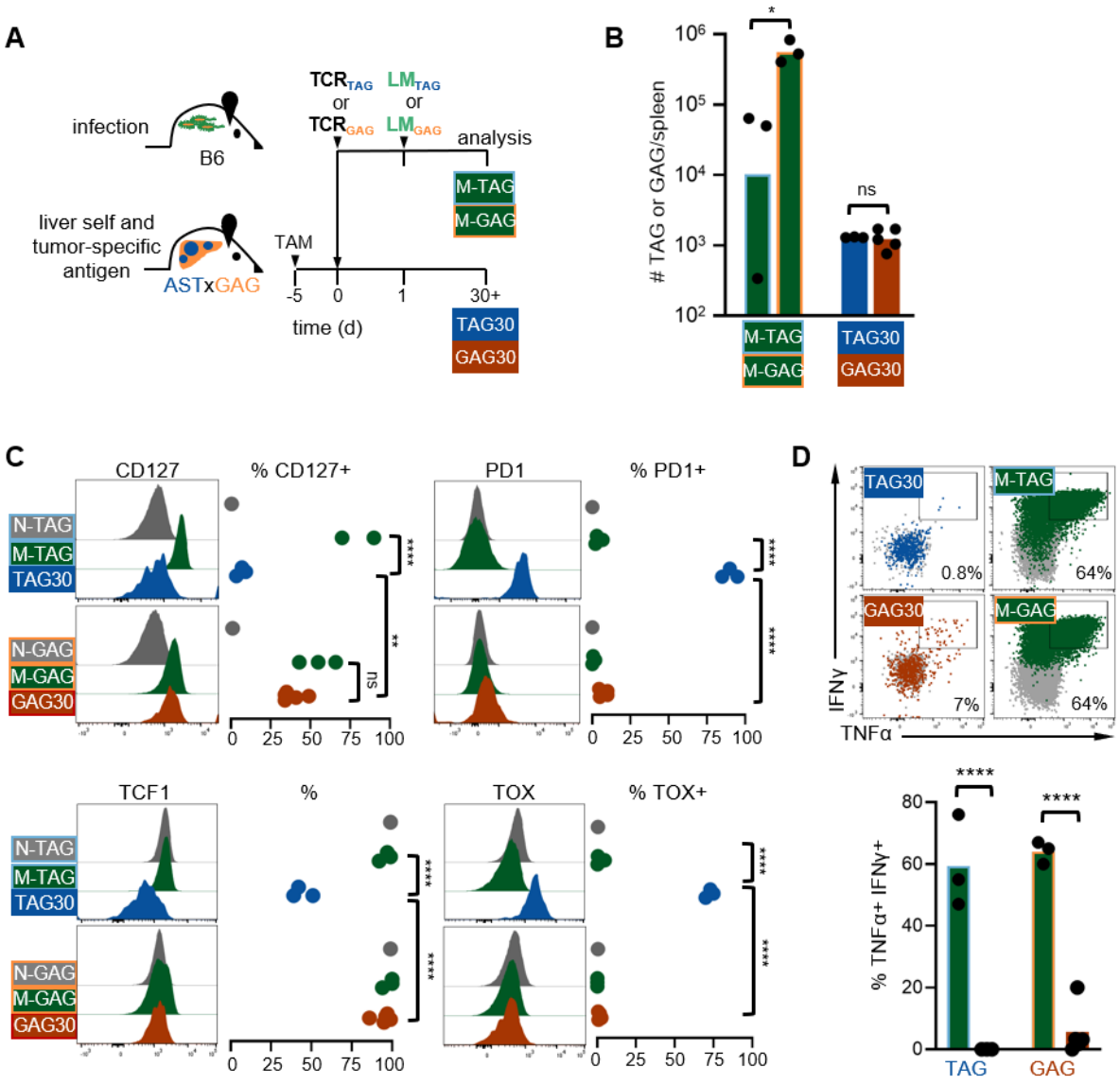

Figure 4.9| Persistent SST in the spleen are memory-like but lack effector function. A. Experimental scheme: naive TCR_{TAG} (Thy1.1) or naive TCR_{GAG} (Thy1.1) were adoptively transferred into *Listeria*-immunized B6 (memory) or into ASTxGAG (Thy1.2). TCR_{TAG} (blue) and TCR_{GAG} (orange) were re-isolated from recipient spleens 30+ days later for flow cytometric analysis. **B.** Absolute cell numbers recovered from spleen. *p<0.05 (one-way ANOVA). **C**. Left, histograms of CD127, TCF1, PD1, and TOX expression. Right, % marker+ as compared to naive; each dot represents an individual mouse. ***p*<0.01, *****p*<0.0001 (one-way ANOVA). **D**. Upper, TNFα and IFNγ production following 4h ex vivo peptide stimulation. Memory TCR_{TAG} (M-TAG) and memory TCR_{GAG} (M-GAG) generated after *Listeria* infection (as in Fig. S1A; green) and no peptide-stimulated cells (gray) are shown for comparison. % TNFα+ IFNγ+ shown in insets and lower graph. Each symbol represents an individual mouse. *****p*<0.0001 (one-way ANOVA). Data representative of at least two independent experiments. All flow plots are gated on live CD8+ Thy1.1+ cells, and flow data for each time point is concatenated from individual biological replicates. n=4-5 mice per group.

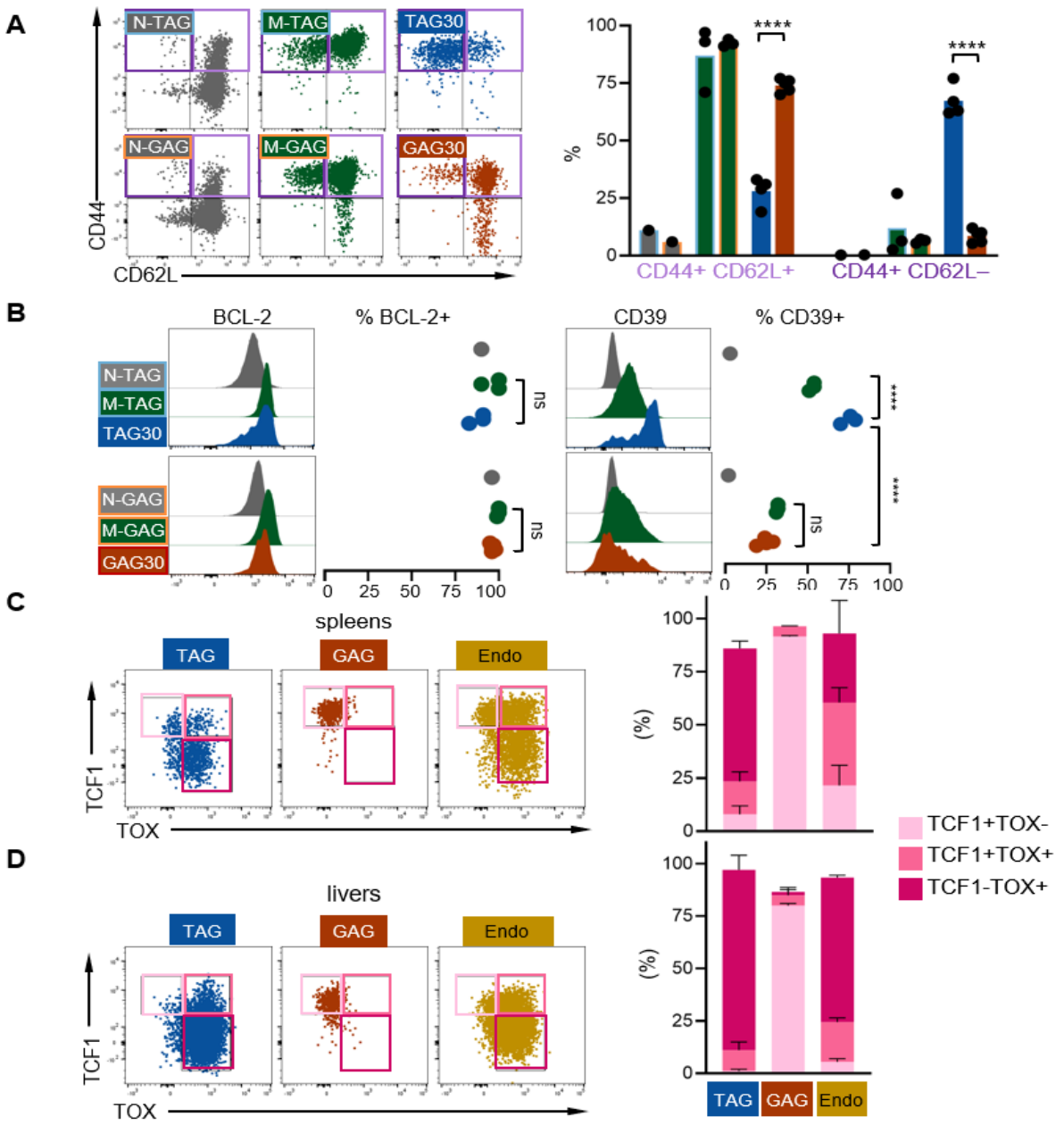

Figure 4.10| Persistent SST in spleens of tumor-bearing hosts have memory-like immunophenotype, and a subset of endogenous PD1+ CD8 T cells share the SST-like TCF1+TOX- profile. A. Left, CD44 and CD62L expression of naive (gray), memory (green) and TCR_{TAG}/TST (blue) and TCR_{GAG}/SST (orange) (as in Fig. 4A). Right, % CD44+CD62L+ and CD44+ CD62L–, each symbol represents an individual mouse. ****p<0.0001 (one-way ANOVA). **B**. Left, histogram BCL2, CD39 expression. Right, % marker+ as compared to naive; each dot represents an individual mouse. Naive (gray), memory (green), TST (blue), SST (orange). ****p<0.0001 (one-way ANOVA). **C, D**. Right, TCF1 and TOX expression of TCR_{TAG}/TST (blue), TCR_{GAG}/SST (orange), and endogenous PD1+ CD8 T cells (gold) in spleens (**C**) and livers (**D**). Left, % cells TCF1+TOX- (light pink), TCF1+TOX+ (pink), and TCF1-TOX+ (dark pink), bars show standard error of the mean (SEM). Data representative of two independent experiments. All flow plots are gated on live CD8+ Thy1.1+ cells, and data is concatenated from biological replicates. n=4-5 mice per group.

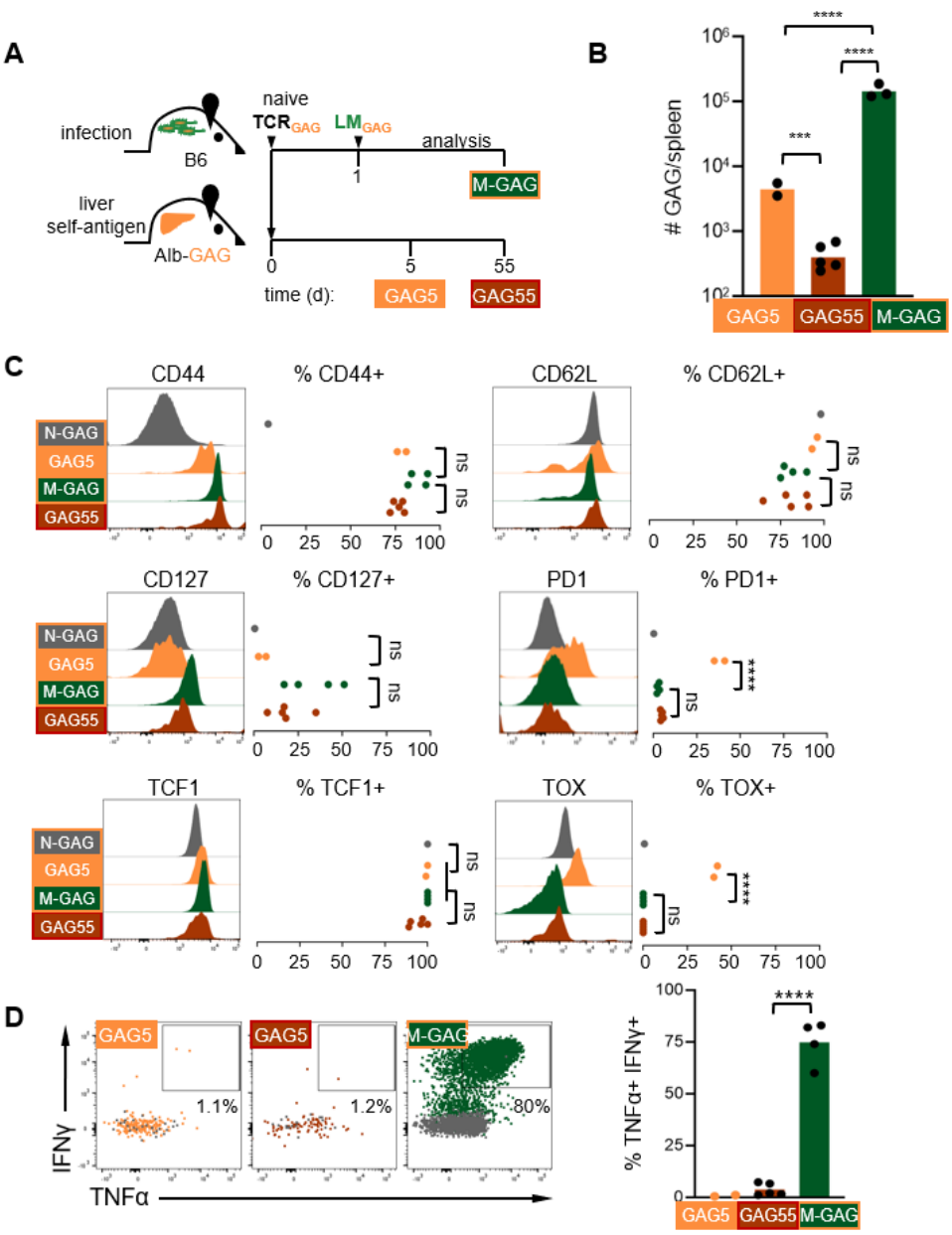

Figure 4.11| SST persisting in non-tumor bearing mice are memory-like but lack effector function. A. Experimental scheme: naive TCR_{GAG} (Thy1.1) were adoptively transferred into B6 infected with LM_{GAG} or into Alb-GAG (Thy1.2). TCR_{GAG} (orange and brown) were re-isolated from recipient spleens 5 and 55 days later for flow cytometric analysis. **B**. Absolute cell numbers recovered from spleen ***p<0.001, ****p<0.0001 (one-way ANOVA). **C**. Left, histograms of CD44, CD127, TCF1, CD62L, PD1, and TOX expression. Right, % marker+ as compared to naive; each dot represents an individual mouse. **D**. TNFα and IFNγ production following 4h *ex vivo* peptide stimulation with % TNFa+ IFNg+ shown in insets and graph on right. Each symbol represents an individual mouse. ****p<0.0001 (one-way ANOVA). Data representative of two independent experiments. All flow plots are gated on live CD8+ Thy1.1+ cells, and data for each time point is concatenated from biological replicates. n=2-5 mice per group.

To test whether the induction of the memory-like dysfunctional state was specific to premalignant/malignant hosts, we adoptively transferred TCR_{GAG} into Alb-GAG hosts and into LM_{GAG}-infected B6 (**Fig. 4.11A**). As late as 55 days post-transfer, memory-like dysfunctional SST were found in the spleens of Alb-GAG (**Fig. 4.11B**) expressing TCF1, CD44, CD62L, and CD127 (**Fig. 4.11C**), and unable to produce effector cytokines (**Fig. 4.11D**).

SST and TST have distinct underlying transcriptional programs

We next asked which transcriptional features were associated with this novel TCF1+ dysfunctional state and how they compared to TCF1- dysfunctional TST by using our previously described transcriptional profiling data obtained in late TCR_{TAG}/TST transferred into AST;Cre-ER^{T2} (Schietinger et al. *Immunity* 2016) and TCR_{GAG} into Alb-GAG hosts (Schietinger et al. *Science* 2012). We found that 628 probes mapping to 535 unique genes were differentially expressed in TCR_{TAG}/TST as compared to TCR_{GAG}/SST (**Fig. 4.12A**). Dysfunction/exhaustion-associated genes such as *Ctla4*, *Gzmk*, *Lag3*, *Epntpd1* (encoding CD39), and *Rgs16*, recently shown to promote inhibit ERK1 activation in exhausted T cells (Weisshaar et al. *Sci Immunol* 2022), were upregulated in TCR_{TAG}/TST (**Fig. 4.12A**). In contrast, genes associated with stem-like/progenitor T cell states and lymphoid homing (*Lef1*, *Tcf7* (encoding TCF1), *Sell* (encoding CD62L), *Ccr7*, *Klf2*, and *Bach2*) were upregulated in TCR_{GAG}/SST (**Fig. 4.12A**). We carried out Gene Set Enrichment Analysis (GSEA) (Mootha et al. *Nat Genet* 2003; Subramanian et al. *Proc Natl Acad Sci U S A* 2005) to identify pathways associated with TCR_{GAG} /SST and interestingly, found enrichment in genes associated with oxidative phosphorylation (**Fig. 4.12B**), also enriched in memory T cells and other quiescent T cells (Chapman, Boothby, and Chi *Nat Rev Immunol* 2020). TCR_{GAG}/SST were also enriched in gene sets associated with memory CD8 T cells (**Fig. 4.12C**) in contrast to exhausted or effector CD8 T cells gene sets, which were enriched in TCR_{TAG}/TST (**Fig. 4.12D**). Thus, while both TCR_{TAG}/TST and TCR_{GAG}/SST lack effector function

and are unable to prevent tumor outgrowth, the underlying transcriptional programs controlling their function and phenotype markedly differ.

TCF1+ memory-like SST do not respond to immune checkpoint blockade

In hosts with tumors and chronic infection, TCF1+PD1^{low} stem/progenitor-like exhausted CD8 T cells localized in secondary lymphoid organs and tertiary lymphoid structures preferentially proliferate and respond to anti-PD1/PDL1 ICB (He et al. *Nature* 2016; Im, Hashimoto, Gerner, Lee, Kissick, Burger, et al. *Nature* 2016; Utzschneider et al. *Immunity* 2016; Jansen et al. *Nature* 2019; Miller et al. *Nat Immunol* 2019; Siddiqui et al. *Immunity* 2019; Eberhardt et al. *Nature* 2021). Thus, we asked whether persistent TCF1+ memory-like SST would respond better to ICB than TCF1- TST. We co-transferred TCR_{TAG}/TST and TCR_{GAG}/SST into TAM-treated ASTxGAG mice (5 days post-TAM), waited 21+ days, by which point SST have entered the TCF1+ PD1-/low state, and treated ASTxGAG with combination anti-PD1/anti-PDL1 antibodies or isotype control (**Fig. 4.13A**). Surprisingly, not only did TCR_{GAG} fail to regain effector function in response to ICB (**Fig. 4.13B**), TCR_{GAG} did not significantly upregulate MKI67 in response to ICB (**Fig. 4.13C**), and we did not observe increased TCR_{GAG} numbers (**Fig. 4.13D**). TCR_{TAG} also failed to regain effector function in response to ICB (**Fig. 4.13B**), consistent to what we previously observed (Schietinger et al. *Immunity* 2016), though TCR_{TAG} did proliferate and show lower PD1 staining in ICB-treated ASTxGAG (**Fig. 4.13C**). Accordingly, we did not observe any slowing of ASTxGAG tumor progression, as measured by liver weight (**Fig. 4.13E**).

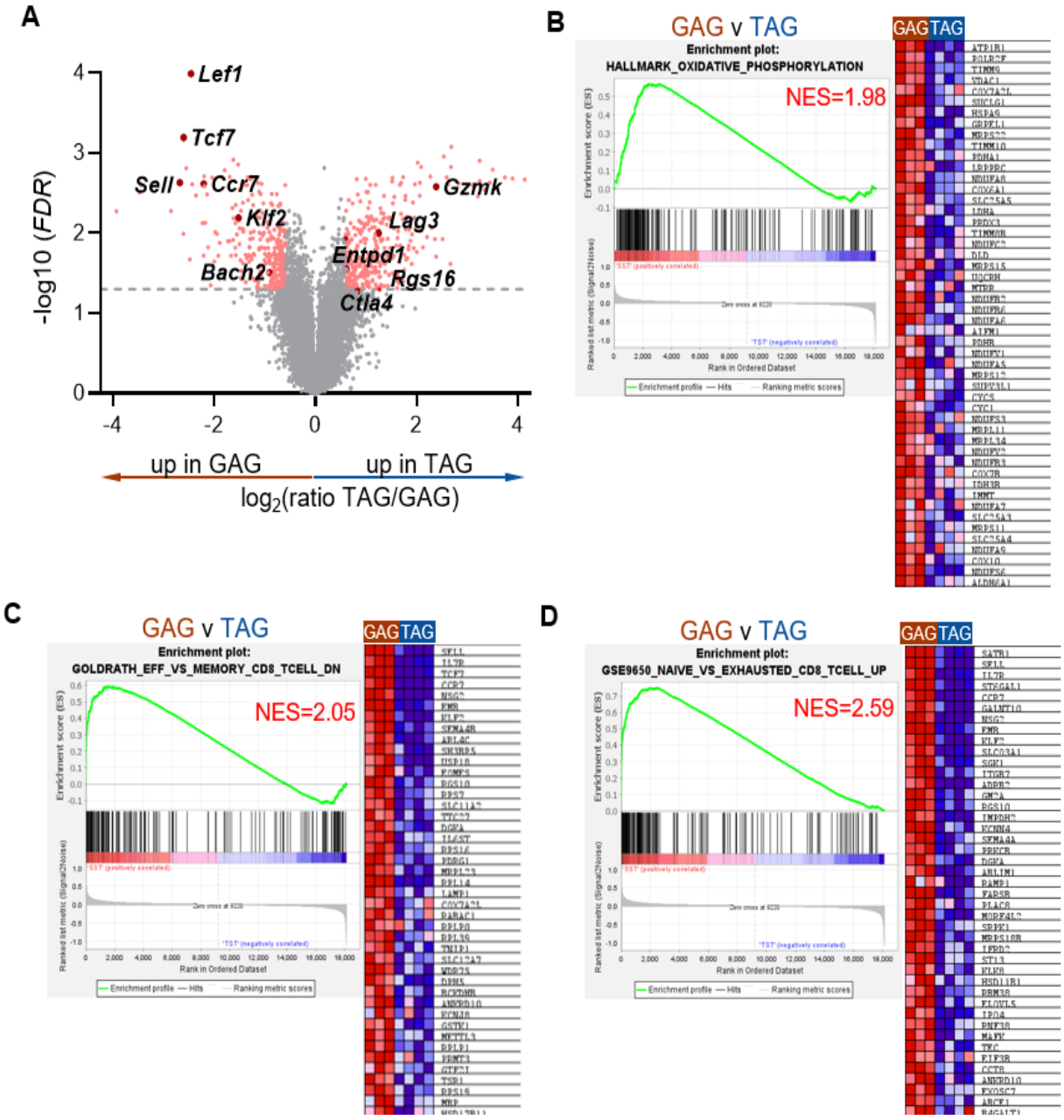

Figure 4.12| SST and TST have distinct underlying transcriptional programs. We analyzed our previously published Illumina microarray data obtained from TCR_{TAG} adoptively transferred into TAM-treated AST;Cre-ER^{T2} mice for 35 days (n=4; blue) [12] and from tolerant TCR_{GAG} from Alb-GAGxTCR_{GAG} (n=3, orange). **A.** Volcano plot showing differences in gene expression in TCR_{TAG} as compared to TCR_{GAG}. Each dot represents one probe, and dots colored in red had |log2 (ratio)| >0.585 (±1.5-fold) and false discovery rate (*FDR*; Benjamini-Hochberg) <0.05. 635 probes associated with 528 unique genes met significance criteria. Selected dysfunction/exhaustion genes upregulated in TCR_{TAG} or quiescence/lymphoid-homing genes upregulated in TCR_{GAG} are shown. For genes with multiple significant probes, the probe with highest -log10(*FDR*) is shown. **B,C,D**. Selected gene sets identified using Gene Set Enrichment Analysis are shown for the comparison of TCR_{TAG} versus $TCR_{GAG;}$ heatmaps shows the top 50 enriched genes from each gene set. NES=normalized enrichment score.

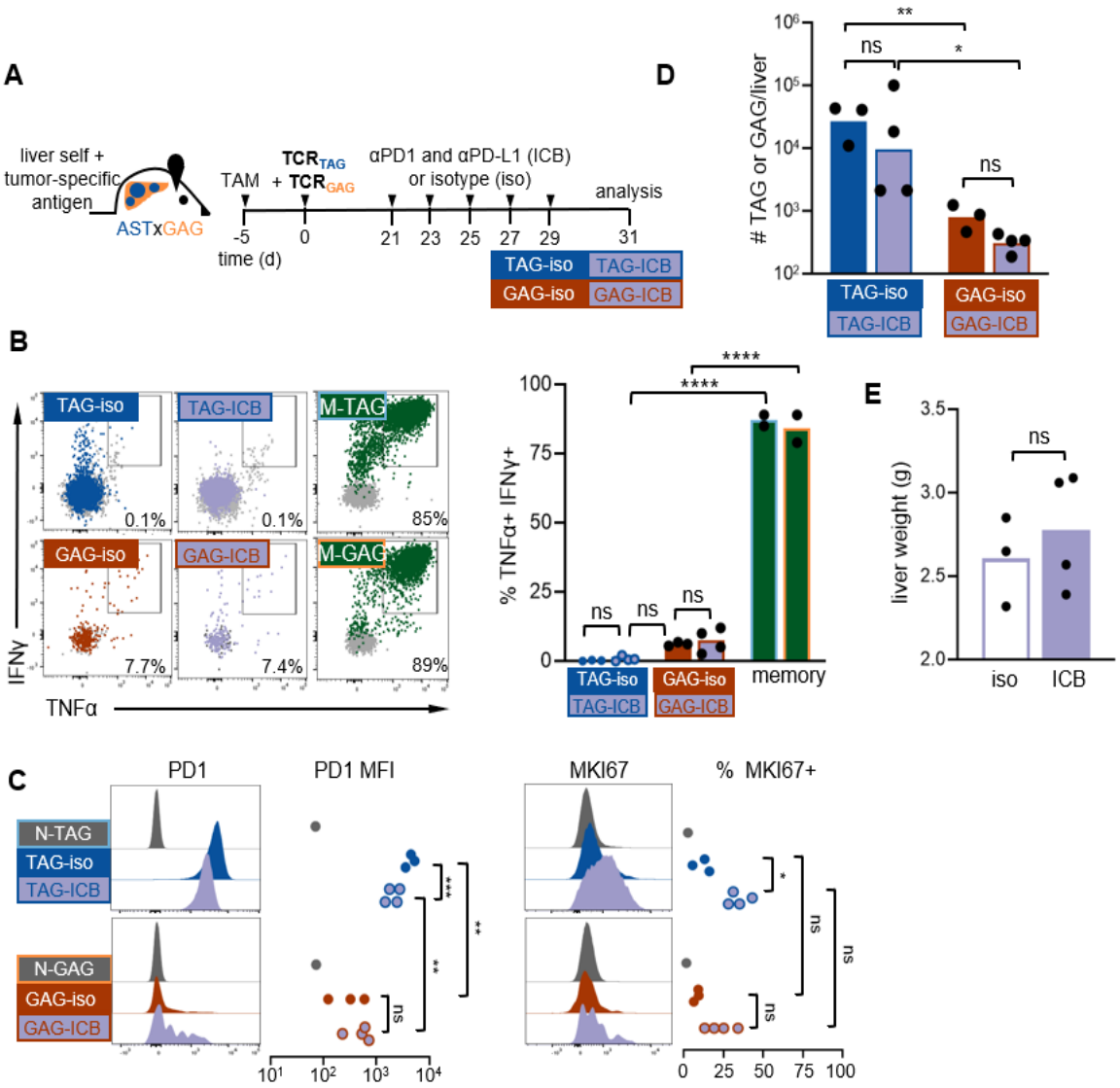

Figure 4.13| TCF1+ memory-like SST do not respond to immune checkpoint blockade. **A.** Experimental scheme: naive TCR_{TAG} (Thy1.12) and naive TCR_{GAG} (Thy1.1) were co-adoptively transferred into TAM-treated ASTxGAG (Thy1.2), and 21 days later, mice were treated with αPD1/PD-L1 antibodies in combination (ICB; purple) or isotype control antibody (iso) every other day. TCR_{TAG} (blue) and TCR_{GAG} (orange) were isolated from recipient livers 2 days following the final treatment for flow cytometric analysis. **B**. Left, TNFα and IFNγ production following 4h ex vivo peptide stimulation. Memory TCR_{TAG} (M-TAG) and memory TCR_{GAG} (M-GAG) generated after *Listeria infection* (as in Fig. S1A; green) and no peptide-stimulated cells (gray) are shown for comparison. % TNFα+ IFNγ+ shown in insets and graph. Each symbol represents an individual mouse. ****p<0.0001 (one-way ANOVA). **C**. Left, histograms of PD1 and MKI67 expression. Right, MFI or % marker+ as compared to naive; each dot represents an individual mouse. *p<0.05, **p<0.01, ***p<0.001 (one-way ANOVA). **D**. Absolute cell numbers recovered from liver. *p<0.05, **p<0.01 (one-way ANOVA). **E**. Liver weights (g) of ASTxGAG at analysis (36 days post-TAM; analyzed by unpaired t-test). Data representative of two independent experiments. All flow plots are gated on live CD8+ Thy1.1+ cells, and flow data for each time point is concatenated from individual biological replicates. n=3-4 mice per group.

To determine if the continued dysfunction was specific to tumor-bearing ASTxGAG hosts, we adoptively transferred TCR_{GAG}/SST into Alb-GAG and treated with anti-PD1/anti-PDL1 or isotype control after TCR_{GAG} had reached a memory-like timepoint (**Fig 4.14A**). As seen in ASTxGAG hosts, neither TCR_{GAG}/SST and endogenous T cells produced effector cytokines upon restimulation with GAG peptide (**Fig 4.14B**). Neither TCR_{GAG}/SST nor endogenous CD8+CD44+ T cells expresses PD1 in either group, as expected at a late timepoint for TCR_{GAG} (**Fig 4.14C**), and cell numbers did not increase with treatment of ICB (**Fig 4.14D**). Thus, despite the memory-like TCF1+ phenotype of SST, ICB treatment does not rescue their function.

The unexpected failure of TCF1+ TCR_{GAG}/SST to proliferate or regain effector function in response to ICB suggests that TCF1 expression and/or associated memory-like transcriptional and phenotypic programs are not sufficient to enable ICB-mediated T cell rescue.

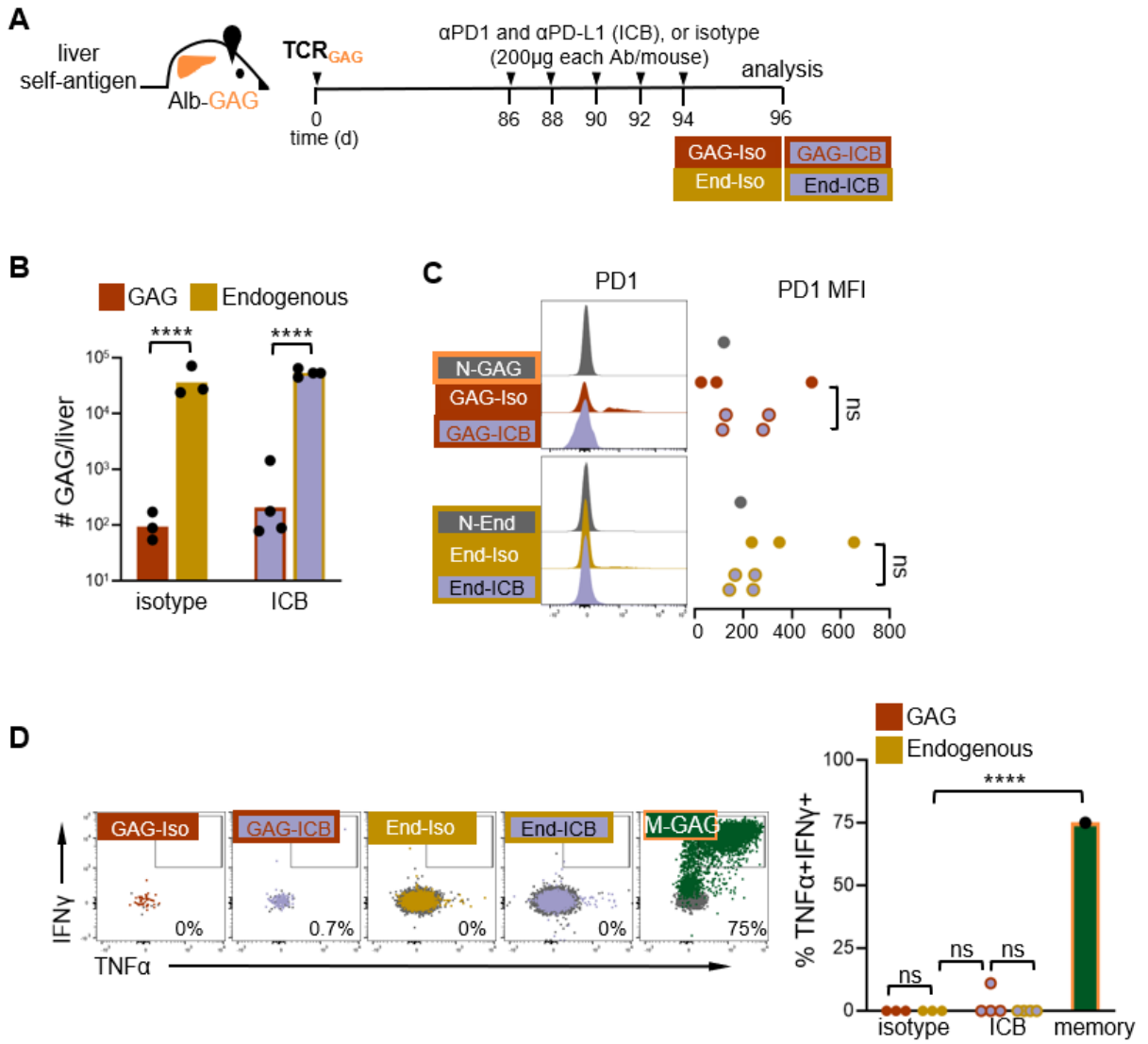

Figure 4.14| SST persisting in non-tumor bearing mice do not rescue with immune checkpoint blockade. A. Experimental scheme: naive TCR_{GAG} (Thy1.1) were adoptively transferred into Alb-GAG (Thy1.2). TCR_{GAG} (orange) and endogenous CD8+CD44+ (gold) were re-isolated from recipient spleens 5 and 55 days later for flow cytometric analysis. **B**. Absolute cell numbers recovered from spleen. ns=not significant, ****p<0.0001 (one-way ANOVA). **C**. Left, histograms of PD1 expression. Right, PD1 MFI as compared to naive level; each dot represents an individual mouse. ns=no significance (one-way ANOVA). **D**. Left, effector cytokine TNFα and INFγ expression following 4h *ex vivo* peptide stimulation (gray, no peptide control). Insets and graph at right shows % INFγ+TNFα+. Each symbol represents an individual mouse. ****p<0.0001 (one-way ANOVA). All flow plots are gated on live CD8+ Thy1.1+ cells, and data for each time point is concatenated from biological replicates. n=3-4 mice per group.

DISCUSSION

To characterize human tumor-reactive T cells from patients, where T cell specificities are usually unknown, researchers have adopted dysfunctional hallmarks identified from studying tumor-specific or viral-specific T cells, including expression of inhibitory receptors such as PD1 and CD39, downregulation of TCF1, and upregulation of TOX (van der Leun, Thommen, and Schumacher *Nat Rev Cancer* 2020; Tooley, Escobar, and Anderson *Trends Cancer* 2022). However, we now find that CD8 T cells specific for SSA enter a previously uncharacterized dysfunctional state immunophenotypically indistinguishable from central memory T cells. Persisting memory-like SST were CD44+ CD62L+ CD127+ TCF1+, and they did not express PD1, CD39, or TOX. Surprisingly, unlike classical memory T cells generated during acute infection, memory-like SST were unable to produce effector cytokines in response to stimulation with cognate antigen, similar to TCF1- TOX+ terminally-differentiated TST. Interestingly, we found that the endogenous tumor-reactive PD1+ CD8 T cell population in ASTxGAG was heterogeneous, with TCF1+TOX1-, TCF1+TOX+, and TCF1-TOX+ subsets present, suggesting that the TCF1+ memory-like state is not unique to TCR_{GAG} but present in T cells specific for other SSA/tumor antigens. In line with this, a recent study profiled the immunophenotype and specificity of tumor-reactive CD8 T cells in patients with melanoma and found that T cells with a memory-like phenotype (PD1-TCF1+TOX-) were present in tumors. These memory-like tumor-infiltrating T cells had specificity for patient-derived melanoma cells but also reacted to non-melanoma cells lines (Oliveira et al. *Nature* 2021), suggesting SSA-specificity. Thus, our findings on TCR_{GAG}/SST in the ASTxGAG model may be applicable to other tumor types and to human patients with cancer.

Our findings have important implications for cancer immunology, demonstrating that (i) tumor antigen type (TSA or SSA) can be an important determinant of tumor-reactive T cell differentiation, (ii) tumor-reactive T cells can lose effector function via classical exhaustion/dysfunction pathways

or through differentiation to a memory-like PD1-TCF+TOX- non-functional state, and (iii) the presence of dysfunctional/exhausted markers (PD1, CD39) or absence of functional/memory-associated transcription factors (TCF1) does not predict whether tumor-reactive CD8 T cells are functional.

Interestingly, CD8 T cell differentiation in response to SSA was conserved whether the antigen was expressed in the context of transformed hepatocytes or non-transformed hepatocytes, suggesting that CD8 T cell differentiation, functional status, and persistence are driven by the nature of the antigen (self/shared- versus tumor-specific) and not by the tumor microenvironment. The failure of self/shared-antigen-reactive T cells to persist has long been attributed to deletional tolerance (Redmond and Sherman *Immunity* 2005). To our surprise, we did not see an increase in the number of apoptotic SST as compared to either TST or to SST responding to their cognate antigen in the context of acute infection. Rather, SST failed to sustain the initial robust proliferation in response to antigen and exited cell cycle prematurely, in contrast to TST or infection-activated SST. Future studies are needed to determine the mechanism by which SST leave cell cycle prematurely while TST do not.

The important question arising is what drives the divergent differentiation paths of TST and SST in our model. Dysfunctional hallmarks such as PD1, CD39, and TOX, are driven by persistent TCR signaling in the setting of tumors or chronic viral infection and dependent on the transcription factor NFAT (Martinez et al. *Immunity* 2015). TCR_{GAG} encounter their cognate GAG antigen in both the spleen and liver of Alb-GAG mice, as suggested by the presence of early division TCR_{GAG} in both organs. However, TCR_{GAG} persisting in the spleen downregulate PD1, maintain TCF1 expression, re-express CD127 and BCL2, and harbor gene expression profiles of quiescent T cells, similar to CD8 T cell differentiation to the memory state during acute infection following pathogen/antigen clearance. Taken together, these findings suggest that SST are not receiving

persistent TCR stimulation, in contrast to TST. TCR_{GAG} may persist in an antigen-free or antigen-low niche within the spleen or other secondary lymphoid organs, though this remains to be investigated. Another determinant of T cell differentiation in tumors is TCR affinity/avidity (Shakiba et al. *J Exp Med* 2022). Comprehensive profiling of TCR affinity/avidity of TIL in patients with melanoma revealed that CD8 T cells specific for neoantigens had higher avidity than SSA specific T cells (Oliveira et al. *Nature* 2021). A recent study using a murine colorectal cancer model found that lower-affinity tumor-infiltrating CD8 T cells have a progenitor phenotype (TCF1+TOX-) while higher affinity T cells maintain a more exhausted phenotype (TCF1-TOX+) with higher proliferation (Hay et al. *Cancer Immunol Res* 2023). Future studies are needed to determine whether it is the lower affinity/avidity of SSA that skews responding T cells to a memory-like state, or whether other differences between SSA and TSA, such as tissue distribution or expression in secondary lymphoid organs, play a role.

Surprisingly, despite having a memory-like phenotype and TCF1 expression, SST failed to regain effector function or even proliferate in response to ICB. Another recent study in a murine lung cancer model found that even though lower-affinity CD8 T cells had a memory-like phenotype (TCF1+) as compared to higher-affinity CD8 T cells, they did not have improved responses to ICB (Burger et al. *Cell* 2021). The failure of SST/TCR_{GAG} to mediate anti-tumor or autoimmune effects with ICB in ASTxGAG demonstrates that TCF1 expression alone does not predict responsiveness to ICB, but it does leave the question open as to why some patients with SST go on to develop irAE after ICB therapy. A recent large retrospective analysis of patients treated with pembrolizumab (anti-PD1) found that those diagnosed with infection were 80% more likely to develop an immune-related adverse event (irAE), though it was not possible to establish whether the infection preceded the irAE or vice versa (Makunts et al. *PLoS One* 2022). Another study in mouse tumor models showed that dendritic cell production of IL12 was required for successful ICB-mediated T cell responses (Garris et al. *Immunity* 2018), suggesting that concurrent

inflammation or infection may determine whether ICB unleashes SST-mediated autoimmune and/or anti-tumor responses. Work from our group suggests that there is a “Goldilocks” range for T cell affinity, in which too high affinity leads to dysfunction while too low affinity induces not dysfunction but functional inertness (Shakiba et al. *J Exp Med* 2022). Lower affinity memory-like SST may not proliferate in the presence of ICB alone but require inflammatory cytokines/dendritic cell priming to push them over the proliferation/effector differentiation threshold.

While many studies have focused on the impact of ICB on tumor-specific CD8 T cell responses in murine cancer models, the ASTxGAG system, in which we can concurrently study tumor-specific and self/shared-antigen specific CD8 T cell responses, allows for the study of ICB-induced anti-tumor responses and irAE. In future studies with the ASTxGAG and similar models, we can dissect antigen-dependent determinants of CD8 T cell differentiation in tumors and determine what regulates ICB efficacy and toxicity.

CHAPTER V

MECHANISMS AFFECTING SELF SPECIFIC T CELL FAILURE TO PERSIST

OVERVIEW

The lack of T cell persistence is an important aspect of peripheral tolerance and the prevention of autoimmunity. However, self-specific T cells that can recognize self-antigen overexpressed on tumors represent an untapped potential for immunotherapies. In the previous chapter, self-specific T cells (SST) in the novel ASTxGAG featuring liver self/shared tumor antigen failed to persist in comparison to tumor neoantigen-specific T cells (TST), regardless of a tumor environment or not. Further probing revealed that SST initially activate and proliferation upon recognition of cognate antigen, but prematurely leave cell cycle after only a few divisions. SST do not undergo increased apoptosis in comparison to TST. This observation suggests that the nature of the antigen affects downstream TCR signaling that influences T cell persistence, proliferation, and/or survival. Thus, we asked several questions in regards to T cell persistence and proliferation to determine the cause of this premature cell cycle exit: lack of optimal priming, failure to express TOX, self-antigen as a tumor antigen, and lower levels of tumor antigen.

RESULTS

Optimal priming of liver self-antigen-specific T cells provides an initial, transient boost in proliferation

To determine if the lack of persistence is due to suboptimal priming of SST, we infected Alb-GAG mice with *Listeria* expressing the GAG antigen (LM_{GAG}) or empty *Listeria* (LM_0) 12 hours before adoptively transferring SST (**Fig 5.1A**). At 3 days post-transfer, the presence of LM_0 allowed SST in both wild-type and Alb-GAG mice to divide more than those without LM_0; however, without the expression of cognate antigen, SST exited cell cycle as previously seen (**Fig 5.1B and 5.1C**). SST within Alb-GAG that had received LM_{GAG} were cycling more than those in Alb-GAG without

LM_{GAG} and were able to continue proliferation with an increase in cell numbers. However, after two weeks, SST were not cycling and had consistent numbers between the two groups (**Fig 5.1D**). Thus, the optimal priming provided by LM_{GAG} is transient, and the signal SST receive to leave cell cycle is dominant over those signals in an acute infection.

TOX overexpression does not rescue liver self-specific T cell persistence

TOX is a DNA binding factor that is required for T cell differentiation during chronic antigen stimulation, such as in tumors or chronic infection (Scott et al. *Nature* 2019a; Khan et al. *Nature* 2019; Wang et al. *J Hepatol* 2019). In these settings, TOX is required for T cell survival and sustained expression of inhibitory receptors, and we have previously seen that TCR_{TAG} upregulate TOX in the tumor environment (Scott et al. *Nature* 2019a). The lack of sustained TOX expression in TCR_{GAG} and the high levels of TOX in TCR_{TAG} (**Fig 4.2B**) led us to hypothesize that TOX plays a role in the lack of TCR_{GAG} persistence and subsequent deletion.

We transduced TCR_{GAG} with a retroviral vector to overexpress TOX-EFGP in TCR_{GAG} and adoptively transferred these T cells into Alb-GAG mice along with EGFP-expressing control TCR_{GAG} **(Fig 5.2A).** TCR_{GAG} overexpressing TOX in WT mice had higher cell numbers than EGFP control counterparts, indicating that TOX played a role in T cell survival (**Fig 5.2C**). Surprisingly, however, TCR_{GAG} within Alb-GAG mice had no significant cell number difference whether they received TOX overexpression or control (**Fig 5.2B**). This finding indicates that the survival signals induced by TOX are not enough to overcome the tolerance phenotype.

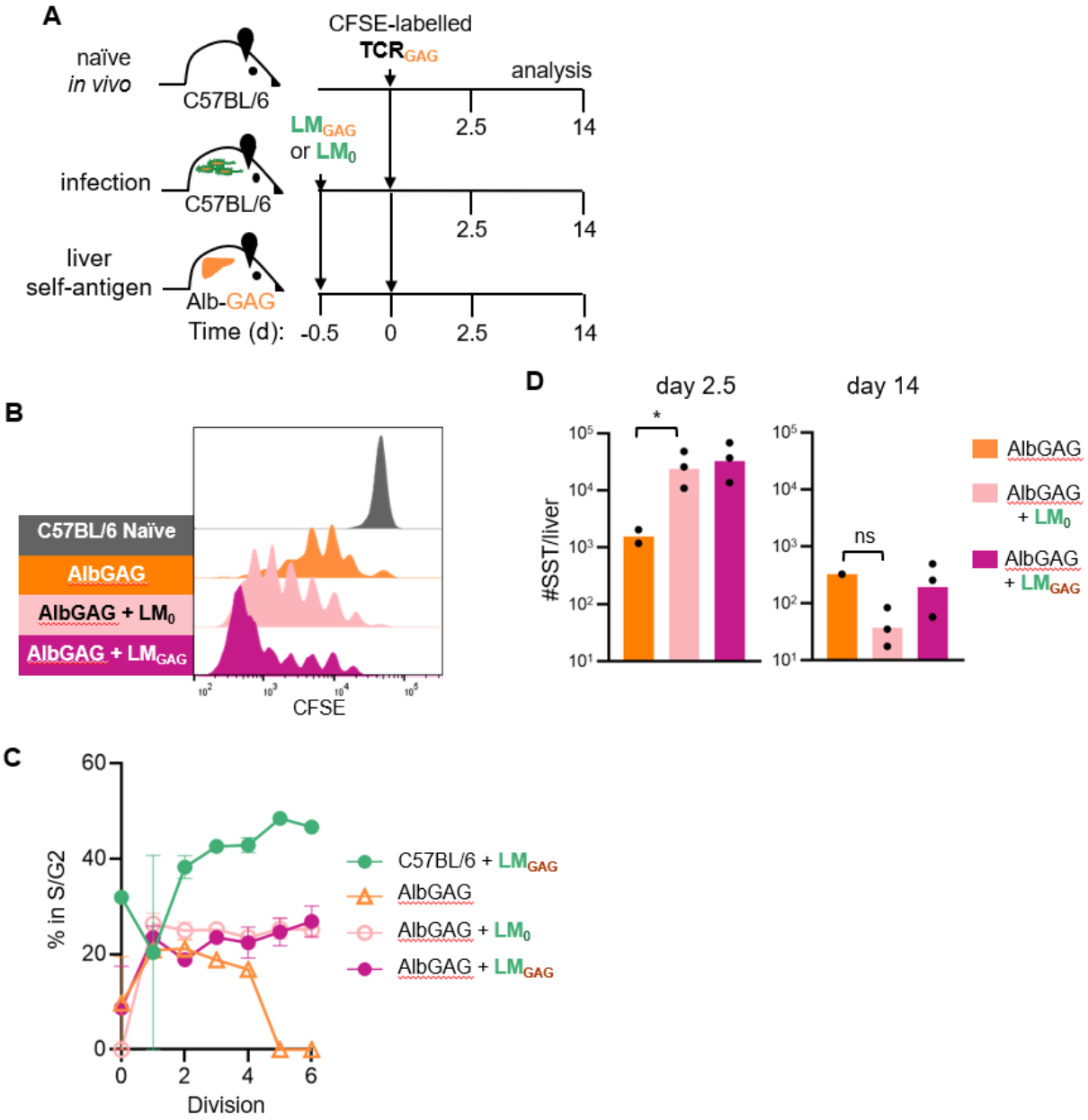

Figure 5.1| Optimal priming does not fully rescue SST function. A. Experimental scheme: naive TCR_{GAG} (Thy1.1) were adoptively transferred into B6 or into Alb-GAG (Thy1.2) following LM_{GAG} 12 hours prior. TCR_{GAG} were re-isolated from recipient spleens 2.5 and 14 days later for flow cytometric analysis. B. CFSE levels at 2.5 days. Naïve (gray), Alb-GAG (orange), Alb-GAG+LM_0 (light pink), and Alb-GAG+ LM_{GAG} (dark pink). C. Percent cells in S/G2 phase by division number at 2.5 days. D. Numbers of TCR_{GAG}recovered from spleens at day 2.5 and 14. All flow plots are gated on live CD8+ Thy1.1+ cells, and data for each timepoint is concatenated from biological replicates. n=2-3 mice per group.

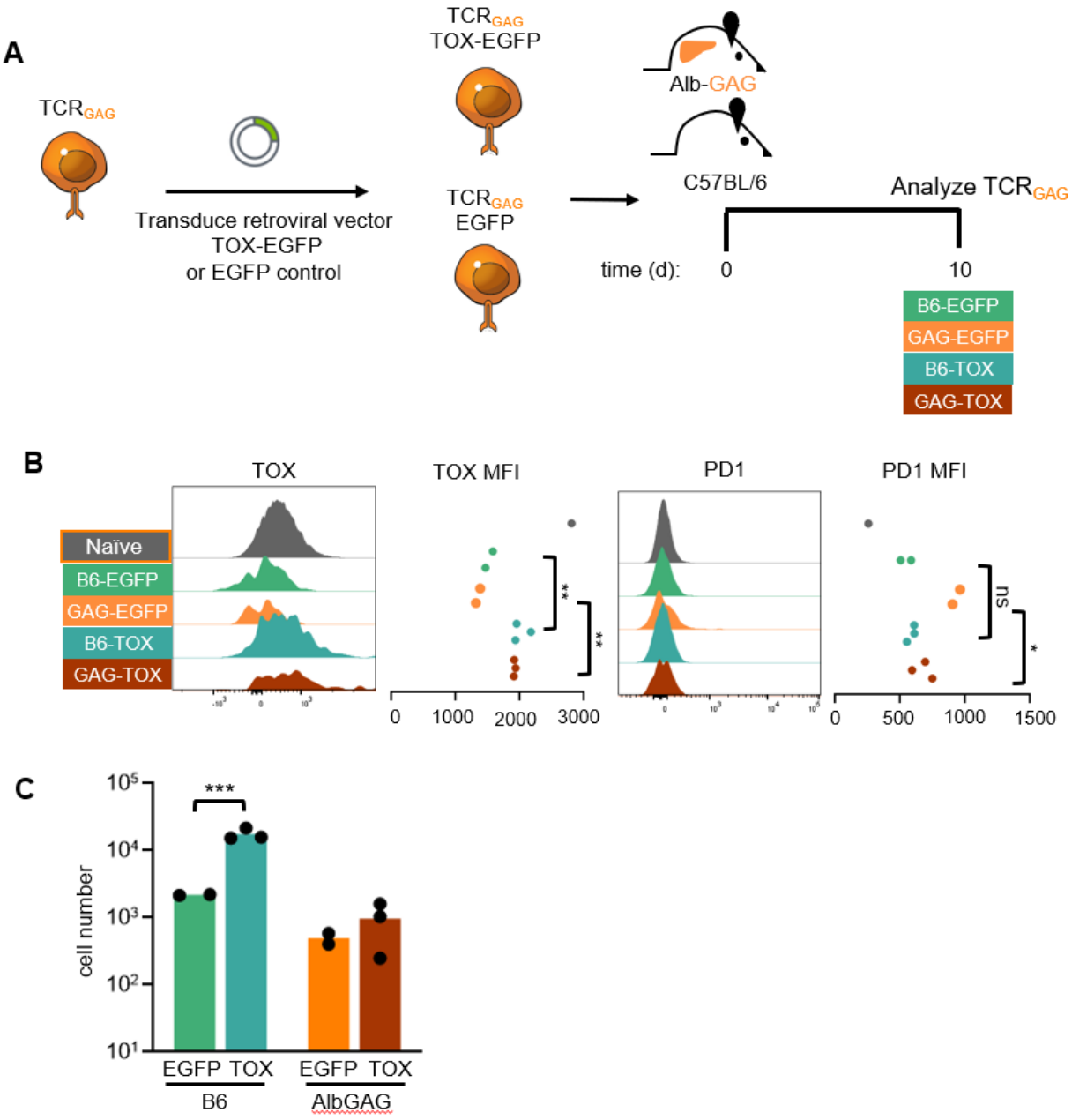

Figure 5.2| TOX overexpression does not overcome tolerogenic signals. A. Experimental scheme. Naïve TCR_{GAG} (Thy1.1) were transduced with retroviral vectors containing TOX-EGFP or control EGFP and adoptively transferred into Alb-GAG or B6 (Thy1.2). TCR_{GAG} were re-isolated from spleens 10 days later. **B**. Left, histogram TOX and PD1 expression. Right, %marker+ as compared to naive level; each dot represents an individual mouse. naïve (gray), EGFP cells in B6 (green), TOX-EGFP cells in B6 (cyan), EGFP in Alb-GAG (orange), TOX-EGFP in Alb-GAG (brown). ns=no significance, *p<0.05, **p<0.01 (one-way ANOVA). **C**. Cell numbers recovered from spleens of WT B6 or Alb-GAG mice. ***P<0.001 (Student's t-test). All flow plots are gated on live CD8+ Thy1.1+GFP+ cells, and data for each timepoint is concatenated from biological replicates. n=2-3 mice per group.

TST do not express higher levels of MYC than SST

c-MYC is well-known as a potent oncogene controlling proliferation and survival in tumor cells (Kortlever et al. *Cell* 2017). In T cells, nonmutated c-MYC is activated downstream of TCR signaling and plays a large role in activating T cell metabolism to support rapid proliferation as well as survival during the effector phase of T cell responses (Gnanaprakasam and Wang *Genes (Basel)* 2017; Rathmell *Immunity* 2011). Previous analyses of the TCR_{TAG} by our group has found that TST have an increase in MYC RNA (data not shown). We thus hypothesized that TST express higher levels of MYC than SST to support proliferation and persistence while the failure to express MYC in SST leads to the exit of cell cycle and the lack pf persistence.

We adoptively transferred CFSE-labeled TCR_{GAG} or TCR_{TAG} into ASTxGAG mice and assessed spleens and livers 60 hours later for MYC expression (**Fig 5.3A**), before we see a dramatic drop in TCR_{GAG} in the spleens (**Fig. 4.3**). Interestingly, even at 60 hours when we see TCR_{GAG}/SST already leaving cell cycle, MYC expression is the same between TCR_{GAG} and TCR_{TAG} (**Fig 5.3B**), indicating that the lack of MYC is not the explanation behind TCR_{GAG}/SST's failure to continue to proliferate and persist in high numbers.

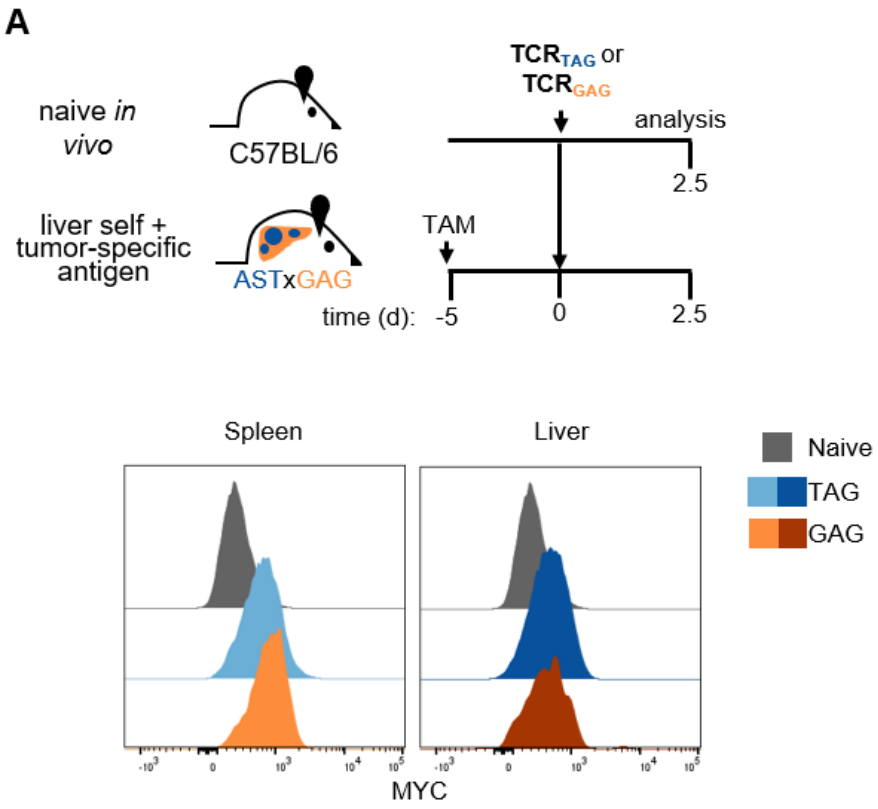

Figure 5.3| SST and TST have similar MYC expression. A. Experimental scheme: naive TCR_{TAG} (Thy1.1) or naive TCR_{GAG} (Thy1.1) were adoptively transferred into TAM-treated ASTxGAG (Thy1.2). TCR_{TAG} (blue) and TCR_{GAG} (orange) were reisolated from recipient spleens and livers 3 days later for flow cytometric analysis. B. Histograms of phosphorylated S6 in spleen and liver. Endogenous CD8+, open. All flow plots are gated on live CD8+ Thy1.1+ cells. All flow plots are gated on live CD8+ Thy1.1+ cells and show data concatenated from all biological replicates. n=3-4 mice per group.

Tumor vs. self-antigen role in persistence

The tumor and self-antigens used in these studies have thus far been different peptides. These antigens are both derived from viral proteins and evoke a TCR cell response in the micromolar range of peptide concentrations; however, there are likely varying degrees of MHC binding and TCR affinity. To address this discrepancy, we sought to utilize the GAG antigen as both a self-antigen and a tumor-specific antigen through a subcutaneous tumor model.

EL-4 cells are a mouse lymphoma cell line on a C57BL/6 background. We transduced a vector expressing the GAG antigen fused to EGFP for simple identification of cells that had taken up the vector. We then sorted these cells by EGFP expression for a homogenous population of EL4-GAG-expressing cells (**Fig 5.4A**). These cells then were injected subcutaneously into WT or Alb-GAG mice and monitored for tumor development before subsequent adoptive transfer of CFSE-labeled TCR_{GAG} and analysis 60 hours post-adoptive transfer (**Fig 5.4B**).

Within the spleen, there were no differences in cell numbers regardless of subcutaneous tumor. However, in the liver, TCR_{GAG} cell numbers were slightly increased with the addition of GAG-expressing tumor (**Fig 5.4C**). Even within the tumor, TCR_{GAG} in B6 mice had much higher cell numbers than those from the self-antigen Alb-GAG environment (**Fig 5.4C**). Having GAG as both the self- and tumor-antigen in this model did not increase the proliferation of TCR_{GAG} in the spleen or liver but did seem to somewhat increase proliferation in the tumor itself (**Fig 5.4D**). PD1 expression did not increase anywhere in the assessed organs (**Fig 5.4D**). Finally, GAG as a shared self/tumor antigen did not rescue effector cytokine function (**Fig 5.4E**). Thus, at an early timepoint of TCR_{GAG} in a shared self/tumor environment, the presence of the tumor antigen only somewhat boosts numbers and proliferation but does not provide additional signals to increase effector function. As the tumors grew quickly in the Alb-GAG mice, it was necessary to perform this experiment at an early timepoint following adoptive transfer. Further studies on

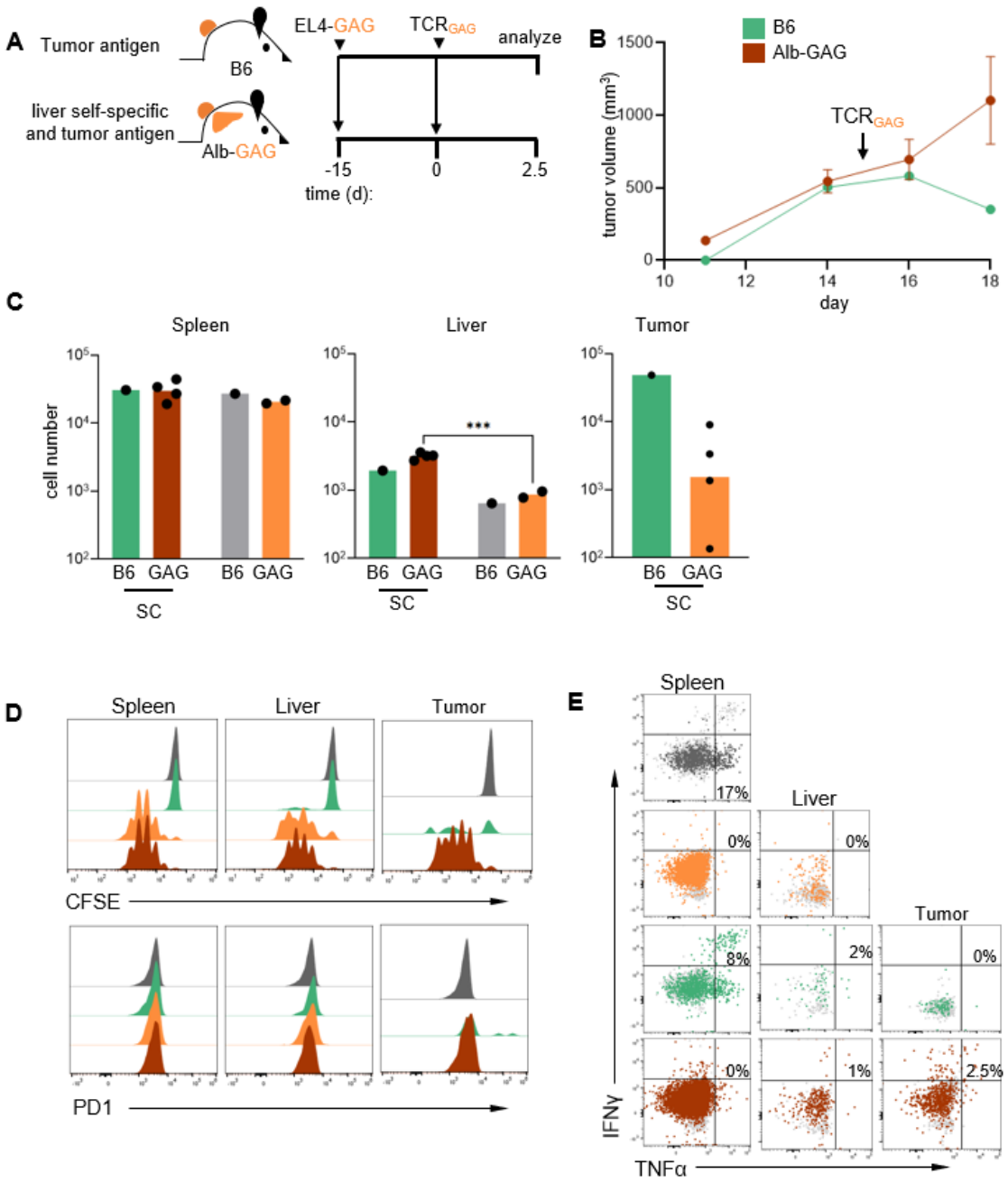

Figure 5.4| GAG as self-antigen and subcutaneous tumor antigen does not improve SST function but does increase proliferation. A. Experimental scheme. EL-4 cells transduced with GAG-EGFP were subcutaneously injected into B6 (green) or Alb-GAG (brown) flanks and allowed to grow for 15 days. CFSE-labelled TCR_{GAG} were then adoptively transferred, and cells recovered 60 hours later from spleens, livers, and tumors. **B.** Tumor volumes of subcutaneous EL-4-GAG tumors. TCR_{GAG} were adoptively transferred on d15. **C.** Absolute cell numbers recovered from spleen, liver, and tumor. SC=subcutaneous tumor. ***p<0.001 (one-way ANOVA). **D**. Histograms of CFSE (top) and PD1 expression (bottom) in spleen, liver, and tumor. **E**. TNFα and INFγ production following 4h *ex vivo* peptide stimulation with % TNFa+ IFNg+ shown in insets. No peptide-stimulated cells (gray) are shown for comparison. All flow plots are gated on live CD8+ Thy1.1+ cells and show data concatenated from all biological replicates. n=1-4 mice per group.

this type of model would be needed to ascertain how T cells persist long-term in a shared self/tumor model using subcutaneous EL4-GAG.

TST do not all activate with lower levels of TAG antigen but still proliferate more than SST

We wondered whether the ability of TST to proliferate faster than SST was due to a greater expression of the TAG antigen upon TAM treatment as compared to the GAG antigen. Unfortunately, there is no antibody available to detect FMLuV GAG antigen to make a direct comparison of the antigen expression levels. Instead, we used the T cells as a readout in the ASTxGAG mice without treatment of TAM. Even without TAM to splice the STOP codon, there are a few cells that still spontaneously express the antigen.

I adoptively transferred CFSE-labelled TCR_{TAG} and TCR_{GAG} into ASTxGAG without treatment of TAM and assessed cell proliferation after 60 hours in the spleen and liver (**Fig 5.5A**). Without high levels of TAG antigen, not all TCR_{TAG} activated as seen by no proliferation. Nearly all TCR_{GAG} were able to proliferate. However, despite fewer activated TCR_{TAG}, these TST were still able to proliferate further than TCR_{GAG}, which still stalled and failed to continue to proliferate after just a few divisions (**Fig 5.5B**). Thus, the amount of antigen expressed in ASTxGAG is not the reason for the failure of TCR_{GAG}/SST to proliferate.

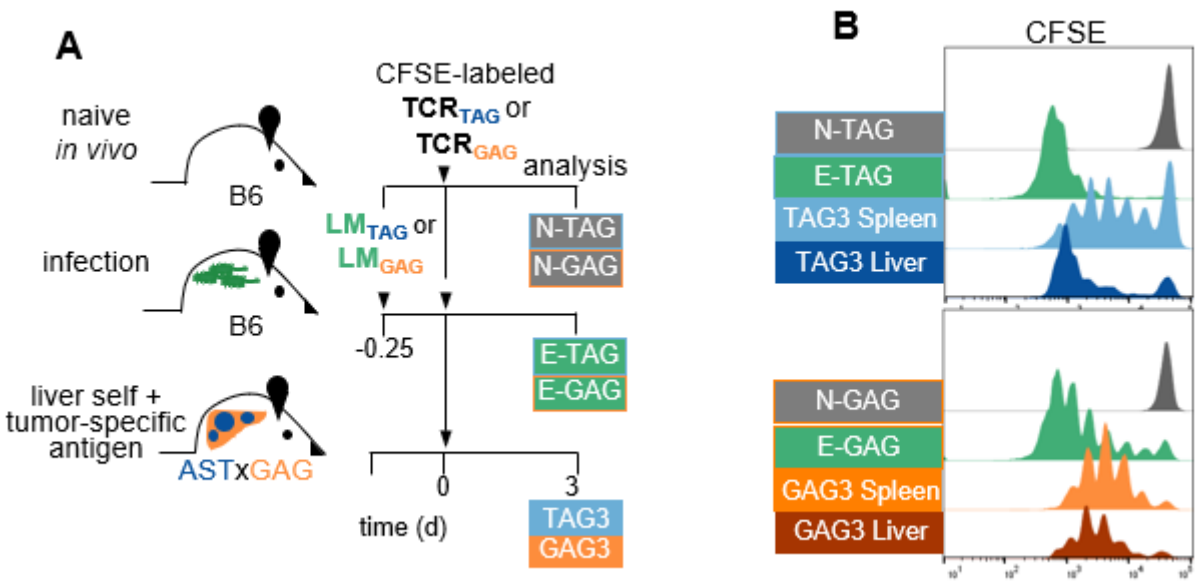

Figure 5.5| TST proliferate better than SST even with lower tumor antigen. A. Experimental scheme: naive TCR_{TAG} (Thy1.1) or naive TCR_{GAG} (Thy1.1) were adoptively transferred into *Listeria*-immunized B6 or ASTxGAG (Thy1.2) without TAM treatment. TCR_{TAG} (blue) and TCR_{GAG} (orange) were reisolated from recipient spleens and livers 3 days later for flow cytometric analysis. **B**. CFSE histograms showing cell proliferation. Data representative data of two independent experiments. All flow plots are gated on live CD8+ Thy1.1+ cells and show data concatenated from all biological replicates. n=3-4 mice per group.

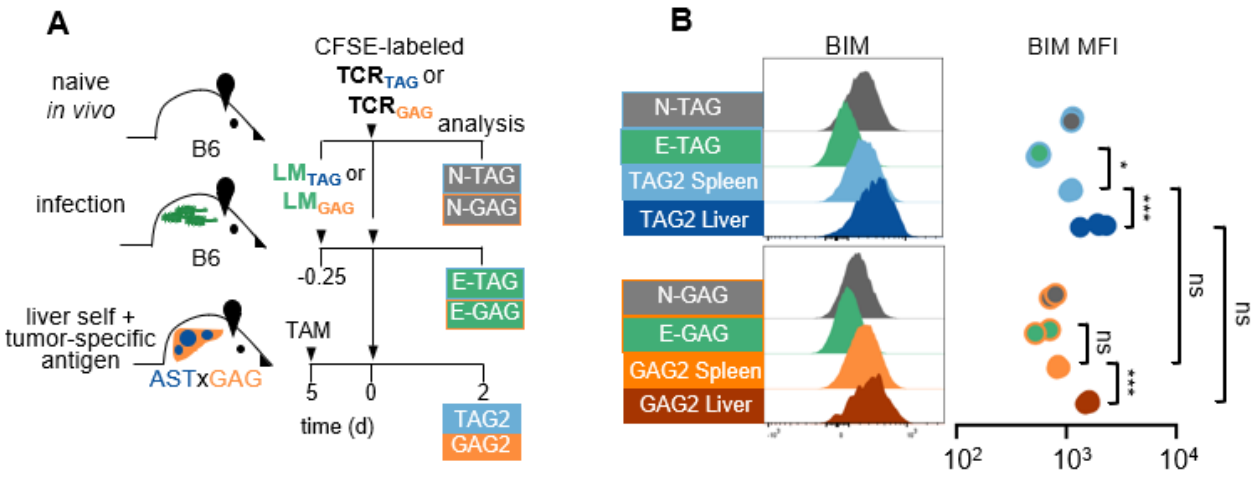

Figure 5.6| SST and TST upregulate BIM at similar levels. Experimental scheme: naive TCR_{TAG} (Thy1.1) or naive TCR_{GAG} (Thy1.1) were adoptively transferred into *Listeria*-immunized B6 or ASTxGAG (Thy1.2) 5 days after TAM treatment. TCR_{TAG} (blue) and TCR_{GAG} (orange) were reisolated from recipient spleens and livers 2 days later for flow cytometric analysis. B. Left, histograms of BIM staining. Right, BIM MFI as compared to naive; each symbol represents an individual mouse. **p*<0.05, ****p*<0.001 (one-way ANOVA). Data representative data of two independent experiments. All flow plots are gated on live CD8+ Thy1.1+ cells and show data concatenated from all biological replicates. n=2-3 mice per group.

CONCLUSIONS

This chapter posed several questions to probe the mechanism behind the lack of SST persistence following encounter with self-antigen. The results regarding the lack of SST persistence posed in this chapter do not fully address the reason why SST fail to persist in comparison to TST in the same tumor environment. However, the results indicate that the premature cell cycle exit is not due to the lack of transcription factor TOX expression or the lack of optimal priming. Rather, it is likely that a complex signaling network is initiated upon self-antigen encounter that requires multiple factors to initiate.

Previous work has shown that deletional tolerance requires the pro-apoptotic protein BIM, and knockout of BIM abrogates apoptosis of SST (Davey et al. *J Exp Med* 2002; Suen and Baldwin *Proc Natl Acad Sci U S A* 2012). However, BIM does not seem to be the driving factor in T cells toward tissue-specific antigen (Suen and Baldwin *Proc Natl Acad Sci U S A* 2012) and we did not see an upregulation of BIM in my studies (**Fig 5.6)**, suggesting a much more complicated route to SST disappearance.

Likewise, MYC is expressed in both TST and SST, which even a slightly higher MYC expression in SST than TST (**Fig 5.3**). This finding suggests that MYC expression is not the sole contributor to TST persistence over SST. Confoundingly, a recent study using CRISPR screens found that MYC and the transcription factor cBAF physically interact with each other to promote a more effector-like phenotype while $MYC^{lo}cBAF^{lo}$ T cells differentiated toward a more memory-like phenotype (Guo et al. *Nature* 2022). However, the fate of MYC-expressing T cells within a tumor environment is much less clear, and indeed, by the results found in our SST/TST model, MYC may play a contrary role in the differentiation to dysfunctional and tolerant states.

Finally, the antigen itself does not seem to be the sole determinant of T cell fate and persistence. Even when GAG acted as a tumor antigen or when the expression levels of GAG were higher in relation to TAG, we did not see a dramatic increase in SST persistence. Further studies using other tumor and self-antigens will be required to ascertain what factors are required and what factors are model or tissue specific.

To design more effect immunotherapies that harness the power of a patient's T cells, we must further understand how the nature of antigens affect T cell fate and differentiation. The mechanisms involved in the disappearance of tissue specific self-reactive T cells are complex and involve several interweaved factors to become hypofunctional.

CHAPTER VI

CONCLUSIONS AND FUTURE DIRECTIONS

CONCLUSIONS

Tumor neoantigens, derived from mutated or fused proteins, are not expressed elsewhere in the host, and T cells with a TCR specific for the mutated peptide should respond toward this neoantigen as if it is foreign. However, we do not see TST respond to our TAG oncogene/neoantigen in our AST;Cre-ER^{T2} mouse model, and several other models and human data show similar T cell hyporesponsiveness with a lack of effector function. On the other hand, cancer cells express self-antigens that can be found elsewhere in the host, such as overexpressed but not mutated proteins. T cells with a TCR specific for the self-antigen should undergo a form of peripheral tolerance in response to recognition of a self-antigen to prevent autoimmune pathology. However, these self-specific T cells represent a ready cytotoxic population that could be harnessed to use a patient's own immune system against their tumors. The work presented in this dissertation has sought to shed further light on T cell responses toward self-antigens and tumor neoantigens.

In chapter III, we attempted to create an *in vitro* model of hepatocellular carcinoma so that we harness our liver cancer mouse model AST;Cre-ER^{T2} and TCR$_{TAG}$ to identify what factors, including the TAG oncogene itself, drove TST dysfunction. Existing 2D methods of generating a cell line from AST;Cre-ER^{T2} mice yielded a cell line that expressed SV40 and could activate TCR$_{TAG}$. We also found that T cells can migrate into the Matrigel matrix and contact peptide-pulsed cells within, indicating that organoid technology could eventually be utilized to study T cell interactions with particular tissue types. However, the organoid technology for livers needs to be advanced further before we can utilize such a model due to the inability to fully differentiate ductal stem cells into hepatocytes that can express albumin.

In chapter IV, we identify that SST and TST responses toward liver self-antigen or liver tumor neoantigen both result in T cell nonfunction; however, SST fail to persist in high numbers in the liver. This failure to persist does not seem to be a massive upregulation of apoptosis in comparison to persistent TST but rather a premature exit in cell cycle soon after recognition of cognate self-antigen.

SST that do remain in the spleen display a memory-like phenotype with high TCF1 and no PD1 expression. Despite this memory-like phenotype, these SST do not respond to ICB, indicating that TCF1 may not be the sole factor in identifying what T cell subset can respond to immune therapies and that memory-like SST might need further priming or activation signals to rescue function and target tumor-associated antigens. In chapter V, we assess other possible mechanisms that might play a role in the premature cell cycle exit of SST. These mechanisms include the use of GAG-expressing *Listeria* to provide an optimal priming condition for SST within the Alb-GAG mice. This optimal priming does transiently rescue the initial proliferation of SST but does not recover higher numbers of SST at later timepoints. This result indicates additional priming may indeed be a way to unleash T cell responses with ICB treatment; however, further studies on this are needed to assess which signals are needed.

In addition to optimal priming, we assessed the expression levels of TOX and MYC in SST versus TST. Overexpression of TOX did not rescue the cell numbers of SST, indicating that the survival and persistence promotion induced by TOX in TST are not enough to override the signals initially received upon recognition of a self-antigen. TST and SST express similar levels of MYC, suggesting MYC is not solely involved in the persistence of TST. Finally, levels of antigen expressed in the ASTxGAG liver do not affect the ability of TST to out proliferate SST.

The results described in this dissertation have contributed to our understanding of T cell responses toward self-antigen and tumor neoantigen in the context of liver mouse models. However, the work presented also raises additional questions and avenues for further research.

FUTURE DIRECTIONS

What is the mechanism behind self-reactive T cell exit of cell cycle?

Chapter V addressed several questions regarding the mechanism behind the premature cell cycle exit of SST: lack of optimal priming, failure to express TOX, self-antigen as a tumor antigen, and lower levels of tumor antigen. However, the experiments performed found that not just one of these factors are required for the cell cycle exit of SST. Rather, it is likely that multiple factors, including the induction of transcription factors by TCR signaling after antigen recognition, play a complex, interrelated role in stopping T cell proliferation. Thus, the question remains: what is the mechanism behind self-reactive T cell exit of cell cycle?

One way to address this question could be to use a library of known apoptosis or survival genes to see what gene, if any, is responsible for the striking lack of persistence in SST. Knocking out certain apoptosis proteins in SST or survival proteins in TST would give clear readouts of T cells surviving or dying. However, given the vast complexity of T cell signaling and fate differentiation and the incomplete answers addressed in Chapter V, it is likely that there is not just one protein responsible for the observed phenotype.

The answer could potentially lie in the downstream signaling that is activated by the individual TCR upon antigen encounter. We probed the upstream signaling briefly in the form of phosphorylated S6 (pS6). pS6 is downstream of the PI3K signaling pathway that is activated upon TCR stimulation. There is no difference between the phosphorylation of pS6 in TCR_{TAG} and

TCR_{GAG} after 60 hours in the premalignant liver environment (**Fig 6.1**), a timepoint when TCR_{GAG} proliferation is already beginning to stop.

What cell is presenting antigen to self- and tumor-reactive T cells?

One factor behind the striking difference in SST and TST persistence may be due to which cell is presenting antigen and providing signals to the T cells. Brief studies looking at the responses of TST and SST upon isolated ASTxGAG hepatocytes show that both SST and TST can activate after three days in culture *in vitro* (**Fig 4.5**); therefore, hepatocytes are capable of presenting antigen directly to SST and TST in our model. However, we did not investigate further as to whether *in vitro* culture alone is sufficient to induce TST and/or SST dysfunction, leaving the ability of hepatocyte signaling effects on TST and SST an open question.

In vivo, T cells are likely to first traffic to the spleen after intravenous adoptive transfer, since transferred cells are detectable in this organ and have upregulated CD44, indicating antigen recognition has occurred. We adoptively transferred CSFE-labeled TCR_{TAG} or TCR_{GAG} into TAM-treated ASTxGAG and analyzed spleens and livers after 3 days (**Fig. 6.2A**). CFSE dilution suggests that it is plausible that TST are activated and begin proliferating and undergoing cell cycle in the spleen and then traffic to the liver, where they continue to proliferate (**Fig 6.2B, C**). SST, on the other hand, see antigen in the spleen and both begin and end proliferation in the spleen with a handful of cells trafficking to the liver, where they may divide once more before exiting cell cycle (**Fig 6.2B, C**).

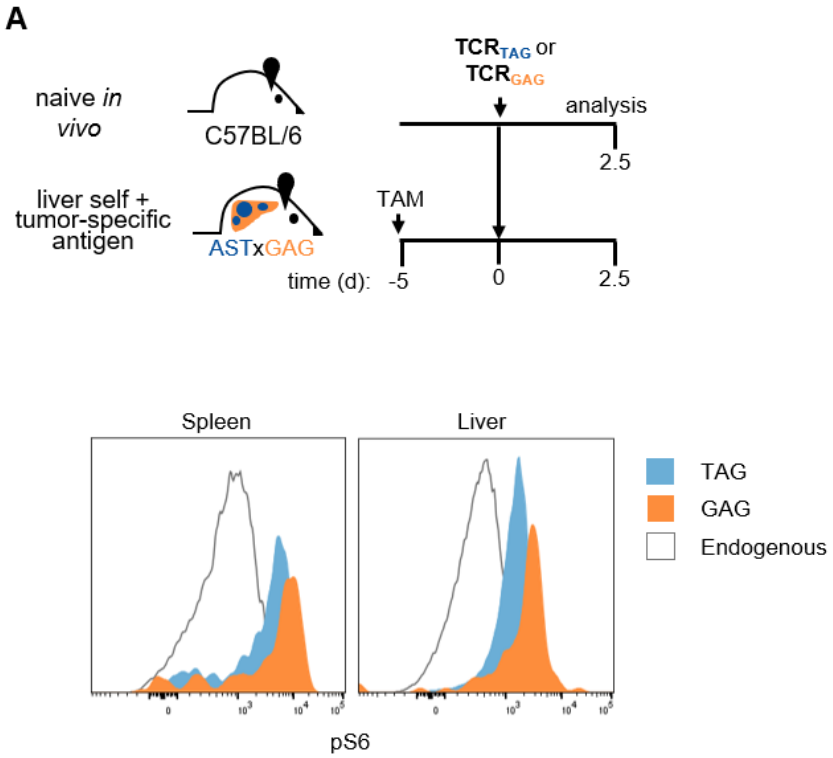

Figure 6.1| SST and TST have similar upstream signaling. Top, Experimental scheme: naive TCR_{TAG} (Thy1.1) or naive TCR_{GAG} (Thy1.1) were adoptively transferred into TAM-treated ASTxGAG (Thy1.2). TCR_{TAG} (blue) and TCR_{GAG} (orange) were reisolated from recipient spleens and livers 3 days later for flow cytometric analysis. Bottom, Histograms of phosphorylated S6 in spleen and liver. Endogenous CD8+, open. All flow plots are gated on live CD8+ Thy1.1+ cells.

Since GAG is a self-antigen, it could be expressed in thymic epithelial cells and splenic dendritic cells. We find very few TCR_{GAG}/SST in Alb-GAG livers, in contrast to TCR_{TAG}/TST, which primarily localize to the liver. To determine if priming location (e.g. liver vs. spleen) plays a role in TCR-TAG and TCR_{GAG}/SST persistence and deletion, a splenectomy could be performed on TAM-treated ASTxGAG mice before adoptively transferring both T cells and subsequent analysis cell numbers as well as effector cytokine production and exhaustion markers could be performed. Combination of this method with a thymectomy can for the evaluation of both thymic epithelial cells and splenic dendritic cells (DC). To eliminate antigen presentation by splenocytes, a bone marrow transplant of β2-microglobulin knockout mice into lethally irradiated ASTxGAG mice could be performed so that GAG antigen will only be presented in hepatocytes and Kupffer cells.

Previous studies have shown that tolerizing DC interact with CD4+ T cells through Fas and TRAIL pathways to induce apoptosis (Qian et al. *J Biol Chem* 2013; Hasegawa and Matsumoto *Front Immunol* 2018). Tolerogenic DC are $CD11b^{HI}Ia^{low}$ and are characterized by low expression of co-stimulatory receptors CD80 and CD86. Enzyme-mediated proximity cell labeling (EXCELL) (Ge et al. *J Am Chem Soc* 2019) can be used to assess which DC populations interact with TCR_{GAG}/SST. This technique relies on the transpeptidase sortase A, which is transduced into cells of interest, such as TCR_{GAG}. Sortase A then transfers biotin-LPETG onto the cell surface of an interacting cell, allowing for the detection of cells that have interacted with TCR_{GAG}/SST by flow cytometry.

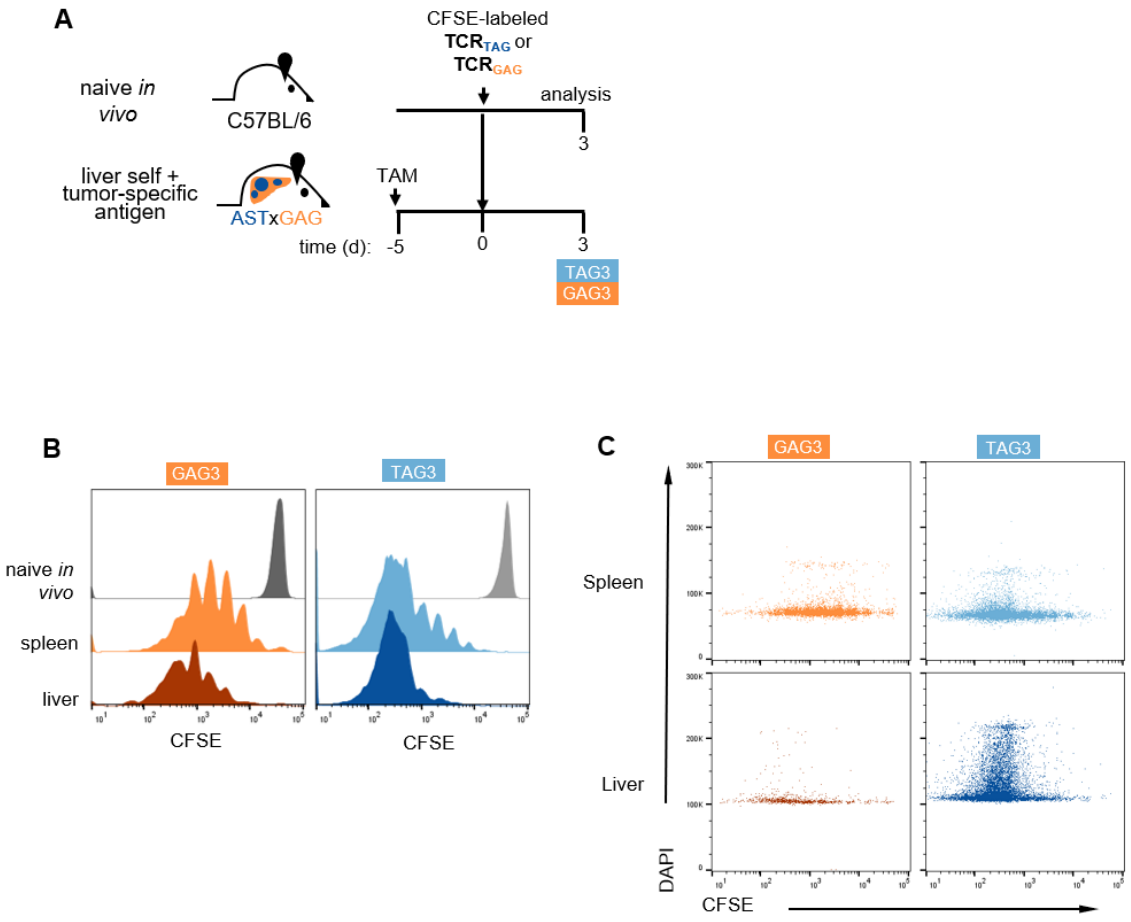

Figure 6.2| SST stop proliferating prematurely. A. Experimental scheme: naive TCR_{TAG} (Thy1.1) or naive TCR_{GAG} (Thy1.1) were adoptively transferred into TAM-treated ASTxGAG (Thy1.2). TCR_{TAG} (blue) and TCR_{GAG} (orange) were reisolated from recipient spleens and livers 3 days later for flow cytometric analysis. **B.** CFSE histograms showing cell proliferation. C. Top, histograms of DAPI staining/DNA content by CFSE dilution/cell division. Data representative data of four independent experiments. All flow plots are gated on live CD8+ Thy1.1+ cells and show data concatenated from all biological replicates. n=3-4 mice per group.

What is the role of TCF1 in SST?

TCF1 is a high mobility group DNA binding protein/transcription factor critical for thymic T cell development. Mice lacking TCF1 have stunted growth of the thymus and greatly reduced T cell numbers (Verbeek et al. *Nature* 1995). *Tcf7-/-* T cells fail to survive and expand during re-infection, suggesting that TCF1 is critical for CD8 memory development (Jeannet et al. *Proc Natl Acad Sci U S A* 2010; Zhou et al. *Immunity* 2010). More recently, TCF1 been shown to be a marker and regulator of long-lived exhausted T cell precursor populations in chronic viral infection and tumor contexts, and TCF1+ T cell populations are thought to be responsible for response to checkpoint blockade (Im, Hashimoto, Gerner, Lee, Kissick, Urger, et al. *Nature* 2016; Wang et al. *Front Immunol* 2019; Siddiqui et al. *Immunity* 2019).

TCF1 is downregulated in terminally differentiated effectors and terminally exhausted CD8+ T cells. However, previous studies suggest that low-affinity peptide ligands induce a lower level of proliferation (Goldrath and Bevan *Immunity* 1999) and a more sustained level of TCF1 (Shakiba et al. *J Exp Med* 2022). The unique phenotype of memory-like SST with TCF1 expression but without effector function despite immune checkpoint blockade treatment is an interesting, previously undescribed subset of T cells. It does appear that ICB downregulates the expression of TCF1 in both TCR_{GAG}/SST and endogenous T cells in the spleen and liver of both tumor-bearing ASTxGAG and non-tumor bearing Alb-GAG mice (**Fig 6.3A, B**); however, MKI67 does not increase to indicate an increase in proliferation in SST. Thus, what is the role of TCF1 in memory-like SST?

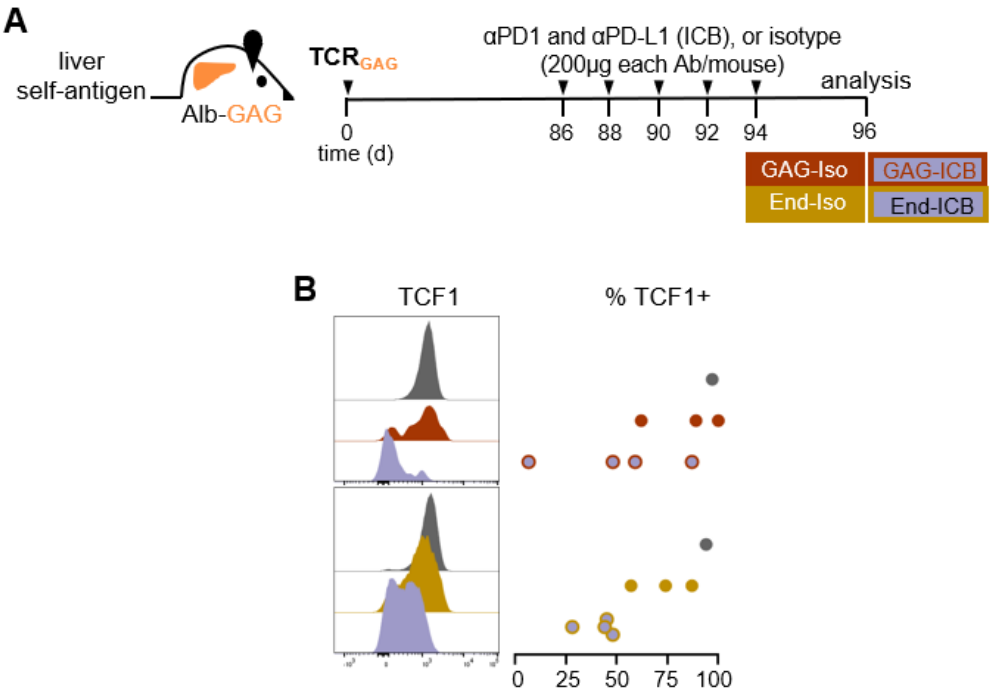

Figure 6.3| Immune checkpoint blockade lowers TCF1 expression. A. Experimental scheme: naive TCR_{GAG} (Thy1.1) were adoptively transferred into Alb-GAG (Thy1.2). TCR_{GAG} (orange) and endogenous CD8+CD44+ (gold) were re-isolated from recipient spleens 5 and 55 days later for flow cytometric analysis. B. Left, histogram of TCF1 expression. Right, % marker+ as compared to naive level; each dot represents an individual mouse. ns=no significance (one-way ANOVA). Data representative data of three independent experiments. All flow plots are gated on live CD8+ Thy1.1+ cells and show data concatenated from all biological replicates. n=3-4 mice per group.

One approach to consider this question would be to generate a knockout of TCF1 in TCR_{GAG}/SST to determine if these T cells develop into the memory-like phenotype we have seen in Alb-GAG and ASTxGAG mice. In addition, a conditional knockout, such a floxed TCF1 mouse crossed with an inducible Cre recombinase would allow for further probing after TCR_{GAG} have reached a memory-like phenotype.

Inflammatory signals have been shown to drive a decrease of TCF1 during infection, and IL-12 especially has been identified as important for TCF1 downregulation. It is possible that ICB induces enough of an inflammatory environment to cause the downregulation of TCF1 seen in TCR_{GAG}/SST following ICB treatment (**Fig 6.3B**). TCF1 overexpression studies could be used to probe the response of TCR_{GAG} during ICB treatment by preventing the downregulation of TCF1 and determine if TCF1 needs to remain high to rescue effector cytokine production.

STUDY LIMITATIONS

One limitation of the work presented here is that only responses toward liver antigens were used. The liver is a unique organ immunologically in that several immunosuppressive mechanisms are in play as the organ filters blood received from the colon and small intestine. The fact that we see TST dysfunction in multiple model systems assuages this fact; however, model systems looking at SST responses are widely varied, and organ specificity should be probed in the future.

Secondly, since the affinity of TCR_{GAG} and TCR_{TAG} are somewhat different, with TCR_{TAG} having a 100-fold higher EC_{50}, the responses of T cells may be confounded by this difference. Both of these peptides are derived from viral peptides and do stimulate in the nanomolar range of peptide. In addition, the slightly lower affinity of the SST TCR is physiologically relevant, as any SST that escapes central tolerance would not have as strong an affinity to peptide as a TST. The ability to measure the affinities has been additionally confounded by the fact that tetramers toward the

GAG pMHC are not available, and the GAG peptide contains several cysteines, making the peptide relatively unstable in culture and long-term storage. We took an indirect approach to assess affinity by culturing SST and TST on hepatocytes isolated from ASTxGAG and found both SST and TST upregulate CD69 by 72 hours in culture, indicating a similar affinity (**Fig 4.4)**. One approach to further probing this limitation would be to use another mouse model system in which the self-antigen is also under the albumin promoter. One such model is the Hep-OVA model, where the well-studied OVA antigen is expressed only in the liver. The OVA model and transgenic CD8 T cells TCR_{OT-I} are well studied in the immunology field and would be an excellent model to compare the responses to TST and the Alb-GAG model.

Finally, the study of SST is limited to what T cells are still alive at time of analysis. We did not observe an increase in apoptosis between SST and persistent TST; however, because cells *in vivo* are quickly cleared upon apoptosis, it is technically challenging to observe apoptotic cells. It may be possible to use a reporter mouse for caspase-3 or another apoptotic protein such as BIM to observe apoptosis in SST and dissect the mechanism behind the lack of persistence.

CONCLUDING REMARKS

The results described in this dissertation address gaps in knowledge that will need to be expanded upon to improve the understanding of T cell biology and therapeutic immunology to harness the power of T cells in cancer. The insights gained on the differential responses to tumor versus self/shared tumor antigen as well as the inability of memory-like TCF1+ SST to respond to ICB in particular highlight the fact that T cells undergo complex, still-unknown signaling regulated by a vast network to undergo tumor-specific dysfunction, self-antigen specific hyporesponsiveness, or functional, effector responses. The identification of a memory-like SST population provides an opportunity to further characterize this unique T cell subset and build a more complete picture of

the mechanisms behind T cell hyporesponsiveness and which T cells respond to ICB. Further understanding of the factors that control T cell differentiation fates may help to develop more specific immunotherapies and inform decisions of personalized treatment regimens. Together, further investigation of these aspects of T cell immunology in cancer and autoimmunity has the potential to significantly impact the future of both basic T cell biology as well as available therapeutics for cancer patients.

REFERENCES

Akbay, E. A., S. Koyama, J. Carretero, A. Altabef, J. H. Tchaicha, C. L. Christensen, O. R. Mikse, A. D. Cherniack, E. M. Beauchamp, T. J. Pugh, M. D. Wilkerson, P. E. Fecci, M. Butaney, J. B. Reibel, M. Soucheray, T. J. Cohoon, P. A. Janne, M. Meyerson, D. N. Hayes, G. I. Shapiro, T. Shimamura, L. M. Sholl, S. J. Rodig, G. J. Freeman, P. S. Hammerman, G. Dranoff, and K. K. Wong. 2013. 'Activation of the PD-1 pathway contributes to immune escape in EGFR-driven lung tumors', *Cancer Discov*, 3: 1355-63.

Alcocer-Gonzalez, J. M., J. Berumen, R. Tamez-Guerra, V. Bermudez-Morales, O. Peralta-Zaragoza, R. Hernandez-Pando, J. Moreno, P. Gariglio, and V. Madrid-Marina. 2006. 'In vivo expression of immunosuppressive cytokines in human papillomavirus-transformed cervical cancer cells', *Viral Immunol*, 19: 481-91.

Anastasiadou, E., D. Stroopinsky, S. Alimperti, A. L. Jiao, A. R. Pyzer, C. Cippitelli, G. Pepe, M. Severa, J. Rosenblatt, M. P. Etna, S. Rieger, B. Kempkes, E. M. Coccia, S. J. H. Sui, C. S. Chen, S. Uccini, D. Avigan, A. Faggioni, P. Trivedi, and F. J. Slack. 2019. 'Epstein–Barr virus-encoded EBNA2 alters immune checkpoint PD-L1 expression by downregulating miR-34a in B-cell lymphomas.' in, *Leukemia*.

Anderson, K. G., I. M. Stromnes, and P. D. Greenberg. 2017. 'Obstacles Posed by the Tumor Microenvironment to T cell Activity: A Case for Synergistic Therapies', *Cancer Cell*, 31: 311-25.

Ansell, S. M., A. M. Lesokhin, I. Borrello, A. Halwani, E. C. Scott, M. Gutierrez, S. J. Schuster, M. M. Millenson, D. Cattry, G. J. Freeman, S. J. Rodig, B. Chapuy, A. H. Ligon, L. Zhu, J. F. Grosso, S. Y. Kim, J. M. Timmerman, M. A. Shipp, and P. Armand. 2015. 'PD-1 blockade with nivolumab in relapsed or refractory Hodgkin's lymphoma', *N Engl J Med*, 372: 311-9.

Aoki, M., H. Aoki, R. Ramanathan, N. C. Hait, and K. Takabe. 2016. 'Sphingosine-1-Phosphate Signaling in Immune Cells and Inflammation: Roles and Therapeutic Potential', *Mediators Inflamm*, 2016: 8606878.

Arroyo Muhr, L. S., Z. Bzhalava, M. Hortlund, C. Lagheden, S. Nordqvist Kleppe, D. Bzhalava, E. Hultin, and J. Dillner. 2017. 'Viruses in cancers among the immunosuppressed', *Int J Cancer*, 141: 2498-504.

Bahl, K., A. Huebner, R. J. Davis, and R. M. Welsh. 2010. 'Analysis of apoptosis of memory T cells and dendritic cells during the early stages of viral infection or exposure to toll-like receptor agonists', *J Virol*, 84: 4866-77.

Baitsch, L., P. Baumgaertner, E. Devevre, S. K. Raghav, A. Legat, L. Barba, S. Wieckowski, H. Bouzourene, B. Deplancke, P. Romero, N. Rufer, and D. E. Speiser. 2011. 'Exhaustion of tumor-specific CD8(+) T cells in metastases from melanoma patients', *J Clin Invest*, 121: 2350-60.

Benechet, A. P., G. De Simone, P. Di Lucia, F. Cilenti, G. Barbiera, N. Le Bert, V. Fumagalli, E. Lusito, F. Moalli, V. Bianchessi, F. Andreata, P. Zordan, E. Bono, L. Giustini, W. V. Bonilla, C. Bleriot, K. Kunasegaran, G. Gonzalez-Aseguinolaza, D. D. Pinschewer, P. T. F. Kennedy, L. Naldini, M. Kuka, F. Ginhoux, A. Cantore, A. Bertoletti, R. Ostuni, L. G. Guidotti, and M. Iannacone. 2019. 'Dynamics and genomic landscape of CD8(+) T cells undergoing hepatic priming', *Nature*, 574: 200-05.

Bermudez-Morales, V. H., O. Peralta-Zaragoza, J. M. Alcocer-Gonzalez, J. Moreno, and V. Madrid-Marina. 2011. 'IL-10 expression is regulated by HPV E2 protein in cervical cancer cells', *Mol Med Rep*, 4: 369-75.

Berner, F., D. Bomze, C. Lichtensteiger, V. Walter, R. Niederer, O. Hasan Ali, N. Wyss, J. Bauer, L. K. Freudenmann, A. Marcu, E. M. Wolfschmitt, S. Haen, T. Gross, M. T. Abdou, S. Diem, S. Knopfli, T. Sinnberg, K. Hofmeister, H. W. Cheng, M. Toma, N. Klumper, M. T. Purde, O. T. Pop, A. K. Jochum, S. Pascolo, M. Joerger, M. Fruh, W. Jochum, H. G. Rammensee, H. Laubli, M. Holzel, J.

Neefjes, J. Walz, and L. Flatz. 2022. 'Autoreactive napsin A-specific T cells are enriched in lung tumors and inflammatory lung lesions during immune checkpoint blockade', *Sci Immunol*, 7: eabn9644.

Bettini, M., L. Blanchfield, A. Castellaw, Q. Zhang, M. Nakayama, M. P. Smeltzer, H. Zhang, K. A. Hogquist, B. D. Evavold, and D. A. Vignali. 2014. 'TCR affinity and tolerance mechanisms converge to shape T cell diabetogenic potential', *J Immunol*, 193: 571-9.

Bhat, P., G. Leggatt, N. Waterhouse, and I. H. Frazer. 2017. 'Interferon-gamma derived from cytotoxic lymphocytes directly enhances their motility and cytotoxicity', *Cell Death Dis*, 8: e2836.

Bowen, D. G., M. Zen, L. Holz, T. Davis, G. W. McCaughan, and P. Bertolino. 2004. 'The site of primary T cell activation is a determinant of the balance between intrahepatic tolerance and immunity', *J Clin Invest*, 114: 701-12.

Bradley, S. D., Z. Chen, B. Melendez, A. Talukder, J. S. Khalili, T. Rodriguez-Cruz, S. Liu, M. Whittington, W. Deng, F. Li, C. Bernatchez, L. G. Radvanyi, M. A. Davies, P. Hwu, and G. Lizee. 2015. 'BRAFV600E Co-opts a Conserved MHC Class I Internalization Pathway to Diminish Antigen Presentation and CD8+ T-cell Recognition of Melanoma', *Cancer Immunol Res*, 3: 602-9.

Brea, E. J., C. Y. Oh, E. Manchado, S. Budhu, S. Gejman R, G. Mo, P. Mondello, J. E. Han, C. A. Jarvis, D. Ulmert, Q. Xiang, A. Y. Chang, R. J. Garippa, T. Merghoub, J. D. Wolchok, N. Rosen, S. W. Lowe, and D. A. Scheinberg. 2016. 'Kinase regulation of Human MHC Class I Molecule Expression on Cancer Cells', *Cancer Immunol Res*, 4: 936-47.

Broutier, L., A. Andersson-Rolf, C. J. Hindley, S. F. Boj, H. Clevers, B. K. Koo, and M. Huch. 2016. 'Culture and establishment of self-renewing human and mouse adult liver and pancreas 3D organoids and their genetic manipulation', *Nat Protoc*, 11: 1724-43.

Burger, M. L., A. M. Cruz, G. E. Crossland, G. Gaglia, C. C. Ritch, S. E. Blatt, A. Bhutkar, D. Canner, T. Kienka, S. Z. Tavana, A. L. Barandiaran, A. Garmilla, J. M. Schenkel, M. Hillman, I. de Los Rios Kobara, A. Li, A. M. Jaeger, W. L. Hwang, P. M. K. Westcott, M. P. Manos, M. M. Holovatska, F. S. Hodi, A. Regev, S. Santagata, and T. Jacks. 2021. 'Antigen dominance hierarchies shape TCF1(+) progenitor CD8 T cell phenotypes in tumors', *Cell*, 184: 4996-5014 e26.

Byrne, E. H., and D. E. Fisher. 2017. 'Immune and molecular correlates in melanoma treated with immune checkpoint blockade', *Cancer*, 123: 2143-53.

Casey, S. C., L. Tong, Y. Li, R. Do, S. Walz, K. N. Fitzgerald, A. M. Gouw, V. Baylot, I. Gutgemann, M. Eilers, and D. W. Felsher. 2016. 'MYC regulates the antitumor immune response through CD47 and PD-L1', *Science*, 352: 227-31.

Chang, H. C., T. H. Hsieh, Y. W. Lee, C. F. Tsai, Y. N. Tsai, C. C. Cheng, and H. W. Wang. 2016. 'c-Myc and viral cofactor Kaposin B co-operate to elicit angiogenesis through modulating miRNome traits of endothelial cells', *BMC Syst Biol*, 10 Suppl 1: 1.

Chapman, N. M., M. R. Boothby, and H. Chi. 2020. 'Metabolic coordination of T cell quiescence and activation', *Nat Rev Immunol*, 20: 55-70.

Coelho, M. A., S. de Carne Trecesson, S. Rana, D. Zecchin, C. Moore, M. Molina-Arcas, P. East, B. Spencer-Dene, E. Nye, K. Barnouin, A. P. Snijders, W. S. Lai, P. J. Blackshear, and J. Downward. 2017. 'Oncogenic RAS Signaling Promotes Tumor Immunoresistance by Stabilizing PD-L1 mRNA', *Immunity*, 47: 1083-99.e6.

Comerford, S. A., N. Schultz, E. A. Hinnant, S. Klapproth, and R. E. Hammer. 2012. 'Comparative analysis of SV40 17kT and LT function in vivo demonstrates that LT's C-terminus re-programs hepatic gene expression and is necessary for tumorigenesis in the liver', *Oncogenesis*, 1: e28.

Cornel, A. M., I. L. Mimpen, and S. Nierkens. 2020. 'MHC Class I Downregulation in Cancer: Underlying Mechanisms and Potential Targets for Cancer Immunotherapy', *Cancers (Basel)*, 12.

Couper, K. N., D. G. Blount, and E. M. Riley. 2008. 'IL-10: the master regulator of immunity to infection', *J Immunol*, 180: 5771-7.

Courtney, A. H., W. L. Lo, and A. Weiss. 2018. 'TCR Signaling: Mechanisms of Initiation and Propagation', *Trends Biochem Sci*, 43: 108-23.

Croft, N. P., C. Shannon-Lowe, A. I. Bell, D. Horst, E. Kremmer, M. E. Ressing, E. J. Wiertz, J. M. Middeldorp, M. Rowe, A. B. Rickinson, and A. D. Hislop. 2009. 'Stage-specific inhibition of MHC class I presentation by the Epstein-Barr virus BNLF2a protein during virus lytic cycle', *PLoS Pathog*, 5: e1000490.

Davey, G. M., C. Kurts, J. F. Miller, P. Bouillet, A. Strasser, A. G. Brooks, F. R. Carbone, and W. R. Heath. 2002. 'Peripheral deletion of autoreactive CD8 T cells by cross presentation of self-antigen occurs by a Bcl-2-inhibitable pathway mediated by Bim', *J Exp Med*, 196: 947-55.

de Martel, C., D. Georges, F. Bray, J. Ferlay, and G. M. Clifford. 2020. 'Global burden of cancer attributable to infections in 2018: a worldwide incidence analysis', *Lancet Glob Health*, 8: e180-e90.

del Campo, A. B., J. A. Kyte, J. Carretero, S. Zinchencko, R. Mendez, G. Gonzalez-Aseguinolaza, F. Ruiz-Cabello, S. Aamdal, G. Gaudernack, F. Garrido, and N. Aptsiauri. 2014. 'Immune escape of cancer cells with beta2-microglobulin loss over the course of metastatic melanoma', *Int J Cancer*, 134: 102-13.

Dijkstra, K. K., C. M. Cattaneo, F. Weeber, M. Chalabi, J. van de Haar, L. F. Fanchi, M. Slagter, D. L. van der Velden, S. Kaing, S. Kelderman, N. van Rooij, M. E. van Leerdam, A. Depla, E. F. Smit, K. J. Hartemink, R. de Groot, M. C. Wolkers, N. Sachs, P. Snaebjornsson, K. Monkhorst, J. Haanen, H. Clevers, T. N. Schumacher, and E. E. Voest. 2018. 'Generation of Tumor-Reactive T Cells by Co-culture of Peripheral Blood Lymphocytes and Tumor Organoids', *Cell*.

Eberhardt, C. S., H. T. Kissick, M. R. Patel, M. A. Cardenas, N. Prokhnevska, R. C. Obeng, T. H. Nasti, C. C. Griffith, S. J. Im, X. Wang, D. M. Shin, M. Carrington, Z. G. Chen, J. Sidney, A. Sette, N. F. Saba, A. Wieland, and R. Ahmed. 2021. 'Functional HPV-specific PD-1(+) stem-like CD8 T cells in head and neck cancer', *Nature*, 597: 279-84.

Eggert, Tobias, Katharina Wolter, Juling Ji, Chi Ma, Tetyana Yevsa, Sabrina Klotz, José Medina-Echeverz, Thomas Longerich, Marshonna Forgues, Florian Reisinger, Mathias Heikenwalder, Xin Wei Wang, Lars Zender, and Tim F. Greten. 2016. 'Distinct Functions of Senescence-Associated Immune Responses in Liver Tumor Surveillance and Tumor Progression', *Cancer Cell*, 30: 533-47.

ElTanbouly, M. A., and R. J. Noelle. 2020. 'Rethinking peripheral T cell tolerance: checkpoints across a T cell's journey', *Nat Rev Immunol*.

Fonseca, S., V. Pereira, C. Lau, M. D. A. Teixeira, M. Bini-Antunes, and M. Lima. 2020. 'Human Peripheral Blood Gamma Delta T Cells: Report on a Series of Healthy Caucasian Portuguese Adults and Comprehensive Review of the Literature', *Cells*, 9.

Forloni, M., S. Albini, M. Z. Limongi, L. Cifaldi, R. Boldrini, M. R. Nicotra, G. Giannini, P. G. Natali, P. Giacomini, and D. Fruci. 2010. 'NF-kappaB, and not MYCN, regulates MHC class I and endoplasmic reticulum aminopeptidases in human neuroblastoma cells', *Cancer Res*, 70: 916-24.

Gaglia, M. M., and K. Munger. 2018. 'More than just oncogenes: mechanisms of tumorigenesis by human viruses', *Curr Opin Virol*, 32: 48-59.

Galluzzi, L., I. Vitale, S. A. Aaronson, J. M. Abrams, D. Adam, P. Agostinis, E. S. Alnemri, L. Altucci, I. Amelio, D. W. Andrews, M. Annicchiarico-Petruzzelli, A. V. Antonov, E. Arama, E. H. Baehrecke, N. A. Barlev, N. G. Bazan, F. Bernassola, M. J. M. Bertrand, K. Bianchi, M. V. Blagosklonny, K. Blomgren, C. Borner, P. Boya, C. Brenner, M. Campanella, E. Candi, D. Carmona-Gutierrez, F. Cecconi, F. K. Chan, N. S. Chandel, E. H. Cheng, J. E. Chipuk, J. A. Cidlowski, A. Ciechanover, G. M. Cohen, M. Conrad, J. R. Cubillos-Ruiz, P. E. Czabotar, V. D'Angiolella, T. M. Dawson, V. L. Dawson, V. De Laurenzi, R. De Maria, K. M. Debatin, R. J. DeBerardinis, M. Deshmukh, N. Di Daniele, F. Di Virgilio, V. M. Dixit, S. J. Dixon, C. S. Duckett, B. D. Dynlacht, W. S. El-Deiry, J. W. Elrod, G. M. Fimia, S. Fulda, A. J. Garcia-Saez, A. D. Garg, C. Garrido, E. Gavathiotis, P. Golstein, E. Gottlieb, D.

R. Green, L. A. Greene, H. Gronemeyer, A. Gross, G. Hajnoczky, J. M. Hardwick, I. S. Harris, M. O. Hengartner, C. Hetz, H. Ichijo, M. Jaattela, B. Joseph, P. J. Jost, P. P. Juin, W. J. Kaiser, M. Karin, T. Kaufmann, O. Kepp, A. Kimchi, R. N. Kitsis, D. J. Klionsky, R. A. Knight, S. Kumar, S. W. Lee, J. J. Lemasters, B. Levine, A. Linkermann, S. A. Lipton, R. A. Lockshin, C. Lopez-Otin, S. W. Lowe, T. Luedde, E. Lugli, M. MacFarlane, F. Madeo, M. Malewicz, W. Malorni, G. Manic, J. C. Marine, S. J. Martin, J. C. Martinou, J. P. Medema, P. Mehlen, P. Meier, S. Melino, E. A. Miao, J. D. Molkentin, U. M. Moll, C. Munoz-Pinedo, S. Nagata, G. Nunez, A. Oberst, M. Oren, M. Overholtzer, M. Pagano, T. Panaretakis, M. Pasparakis, J. M. Penninger, D. M. Pereira, S. Pervaiz, M. E. Peter, M. Piacentini, P. Pinton, J. H. M. Prehn, H. Puthalakath, G. A. Rabinovich, M. Rehm, R. Rizzuto, C. M. P. Rodrigues, D. C. Rubinsztein, T. Rudel, K. M. Ryan, E. Sayan, L. Scorrano, F. Shao, Y. Shi, J. Silke, H. U. Simon, A. Sistigu, B. R. Stockwell, A. Strasser, G. Szabadkai, S. W. G. Tait, D. Tang, N. Tavernarakis, A. Thorburn, Y. Tsujimoto, B. Turk, T. Vanden Berghe, P. Vandenabeele, M. G. Vander Heiden, A. Villunger, H. W. Virgin, K. H. Vousden, D. Vucic, E. F. Wagner, H. Walczak, D. Wallach, Y. Wang, J. A. Wells, W. Wood, J. Yuan, Z. Zakeri, B. Zhivotovsky, L. Zitvogel, G. Melino, and G. Kroemer. 2018. 'Molecular mechanisms of cell death: recommendations of the Nomenclature Committee on Cell Death 2018', *Cell Death Differ*, 25: 486-541.

Galluzzi, L., I. Vitale, S. Warren, S. Adjemian, P. Agostinis, A. B. Martinez, T. A. Chan, G. Coukos, S. Demaria, E. Deutsch, D. Draganov, R. L. Edelson, S. C. Formenti, J. Fucikova, L. Gabriele, U. S. Gaipl, S. R. Gameiro, A. D. Garg, E. Golden, J. Han, K. J. Harrington, A. Hemminki, J. W. Hodge, D. M. S. Hossain, T. Illidge, M. Karin, H. L. Kaufman, O. Kepp, G. Kroemer, J. J. Lasarte, S. Loi, M. T. Lotze, G. Manic, T. Merghoub, A. A. Melcher, K. L. Mossman, F. Prosper, O. Rekdal, M. Rescigno, C. Riganti, A. Sistigu, M. J. Smyth, R. Spisek, J. Stagg, B. E. Strauss, D. Tang, K. Tatsuno, S. W. van Gool, P. Vandenabeele, T. Yamazaki, D. Zamarin, L. Zitvogel, A. Cesano, and F. M. Marincola. 2020. 'Consensus guidelines for the definition, detection and interpretation of immunogenic cell death', *J Immunother Cancer*, 8.

Garris, C. S., S. P. Arlauckas, R. H. Kohler, M. P. Trefny, S. Garren, C. Piot, C. Engblom, C. Pfirschke, M. Siwicki, J. Gungabeesoon, G. J. Freeman, S. E. Warren, S. Ong, E. Browning, C. G. Twitty, R. H. Pierce, M. H. Le, A. P. Algazi, A. I. Daud, S. I. Pai, A. Zippelius, R. Weissleder, and M. J. Pittet. 2018. 'Successful Anti-PD-1 Cancer Immunotherapy Requires T Cell-Dendritic Cell Crosstalk Involving the Cytokines IFN-gamma and IL-12', *Immunity*, 49: 1148-61 e7.

Ge, Y., L. Chen, S. Liu, J. Zhao, H. Zhang, and P. R. Chen. 2019. 'Enzyme-Mediated Intercellular Proximity Labeling for Detecting Cell-Cell Interactions', *J Am Chem Soc*, 141: 1833-37.

Gettinger, S., J. Choi, K. Hastings, A. Truini, I. Datar, R. Sowell, A. Wurtz, W. Dong, G. Cai, M. Ann Melnick, V. Y. Du, J. Schlessinger, S. B. Goldberg, A. Chiang, M. F. Sanmamed, I. Melero, J. Agorreta, L. Montuenga, R. Lifton, S. Ferrone, P. Kavathas, D. L. Rimm, S. M. Kaech, K. Schalper, R. S. Herbst, and K. Politi. 2017. 'Impaired HLA Class I Antigen Processing and Presentation as a Mechanism of Acquired Resistance to Immune Checkpoint Inhibitors in Lung Cancer', *Cancer Discov*, 7: 1420-35.

Gharagozloo, M., S. Mahmoud, C. Simard, T. M. Mahvelati, A. Amrani, and D. Gris. 2018. 'The Dual Immunoregulatory function of Nlrp12 in T Cell-Mediated Immune Response: Lessons from Experimental Autoimmune Encephalomyelitis', *Cells*, 7.

Gnanaprakasam, J. N., and R. Wang. 2017. 'MYC in Regulating Immunity: Metabolism and Beyond', *Genes (Basel)*, 8.

Goldrath, A. W., and M. J. Bevan. 1999. 'Low-affinity ligands for the TCR drive proliferation of mature CD8+ T cells in lymphopenic hosts', *Immunity*, 11: 183-90.

Green, D. R., T. Ferguson, L. Zitvogel, and G. Kroemer. 2009. 'Immunogenic and tolerogenic cell death', *Nat Rev Immunol*, 9: 353-63.

Green, M. R., S. Monti, S. J. Rodig, P. Juszczynski, T. Currie, E. O'Donnell, B. Chapuy, K. Takeyama, D. Neuberg, T. R. Golub, J. L. Kutok, and M. A. Shipp. 2010. 'Integrative analysis reveals selective 9p24.1 amplification, increased PD-1 ligand expression, and further induction via JAK2 in nodular sclerosing Hodgkin lymphoma and primary mediastinal large B-cell lymphoma', *Blood*, 116: 3268-77.

Griguolo, G., T. Pascual, M. V. Dieci, V. Guarneri, and A. Prat. 2019. 'Interaction of host immunity with HER2-targeted treatment and tumor heterogeneity in HER2-positive breast cancer', *J Immunother Cancer*, 7: 90.

Gros, A., P. F. Robbins, X. Yao, Y. F. Li, S. Turcotte, E. Tran, J. R. Wunderlich, A. Mixon, S. Farid, M. E. Dudley, K. Hanada, J. R. Almeida, S. Darko, D. C. Douek, J. C. Yang, and S. A. Rosenberg. 2014. 'PD-1 identifies the patient-specific CD8(+) tumor-reactive repertoire infiltrating human tumors', *J Clin Invest*, 124: 2246-59.

Guo, A., H. Huang, Z. Zhu, M. J. Chen, H. Shi, S. Yuan, P. Sharma, J. P. Connelly, S. Liedmann, Y. Dhungana, Z. Li, D. Haydar, M. Yang, H. Beere, J. T. Yustein, C. DeRenzo, S. M. Pruett-Miller, J. C. Crawford, G. Krenciute, C. W. M. Roberts, H. Chi, and D. R. Green. 2022. 'cBAF complex components and MYC cooperate early in CD8(+) T cell fate', *Nature*, 607: 135-41.

Gupta, P. K., J. Godec, D. Wolski, E. Adland, K. Yates, K. E. Pauken, C. Cosgrove, C. Ledderose, W. G. Junger, S. C. Robson, E. J. Wherry, G. Alter, P. J. Goulder, P. Klenerman, A. H. Sharpe, G. M. Lauer, and W. N. Haining. 2015. 'CD39 Expression Identifies Terminally Exhausted CD8+ T Cells', *PLoS Pathog*, 11: e1005177.

Guy, C., D. M. Mitrea, P. C. Chou, J. Temirov, K. M. Vignali, X. Liu, H. Zhang, R. Kriwacki, M. P. Bruchez, S. C. Watkins, C. J. Workman, and D. A. A. Vignali. 2022. 'LAG3 associates with TCR-CD3 complexes and suppresses signaling by driving co-receptor-Lck dissociation', *Nat Immunol*, 23: 757-67.

Hanahan, D., and R. A. Weinberg. 2011. 'Hallmarks of cancer: the next generation', *Cell*, 144: 646-74.

Hannesdottir, L., P. Tymoszuk, N. Parajuli, M. H. Wasmer, S. Philipp, N. Daschil, S. Datta, J. B. Koller, C. H. Tripp, P. Stoitzner, E. Muller-Holzner, G. J. Wiegers, V. Sexl, A. Villunger, and W. Doppler. 2013. 'Lapatinib and doxorubicin enhance the Stat1-dependent antitumor immune response', *Eur J Immunol*, 43: 2718-29.

Hansen, T. H., and M. Bouvier. 2009. 'MHC class I antigen presentation: learning from viral evasion strategies', *Nat Rev Immunol*, 9: 503-13.

Hasegawa, H., and T. Matsumoto. 2018. 'Mechanisms of Tolerance Induction by Dendritic Cells In Vivo', *Front Immunol*, 9: 350.

Hasim, A., M. Abudula, R. Aimiduo, J. Q. Ma, Z. Jiao, G. Akula, T. Wang, and A. Abudula. 2012. 'Post-transcriptional and epigenetic regulation of antigen processing machinery (APM) components and HLA-I in cervical cancers from Uighur women', *PLoS ONE*, 7: e44952.

Haslam, A., J. Gill, and V. Prasad. 2020. 'Estimation of the Percentage of US Patients With Cancer Who Are Eligible for Immune Checkpoint Inhibitor Drugs', *JAMA Netw Open*, 3: e200423.

Havel, J. J., D. Chowell, and T. A. Chan. 2019. 'The evolving landscape of biomarkers for checkpoint inhibitor immunotherapy', *Nat Rev Cancer*, 19: 133-50.

Hay, Z. L. Z., J. R. Knapp, R. E. Magallon, B. P. O'Connor, and J. E. Slansky. 2023. 'Low TCR Binding Strength Results in Increased Progenitor-like CD8+ Tumor-Infiltrating Lymphocytes', *Cancer Immunol Res*, 11: 570-82.

He, R., S. Hou, C. Liu, A. Zhang, Q. Bai, M. Han, Y. Yang, G. Wei, T. Shen, X. Yang, L. Xu, X. Chen, Y. Hao, P. Wang, C. Zhu, J. Ou, H. Liang, T. Ni, X. Zhang, X. Zhou, K. Deng, Y. Chen, Y. Luo, J. Xu, H. Qi, Y. Wu, and L. Ye. 2016. 'Follicular CXCR5- expressing CD8(+) T cells curtail chronic viral infection', *Nature*, 537: 412-28.

Hislop, A. D., M. E. Ressing, D. van Leeuwen, V. A. Pudney, D. Horst, D. Koppers-Lalic, N. P. Croft, J. J. Neefjes, A. B. Rickinson, and E. J. Wiertz. 2007. 'A CD8+ T cell immune evasion protein specific to Epstein-Barr virus and its close relatives in Old World primates', *J Exp Med*, 204: 1863-73.

Hoare, M., Y. Ito, T. W. Kang, M. P. Weekes, N. J. Matheson, D. A. Patten, S. Shetty, A. J. Parry, S. Menon, R. Salama, R. Antrobus, K. Tomimatsu, W. Howat, P. J. Lehner, L. Zender, and M. Narita. 2016. 'NOTCH1 mediates a switch between two distinct secretomes during senescence', *Nat Cell Biol*, 18: 979-92.

Hofer, M., and M. P. Lutolf. 2021. 'Engineering organoids', *Nat Rev Mater*, 6: 402-20.

Huang, H., E. Langenkamp, M. Georganaki, A. Loskog, P. F. Fuchs, L. C. Dieterich, J. Kreuger, and A. Dimberg. 2015. 'VEGF suppresses T-lymphocyte infiltration in the tumor microenvironment through inhibition of NF-kappaB-induced endothelial activation', *FASEB J*, 29: 227-38.

Huch, M., C. Dorrell, S. F. Boj, J. H. van Es, V. S. Li, M. van de Wetering, T. Sato, K. Hamer, N. Sasaki, M. J. Finegold, A. Haft, R. G. Vries, M. Grompe, and H. Clevers. 2013. 'In vitro expansion of single Lgr5+ liver stem cells induced by Wnt-driven regeneration', *Nature*, 494: 247-50.

Huch, M., H. Gehart, R. van Boxtel, K. Hamer, F. Blokzijl, M. M. Verstegen, E. Ellis, M. van Wenum, S. A. Fuchs, J. de Ligt, M. van de Wetering, N. Sasaki, S. J. Boers, H. Kemperman, J. de Jonge, J. N. Ijzermans, E. E. Nieuwenhuis, R. Hoekstra, S. Strom, R. R. Vries, L. J. van der Laan, E. Cuppen, and H. Clevers. 2015. 'Long-term culture of genome-stable bipotent stem cells from adult human liver', *Cell*, 160: 299-312.

Hui, E., J. Cheung, J. Zhu, X. Su, M. J. Taylor, H. A. Wallweber, D. K. Sasmal, J. Huang, J. M. Kim, I. Mellman, and R. D. Vale. 2017. 'T cell costimulatory receptor CD28 is a primary target for PD-1-mediated inhibition', *Science*, 355: 1428-33.

Hwang, J. R., Y. Byeon, D. Kim, and S. G. Park. 2020. 'Recent insights of T cell receptor-mediated signaling pathways for T cell activation and development', *Exp Mol Med*, 52: 750-61.

Im, S. J., M. Hashimoto, M. Y. Gerner, J. Lee, H. T. Kissick, M. C. Burger, Q. Shan, J. S. Hale, J. Lee, T. H. Nasti, A. H. Sharpe, G. J. Freeman, R. N. Germain, H. I. Nakaya, H. H. Xue, and R. Ahmed. 2016. 'Defining CD8+ T cells that provide the proliferative burst after PD-1 therapy', *Nature*, 537: 417-21.

Im, S. J., M. Hashimoto, M. Y. Gerner, J. Lee, H. T. Kissick, M. C. B. Urger, Q. Shan, J. S. Hale, J. Lee, T. H. Nasti, A. H. Sharpe, G. J. Freeman, R. N. Germain, H. I. Nakaya, H. H. Xue, and R. Ahmed. 2016. 'Defining CD8(+) T cells that provide the proliferative burst after PD-1 therapy', *Nature*, 537: 417-+.

Inoue, M., K. Mimura, S. Izawa, K. Shiraishi, A. Inoue, S. Shiba, M. Watanabe, T. Maruyama, Y. Kawaguchi, S. Inoue, T. Kawasaki, A. Choudhury, R. Katoh, H. Fujii, R. Kiessling, and K. Kono. 2012. 'Expression of MHC Class I on breast cancer cells correlates inversely with HER2 expression', *Oncoimmunology*, 1: 1104-10.

James, K. D., W. E. Jenkinson, and G. Anderson. 2018. 'T-cell egress from the thymus: Should I stay or should I go?', *J Leukoc Biol*, 104: 275-84.

Jansen, C. S., N. Prokhnevska, V. A. Master, M. G. Sanda, J. W. Carlisle, M. A. Bilen, M. Cardenas, S. Wilkinson, R. Lake, A. G. Sowalsky, R. M. Valanparambil, W. H. Hudson, D. McGuire, K. Melnick, A. I. Khan, K. Kim, Y. M. Chang, A. Kim, C. P. Filson, M. Alemozaffar, A. O. Osunkoya, P. Mullane, C. Ellis, R. Akondy, S. J. Im, A. O. Kamphorst, A. Reyes, Y. Liu, and H. Kissick. 2019. 'An intra-tumoral niche maintains and differentiates stem-like CD8 T cells', *Nature*, 576: 465-70.

Jeannet, G., C. Boudousquie, N. Gardiol, J. Kang, J. Huelsken, and W. Held. 2010. 'Essential role of the Wnt pathway effector Tcf-1 for the establishment of functional CD8 T cell memory', *Proc Natl Acad Sci U S A*, 107: 9777-82.

Jiao, L., J. Chen, X. Wu, B. Cai, Z. Su, and L. Wang. 2020. 'Correlation of CpG methylation of the Pdcd1 gene with PD-1 expression on CD8(+) T cells and medical laboratory indicators in chronic hepatitis B infection', *J Gene Med*, 22: e3148.

Johnson, D. B., C. A. Nebhan, J. J. Moslehi, and J. M. Balko. 2022. 'Immune-checkpoint inhibitors: long-term implications of toxicity', *Nat Rev Clin Oncol*, 19: 254-67.

Jorgovanovic, D., M. Song, L. Wang, and Y. Zhang. 2020. 'Roles of IFN-gamma in tumor progression and regression: a review', *Biomark Res*, 8: 49.

Kansara, M., H. S. Leong, D. M. Lin, S. Popkiss, P. Pang, D. W. Garsed, C. R. Walkley, C. Cullinane, J. Ellul, N. M. Haynes, R. Hicks, M. L. Kuijjer, A. M. Cleton-Jansen, P. W. Hinds, M. J. Smyth, and D. M. Thomas. 2013. 'Immune response to RB1-regulated senescence limits radiation-induced osteosarcoma formation', *J Clin Invest*, 123: 5351-60.

Khan, G., C. Fitzmaurice, M. Naghavi, and L. A. Ahmed. 2020. 'Global and regional incidence, mortality and disability-adjusted life-years for Epstein-Barr virus-attributable malignancies, 1990-2017', *BMJ Open*, 10: e037505.

Khan, O., J. R. Giles, S. McDonald, S. Manne, S. F. Ngiow, K. P. Patel, M. T. Werner, A. C. Huang, K. A. Alexander, J. E. Wu, J. Attanasio, P. Yan, S. M. George, B. Bengsch, R. P. Staupe, G. Donahue, W. Xu, R. K. Amaravadi, X. Xu, G. C. Karakousis, T. C. Mitchell, L. M. Schuchter, J. Kaye, S. L. Berger, and E. J. Wherry. 2019. 'TOX transcriptionally and epigenetically programs CD8(+) T cell exhaustion', *Nature*, 571: 211-18.

Kortlever, R. M., N. M. Sodir, C. H. Wilson, D. L. Burkhart, L. Pellegrinet, L. Brown Swigart, T. D. Littlewood, and G. I. Evan. 2017. 'Myc Cooperates with Ras by Programming Inflammation and Immune Suppression', *Cell*, 171: 1301-15.e14.

Krummel, M. F., and J. P. Allison. 1995. 'CD28 and CTLA-4 have opposing effects on the response of T cells to stimulation', *J Exp Med*, 182: 459-65.

Krummel, M. F., F. Bartumeus, and A. Gerard. 2016. 'T cell migration, search strategies and mechanisms', *Nat Rev Immunol*, 16: 193-201.

Krump, N. A., and J. You. 2018. 'Molecular mechanisms of viral oncogenesis in humans', *Nat Rev Microbiol*, 16: 684-98.

Kumar, B. V., T. J. Connors, and D. L. Farber. 2018. 'Human T Cell Development, Localization, and Function throughout Life', *Immunity*, 48: 202-13.

Kurtulus, S., A. Madi, G. Escobar, M. Klapholz, J. Nyman, E. Christian, M. Pawlak, D. Dionne, J. Xia, O. Rozenblatt-Rosen, V. K. Kuchroo, A. Regev, and A. C. Anderson. 2019. 'Checkpoint Blockade Immunotherapy Induces Dynamic Changes in PD-1(-)CD8(+) Tumor-Infiltrating T Cells', *Immunity*, 50: 181-94 e6.

Langowski, J. L., X. Zhang, L. Wu, J. D. Mattson, T. Chen, K. Smith, B. Basham, T. McClanahan, R. A. Kastelein, and M. Oft. 2006. 'IL-23 promotes tumour incidence and growth', *Nature*, 442: 461-5.

Lee, J., E. Ahn, H. T. Kissick, and R. Ahmed. 2015. 'Reinvigorating Exhausted T Cells by Blockade of the PD-1 Pathway', *For Immunopathol Dis Therap*, 6: 7-17.

Legut, M., D. K. Cole, and A. K. Sewell. 2015. 'The promise of gammadelta T cells and the gammadelta T cell receptor for cancer immunotherapy', *Cell Mol Immunol*, 12: 656-68.

Leko, V., and S. A. Rosenberg. 2020. 'Identifying and Targeting Human Tumor Antigens for T Cell-Based Immunotherapy of Solid Tumors', *Cancer Cell*, 38: 454-72.

Li, H., A. M. van der Leun, I. Yofe, Y. Lubling, D. Gelbard-Solodkin, A. C. J. van Akkooi, M. van den Braber, E. A. Rozeman, Jbag Haanen, C. U. Blank, H. M. Horlings, E. David, Y. Baran, A. Bercovich, A. Lifshitz, T. N. Schumacher, A. Tanay, and I. Amit. 2019. 'Dysfunctional CD8 T Cells Form a Proliferative, Dynamically Regulated Compartment within Human Melanoma', *Cell*, 176: 775-89 e18.

Li, J., S. K. Figueira, A. C. Vrazo, B. F. Binkowski, B. L. Butler, Y. Tabata, A. Filipovich, M. B. Jordan, and K. A. Risma. 2014. 'Real-time detection of CTL function reveals distinct patterns of caspase activation mediated by Fas versus granzyme B', *J Immunol*, 193: 519-28.

Li, M. O., Y. Y. Wan, S. Sanjabi, A. K. Robertson, and R. A. Flavell. 2006. 'Transforming growth factor-beta regulation of immune responses', *Annu Rev Immunol*, 24: 99-146.

Li, P., T. Huang, Q. Zou, D. Liu, Y. Wang, X. Tan, Y. Wei, and H. Qiu. 2019. 'FGFR2 Promotes Expression of PD-L1 in Colorectal Cancer via the JAK/STAT3 Signaling Pathway', *J Immunol*, 202: 3065-75.

Lu, W. J., and J. M. Abrams. 2006. 'Lessons from p53 in non-mammalian models', *Cell Death Differ*, 13: 909-12.

Macian, F., F. Garcia-Cozar, S. H. Im, H. F. Horton, M. C. Byrne, and A. Rao. 2002. 'Transcriptional mechanisms underlying lymphocyte tolerance', *Cell*, 109: 719-31.

Makunts, T., K. Burkhart, R. Abagyan, and P. Lee. 2022. 'Retrospective analysis of clinical trial safety data for pembrolizumab reveals the effect of co-occurring infections on immune-related adverse events', *PLoS One*, 17: e0263402.

Mandai, M., J. Hamanishi, K. Abiko, N. Matsumura, T. Baba, and I. Konishi. 2016. 'Dual Faces of IFNgamma in Cancer Progression: A Role of PD-L1 Induction in the Determination of Pro- and Antitumor Immunity', *Clin Cancer Res*, 22: 2329-34.

Markosyan, N., J. Li, Y. H. Sun, L. P. Richman, J. H. Lin, F. Yan, L. Quinones, Y. Sela, T. Yamazoe, N. Gordon, J. W. Tobias, K. T. Byrne, A. J. Rech, G. A. FitzGerald, B. Z. Stanger, and R. H. Vonderheide. 2019. 'Tumor cell-intrinsic EPHA2 suppresses anti-tumor immunity by regulating PTGS2 (COX-2)', *J Clin Invest*, 129: 3594-609.

Martinez, G. J., R. M. Pereira, T. Aijo, E. Y. Kim, F. Marangoni, M. E. Pipkin, S. Togher, V. Heissmeyer, Y. C. Zhang, S. Crotty, E. D. Lamperti, K. M. Ansel, T. R. Mempel, H. Lahdesmaki, P. G. Hogan, and A. Rao. 2015. 'The transcription factor NFAT promotes exhaustion of activated CD8(+) T cells', *Immunity*, 42: 265-78.

McCormick, C., and D. Ganem. 2005. 'The kaposin B protein of KSHV activates the p38/MK2 pathway and stabilizes cytokine mRNAs', *Science*, 307: 739-41.

McLane, L. M., M. S. Abdel-Hakeem, and E. J. Wherry. 2019. 'CD8 T Cell Exhaustion During Chronic Viral Infection and Cancer', *Annu Rev Immunol*.

Miller, B. C., D. R. Sen, R. Al Abosy, K. Bi, Y. V. Virkud, M. W. LaFleur, K. B. Yates, A. Lako, K. Felt, G. S. Naik, M. Manos, E. Gjini, J. R. Kuchroo, J. J. Ishizuka, J. L. Collier, G. K. Griffin, S. Maleri, D. E. Comstock, S. A. Weiss, F. D. Brown, A. Panda, M. D. Zimmer, R. T. Manguso, F. S. Hodi, S. J. Rodig, A. H. Sharpe, and W. N. Haining. 2019. 'Subsets of exhausted CD8(+) T cells differentially mediate tumor control and respond to checkpoint blockade', *Nat Immunol*, 20: 326-36.

Moasser, M. M. 2007. 'The oncogene HER2: its signaling and transforming functions and its role in human cancer pathogenesis', *Oncogene*, 26: 6469-87.

Mognol, G. P., R. Spreafico, V. Wong, J. P. Scott-Browne, S. Togher, A. Hoffmann, P. G. Hogan, A. Rao, and S. Trifari. 2017. 'Exhaustion-associated regulatory regions in CD8(+) tumor-infiltrating T cells', *Proc Natl Acad Sci U S A*, 114: E2776-E85.

Moore, P. S., and Y. Chang. 2010. 'Why do viruses cause cancer? Highlights of the first century of human tumour virology', *Nat Rev Cancer*, 10: 878-89.

Mootha, V. K., C. M. Lindgren, K. F. Eriksson, A. Subramanian, S. Sihag, J. Lehar, P. Puigserver, E. Carlsson, M. Ridderstrale, E. Laurila, N. Houstis, M. J. Daly, N. Patterson, J. P. Mesirov, T. R. Golub, P. Tamayo, B. Spiegelman, E. S. Lander, J. N. Hirschhorn, D. Altshuler, and L. C. Groop. 2003. 'PGC-1alpha-responsive genes involved in oxidative phosphorylation are coordinately downregulated in human diabetes', *Nat Genet*, 34: 267-73.

Morimoto, J., X. Tan, R. M. Teague, C. Ohlen, and P. D. Greenberg. 2007. 'Induction of tolerance in CD8+ T cells to a transgenic autoantigen expressed in the liver does not require cross-presentation', *J Immunol*, 178: 6849-60.

Mueller, D. L. 2010. 'Mechanisms maintaining peripheral tolerance', *Nat Immunol*, 11: 21-7.

Munoz-Fontela, C., A. Mandinova, S. A. Aaronson, and S. W. Lee. 2016. 'Emerging roles of p53 and other tumour-suppressor genes in immune regulation', *Nat Rev Immunol*, 16: 741-50.

Nagy, J. A., S. H. Chang, A. M. Dvorak, and H. F. Dvorak. 2009. 'Why are tumour blood vessels abnormal and why is it important to know?', *Br J Cancer*, 100: 865-9.

Nakayama, A., H. Abe, A. Kunita, R. Saito, T. Kanda, H. Yamashita, Y. Seto, S. Ishikawa, and M. Fukayama. 2019. 'Viral loads correlate with upregulation of PD-L1 and worse patient prognosis in Epstein-Barr Virus-associated gastric carcinoma', *PLoS ONE*, 14: e0211358.

Nishino, M., A. Giobbie-Hurder, H. Hatabu, N. H. Ramaiya, and F. S. Hodi. 2016. 'Incidence of Programmed Cell Death 1 Inhibitor-Related Pneumonitis in Patients With Advanced Cancer: A Systematic Review and Meta-analysis', *JAMA Oncol*, 2: 1607-16.

Nussing, S., J. A. Trapani, and I. A. Parish. 2020. 'Revisiting T Cell Tolerance as a Checkpoint Target for Cancer Immunotherapy', *Front Immunol*, 11: 589641.

Ohlen, C., M. Kalos, L. E. Cheng, A. C. Shur, D. J. Hong, B. D. Carson, N. C. Kokot, C. G. Lerner, B. D. Sather, E. S. Huseby, and P. D. Greenberg. 2002. 'CD8(+) T cell tolerance to a tumor-associated antigen is maintained at the level of expansion rather than effector function', *J Exp Med*, 195: 1407-18.

Ohlen, C., M. Kalos, D. J. Hong, A. C. Shur, and P. D. Greenberg. 2001. 'Expression of a tolerizing tumor antigen in peripheral tissue does not preclude recovery of high-affinity CD8+ T cells or CTL immunotherapy of tumors expressing the antigen', *J Immunol*, 166: 2863-70.

Oliveira, G., K. Stromhaug, S. Klaeger, T. Kula, D. T. Frederick, P. M. Le, J. Forman, T. Huang, S. Li, W. Zhang, Q. Xu, N. Cieri, K. R. Clauser, S. A. Shukla, D. Neuberg, S. Justesen, G. MacBeath, S. A. Carr, E. F. Fritsch, N. Hacohen, M. Sade-Feldman, K. J. Livak, G. M. Boland, P. A. Ott, D. B. Keskin, and C. J. Wu. 2021. 'Phenotype, specificity and avidity of antitumour CD8(+) T cells in melanoma', *Nature*, 596: 119-25.

Pandey, N. V. 2020. 'DNA viruses and cancer: insights from evolutionary biology', *Virusdisease*, 31: 1-9.

Paulsen, S. J., M. M. Rosenkilde, J. Eugen-Olsen, and T. N. Kledal. 2005. 'Epstein-Barr virus-encoded BILF1 is a constitutively active G protein-coupled receptor', *J Virol*, 79: 536-46.

Pedersen, M. H., B. L. Hood, H. C. Beck, T. P. Conrads, H. J. Ditzel, and R. Leth-Larsen. 2017. 'Downregulation of antigen presentation-associated pathway proteins is linked to poor outcome in triple-negative breast cancer patient tumors', *Oncoimmunology*, 6: e1305531.

Peng, W. C., C. Y. Logan, M. Fish, T. Anbarchian, F. Aguisanda, A. Alvarez-Varela, P. Wu, Y. Jin, J. Zhu, B. Li, M. Grompe, B. Wang, and R. Nusse. 2018. 'Inflammatory Cytokine TNFalpha Promotes the Long-Term Expansion of Primary Hepatocytes in 3D Culture', *Cell*, 175: 1607-19 e15.

Petrazzuolo, A., M. Perez-Lanzon, I. Martins, P. Liu, O. Kepp, V. Minard-Colin, M. C. Maiuri, and G. Kroemer. 2021. 'Pharmacological inhibitors of anaplastic lymphoma kinase (ALK) induce immunogenic cell death through on-target effects', *Cell Death Dis*, 12: 713.

Petrelli, F., G. Grizzi, M. Ghidini, A. Ghidini, M. Ratti, S. Panni, M. Cabiddu, M. Ghilardi, K. Borgonovo, M. C. Parati, G. Tomasello, S. Barni, A. Berruti, and M. Brighenti. 2020. 'Immune-related Adverse Events and Survival in Solid Tumors Treated With Immune Checkpoint Inhibitors: A Systematic Review and Meta-Analysis', *J Immunother*, 43: 1-7.

Pfaffl, M. W. 2001. 'A new mathematical model for relative quantification in real-time RT-PCR', *Nucleic Acids Res*, 29: e45.

Philip, M., L. Fairchild, L. Sun, E. L. Horste, S. Camara, M. Shakiba, A. C. Scott, A. Viale, P. Lauer, T. Merghoub, M. D. Hellmann, J. D. Wolchok, C. S. Leslie, and A. Schietinger. 2017. 'Chromatin states define tumour-specific T cell dysfunction and reprogramming', *Nature*, 545: 452-56.

Philip, M., and A. Schietinger. 2019. 'Heterogeneity and fate choice: T cell exhaustion in cancer and chronic infections', *Curr Opin Immunol*, 58: 98-103.

———. 2021. 'CD8(+) T cell differentiation and dysfunction in cancer', *Nat Rev Immunol*.

———. 2022. 'CD8(+) T cell differentiation and dysfunction in cancer', *Nat Rev Immunol*, 22: 209-23.

Postow, M. A., R. Sidlow, and M. D. Hellmann. 2018. 'Immune-Related Adverse Events Associated with Immune Checkpoint Blockade', *N Engl J Med*, 378: 158-68.

Pylayeva-Gupta, Y., S. Das, J. S. Handler, C. H. Hajdu, M. Coffre, S. B. Koralov, and D. Bar-Sagi. 2016. 'IL35-Producing B Cells Promote the Development of Pancreatic Neoplasia', *Cancer Discov*, 6: 247-55.

Pylayeva-Gupta, Y., K. E. Lee, C. H. Hajdu, G. Miller, and D. Bar-Sagi. 2012. 'Oncogenic Kras-induced GM-CSF production promotes the development of pancreatic neoplasia', *Cancer Cell*, 21: 836-47.

Qian, C., L. Qian, Y. Yu, H. An, Z. Guo, Y. Han, Y. Chen, Y. Bai, Q. Wang, and X. Cao. 2013. 'Fas signal promotes the immunosuppressive function of regulatory dendritic cells via the ERK/beta-catenin pathway', *J Biol Chem*, 288: 27825-35.

Rathmell, J. C. 2011. 'T cell Myc-tabolism', *Immunity*, 35: 845-6.

Redmond, W. L., B. C. Marincek, and L. A. Sherman. 2005. 'Distinct requirements for deletion versus anergy during CD8 T cell peripheral tolerance in vivo', *J Immunol*, 174: 2046-53.

Redmond, W. L., and L. A. Sherman. 2005. 'Peripheral tolerance of CD8 T lymphocytes', *Immunity*, 22: 275-84.

Rivas, C., S. A. Aaronson, and C. Munoz-Fontela. 2010. 'Dual Role of p53 in Innate Antiviral Immunity', *Viruses*, 2: 298-313.

Roemer, M. G., R. H. Advani, A. H. Ligon, Y. Natkunam, R. A. Redd, H. Homer, C. F. Connelly, H. H. Sun, S. E. Daadi, G. J. Freeman, P. Armand, B. Chapuy, D. de Jong, R. T. Hoppe, D. S. Neuberg, S. J. Rodig, and M. A. Shipp. 2016. 'PD-L1 and PD-L2 Genetic Alterations Define Classical Hodgkin Lymphoma and Predict Outcome', *J Clin Oncol*, 34: 2690-7.

Roetman, J. J., M. K. I. Apostolova, and M. Philip. 2022. 'Viral and cellular oncogenes promote immune evasion', *Oncogene*, 41: 921-29.

Rosenberg, S. A., and D. E. White. 1996. 'Vitiligo in patients with melanoma: normal tissue antigens can be targets for cancer immunotherapy', *J Immunother Emphasis Tumor Immunol*, 19: 81-4.

Rous, P. 1911. 'A SARCOMA OF THE FOWL TRANSMISSIBLE BY AN AGENT SEPARABLE FROM THE TUMOR CELLS', *J Exp Med*, 13: 397-411.

Russell, M. L., A. Souquette, D. M. Levine, S. A. Schattgen, E. K. Allen, G. Kuan, N. Simon, A. Balmaseda, A. Gordon, P. G. Thomas, F. A. th Matsen, and P. Bradley. 2022. 'Combining genotypes and T cell receptor distributions to infer genetic loci determining V(D)J recombination probabilities', *Elife*, 11.

Sade-Feldman, M., Y. J. Jiao, J. H. Chen, M. S. Rooney, M. Barzily-Rokni, J. P. Eliane, S. L. Bjorgaard, M. R. Hammond, H. Vitzthum, S. M. Blackmon, D. T. Frederick, M. Hazar-Rethinam, B. A. Nadres, E. E. Van Seventer, S. A. Shukla, K. Yizhak, J. P. Ray, D. Rosebrock, D. Livitz, V. Adalsteinsson, G. Getz, L. M. Duncan, B. Li, R. B. Corcoran, D. P. Lawrence, A. Stemmer-Rachamimov, G. M. Boland, D. A. Landau, K. T. Flaherty, R. J. Sullivan, and N. Hacohen. 2017. 'Resistance to checkpoint blockade therapy through inactivation of antigen presentation', *Nat Commun*, 8: 1136.

Sade-Feldman, M., K. Yizhak, S. L. Bjorgaard, J. P. Ray, C. G. de Boer, R. W. Jenkins, D. J. Lieb, J. H. Chen, D. T. Frederick, M. Barzily-Rokni, S. S. Freeman, A. Reuben, P. J. Hoover, A. C. Villani, E. Ivanova, A. Portell, P. H. Lizotte, A. R. Aref, J. P. Eliane, M. R. Hammond, H. Vitzthum, S. M. Blackmon, B. Li, V. Gopalakrishnan, S. M. Reddy, Z. A. Cooper, C. P. Paweletz, D. A. Barbie, A. Stemmer-

Rachamimov, K. T. Flaherty, J. A. Wargo, G. M. Boland, R. J. Sullivan, G. Getz, and N. Hacohen. 2018. 'Defining T Cell States Associated with Response to Checkpoint Immunotherapy in Melanoma', *Cell*, 175: 998-1013 e20.

Sapkota, B., C. E. Hill, and B. P. Pollack. 2013. 'Vemurafenib enhances MHC induction in BRAF(V600E) homozygous melanoma cells', *Oncoimmunology*, 2: e22890.

Schietinger A, Delrow JJ, Basom RS, Blattman JN, Greenberg PD. 2012. 'Rescued Tolerant CD8 T Cells Are Preprogrammed to Reestablish the Tolerant State', *Science*, 335.

Schietinger, A., J. J. Delrow, R. S. Basom, J. N. Blattman, and P. D. Greenberg. 2012. 'Rescued tolerant CD8 T cells are preprogrammed to reestablish the tolerant state', *Science*, 335: 723-7.

Schietinger, A., and P. D. Greenberg. 2014. 'Tolerance and exhaustion: defining mechanisms of T cell dysfunction', *Trends Immunol*, 35: 51-60.

Schietinger, A., M. Philip, V. E. Krisnawan, E. Y. Chiu, J. J. Delrow, R. S. Basom, P. Lauer, D. G. Brockstedt, S. E. Knoblaugh, G. J. Hammerling, T. D. Schell, N. Garbi, and P. D. Greenberg. 2016. 'Tumor-Specific T Cell Dysfunction Is a Dynamic Antigen-Driven Differentiation Program Initiated Early during Tumorigenesis', *Immunity*, 45: 389-401.

Schietinger, A., M. Philip, and H. Schreiber. 2008. 'Specificity in cancer immunotherapy', *Semin Immunol*, 20: 276-85.

Schievella, A. R., J. H. Chen, J. R. Graham, and L. L. Lin. 1997. 'MADD, a novel death domain protein that interacts with the type 1 tumor necrosis factor receptor and activates mitogen-activated protein kinase', *J Biol Chem*, 272: 12069-75.

Schneider, J. W., and D. P. Dittmer. 2017. 'Diagnosis and Treatment of Kaposi Sarcoma', *Am J Clin Dermatol*, 18: 529-39.

Schoenfeld, A. J., and M. D. Hellmann. 2020. 'Acquired Resistance to Immune Checkpoint Inhibitors', *Cancer Cell*, 37: 443-55.

Scott, A. C., F. Dundar, P. Zumbo, S. S. Chandran, C. A. Klebanoff, M. Shakiba, P. Trivedi, L. Menocal, H. Appleby, S. J. Camara, D. Zamarin, T. Walther, A. C. Snyder, M. R. Femia, E. A. Comen, H. Y. Wen, M. D. Hellmann, N. Anandasabapathy, Y. Liu, N. K. Altorki, P. Lauer, O. Levy, M. Glickman, J. Kaye, D. Betel, M. Philip, and A. Schietinger. 2019a. 'TOX is a critical regulator of tumour-specific T cell differentiation', *Nature*.

———. 2019b. 'TOX is a critical regulator of tumour-specific T cell differentiation', *Nature*, 571: 270-74.

Shakiba, M., P. Zumbo, G. Espinosa-Carrasco, L. Menocal, F. Dundar, S. E. Carson, E. M. Bruno, F. J. Sanchez-Rivera, S. W. Lowe, S. Camara, R. P. Koche, V. P. Reuter, N. D. Socci, B. Whitlock, F. Tamzalit, M. Huse, M. D. Hellmann, D. K. Wells, N. A. Defranoux, D. Betel, M. Philip, and A. Schietinger. 2022. 'TCR signal strength defines distinct mechanisms of T cell dysfunction and cancer evasion', *J Exp Med*, 219.

Siddiqui, I., K. Schaeuble, V. Chennupati, S. A. Fuertes Marraco, S. Calderon-Copete, D. Pais Ferreira, S. J. Carmona, L. Scarpellino, D. Gfeller, S. Pradervand, S. A. Luther, D. E. Speiser, and W. Held. 2019. 'Intratumoral Tcf1(+)PD-1(+)CD8(+) T Cells with Stem-like Properties Promote Tumor Control in Response to Vaccination and Checkpoint Blockade Immunotherapy', *Immunity*, 50: 195-211 e10.

Smith, T. R., G. Verdeil, K. Marquardt, and L. A. Sherman. 2014. 'Contribution of TCR signaling strength to CD8+ T cell peripheral tolerance mechanisms', *J Immunol*, 193: 3409-16.

Spranger, S., R. Bao, and T. F. Gajewski. 2015. 'Melanoma-intrinsic beta-catenin signalling prevents anti-tumour immunity', *Nature*, 523: 231-5.

Stahl, S., T. Sacher, A. Bechtold, U. Protzer, R. Ganss, G. J. Hammerling, B. Arnold, and N. Garbi. 2009. 'Tumor agonist peptides break tolerance and elicit effective CTL responses in an inducible mouse model of hepatocellular carcinoma', *Immunol Lett*, 123: 31-7.

Stanley, M. 2017. 'Tumour virus vaccines: hepatitis B virus and human papillomavirus.' in, *Philos Trans R Soc Lond B Biol Sci*.

Staveley-O'Carroll, K., T. D. Schell, M. Jimenez, L. M. Mylin, M. J. Tevethia, S. P. Schoenberger, and S. S. Tevethia. 2003. 'In vivo ligation of CD40 enhances priming against the endogenous tumor antigen and promotes CD8+ T cell effector function in SV40 T antigen transgenic mice', *J Immunol*, 171: 697-707.

Strong, M. J., T. Laskow, H. Nakhoul, E. Blanchard, Y. Liu, X. Wang, M. Baddoo, Z. Lin, Q. Yin, and E. K. Flemington. 2015. 'Latent Expression of the Epstein-Barr Virus (EBV)-Encoded Major Histocompatibility Complex Class I TAP Inhibitor, BNLF2a, in EBV-Positive Gastric Carcinomas', *J Virol*, 89: 10110-4.

Subramanian, A., P. Tamayo, V. K. Mootha, S. Mukherjee, B. L. Ebert, M. A. Gillette, A. Paulovich, S. L. Pomeroy, T. R. Golub, E. S. Lander, and J. P. Mesirov. 2005. 'Gene set enrichment analysis: a knowledge-based approach for interpreting genome-wide expression profiles', *Proc Natl Acad Sci U S A*, 102: 15545-50.

Suen, A. Y., and T. A. Baldwin. 2012. 'Proapoptotic protein Bim is differentially required during thymic clonal deletion to ubiquitous versus tissue-restricted antigens', *Proc Natl Acad Sci U S A*, 109: 893-8.

Sugiyama, E., Y. Togashi, Y. Takeuchi, S. Shinya, Y. Tada, K. Kataoka, K. Tane, E. Sato, G. Ishii, K. Goto, Y. Shintani, M. Okumura, M. Tsuboi, and H. Nishikawa. 2020. 'Blockade of EGFR improves responsiveness to PD-1 blockade in EGFR-mutated non-small cell lung cancer', *Sci Immunol*, 5.

Tau, G., and P. Rothman. 1999. 'Biologic functions of the IFN-gamma receptors', *Allergy*, 54: 1233-51.

Tay, S. S., Y. C. Wong, D. M. McDonald, N. A. Wood, B. Roediger, F. Sierro, C. McGuffog, I. E. Alexander, G. A. Bishop, J. R. Gamble, W. Weninger, G. W. McCaughan, P. Bertolino, and D. G. Bowen. 2014. 'Antigen expression level threshold tunes the fate of CD8 T cells during primary hepatic immune responses', *Proc Natl Acad Sci U S A*, 111: E2540-9.

Teague, R. M., P. D. Greenberg, C. Fowler, M. Z. Huang, X. Tan, J. Morimoto, M. L. Dossett, E. S. Huseby, and C. Öhlén. 2008. 'Peripheral CD8+ T cell tolerance to self-proteins is regulated proximally at the T cell receptor', *Immunity*, 28: 662-74.

Thommen, D. S., J. Schreiner, P. Muller, P. Herzig, A. Roller, A. Belousov, P. Umana, P. Pisa, C. Klein, M. Bacac, O. S. Fischer, W. Moersig, S. Savic Prince, V. Levitsky, V. Karanikas, D. Lardinois, and A. Zippelius. 2015. 'Progression of Lung Cancer Is Associated with Increased Dysfunction of T Cells Defined by Coexpression of Multiple Inhibitory Receptors', *Cancer Immunol Res*, 3: 1344-55.

Thompson, E. D., H. L. Enriquez, Y. X. Fu, and V. H. Engelhard. 2010. 'Tumor masses support naive T cell infiltration, activation, and differentiation into effectors', *J Exp Med*, 207: 1791-804.

Tooley, K. A., G. Escobar, and A. C. Anderson. 2022. 'Spatial determinants of CD8(+) T cell differentiation in cancer', *Trends Cancer*.

Toso, Alberto, Ajinkya Revandkar, Diletta DiMitri, Ilaria Guccini, Michele Proietti, Manuela Sarti, Sandra Pinton, Jiangwen Zhang, Madhuri Kalathur, Gianluca Civenni, David Jarrossay, Erica Montani, Camilla Marini, Ramon Garcia-Escudero, Eugenio Scanziani, Fabio Grassi, Pier Paolo Pandolfi, Carlo V. Catapano, and Andrea Alimonti. 2014. 'Enhancing chemotherapy efficacy in pten-deficient prostate tumors by activating the senescence-associated antitumor immunity', *Cell Reports*.

Trapani, J. A., and M. J. Smyth. 2002. 'Functional significance of the perforin/granzyme cell death pathway', *Nat Rev Immunol*, 2: 735-47.

Tsurumi, T., M. Fujita, and A. Kudoh. 2005. 'Latent and lytic Epstein-Barr virus replication strategies', *Rev Med Virol*, 15: 3-15.

Twomey, J. D., and B. Zhang. 2021. 'Cancer Immunotherapy Update: FDA-Approved Checkpoint Inhibitors and Companion Diagnostics', *AAPS J*, 23: 39.

Utzschneider, D. T., M. Charmoy, V. Chennupati, L. Pousse, D. P. Ferreira, S. Calderon-Copete, M. Danilo, F. Alfei, M. Hofmann, D. Wieland, S. Pradervand, R. Thimme, D. Zehn, and W. Held. 2016. 'T Cell

Factor 1-Expressing Memory-like CD8(+) T Cells Sustain the Immune Response to Chronic Viral Infections', *Immunity*, 45: 415-27.

Uzhachenko, R. V., V. Bharti, Z. Ouyang, A. Blevins, S. Mont, N. Saleh, H. A. Lawrence, C. Shen, S. C. Chen, G. D. Ayers, D. G. DeNardo, C. Arteaga, A. Richmond, and A. E. Vilgelm. 2021. 'Metabolic modulation by CDK4/6 inhibitor promotes chemokine-mediated recruitment of T cells into mammary tumors', *Cell Rep*, 35: 108944.

van der Leun, A. M., D. S. Thommen, and T. N. Schumacher. 2020. 'CD8(+) T cell states in human cancer: insights from single-cell analysis', *Nat Rev Cancer*.

Verbeek, S., D. Izon, F. Hofhuis, E. Robanus-Maandag, H. te Riele, M. van de Wetering, M. Oosterwegel, A. Wilson, H. R. MacDonald, and H. Clevers. 1995. 'An HMG-box-containing T-cell factor required for thymocyte differentiation', *Nature*, 374: 70-4.

Viramontes, K. M., E. N. Neubert, J. M. DeRogatis, and R. Tinoco. 2022. 'PD-1 Immune Checkpoint Blockade and PSGL-1 Inhibition Synergize to Reinvigorate Exhausted T Cells', *Front Immunol*, 13: 869768.

Voskoboinik, I., J. C. Whisstock, and J. A. Trapani. 2015. 'Perforin and granzymes: function, dysfunction and human pathology', *Nat Rev Immunol*, 15: 388-400.

Wang, X., Q. He, H. Shen, A. Xia, W. Tian, W. Yu, and B. Sun. 2019. 'TOX promotes the exhaustion of antitumor CD8(+) T cells by preventing PD1 degradation in hepatocellular carcinoma', *J Hepatol*, 71: 731-41.

Wang, X., J. Li, K. Dong, F. Lin, M. Long, Y. Ouyang, J. Wei, X. Chen, Y. Weng, T. He, and H. Zhang. 2015. 'Tumor suppressor miR-34a targets PD-L1 and functions as a potential immunotherapeutic target in acute myeloid leukemia', *Cell Signal*, 27: 443-52.

Wang, Y., J. Hu, Y. Li, M. Xiao, H. Wang, Q. Tian, Z. Li, J. Tang, L. Hu, Y. Tan, X. Zhou, R. He, Y. Wu, L. Ye, Z. Yin, Q. Huang, and L. Xu. 2019. 'The Transcription Factor TCF1 Preserves the Effector Function of Exhausted CD8 T Cells During Chronic Viral Infection', *Front Immunol*, 10: 169.

Wang, Y. J., R. Fletcher, J. Yu, and L. Zhang. 2018. 'Immunogenic effects of chemotherapy-induced tumor cell death', *Genes Dis*, 5: 194-203.

Weisshaar, N., J. Wu, Y. Ming, A. Madi, A. Hotz-Wagenblatt, S. Ma, A. Mieg, M. Hering, F. Zettl, K. Mohr, T. Schlimbach, N. Ten Bosch, F. Hertel, L. Muller, H. Byren, M. Wang, H. Borgers, M. Munz, L. Schmitt, F. van der Hoeven, U. Kloz, R. Carretero, N. Schleussner, R. F. Jackstadt, I. Hofmann, and G. Cui. 2022. 'Rgs16 promotes antitumor CD8(+) T cell exhaustion', *Sci Immunol*, 7: eabh1873.

Wienand, K., B. Chapuy, C. Stewart, A. J. Dunford, D. Wu, J. Kim, A. Kamburov, T. R. Wood, F. Z. Cader, M. D. Ducar, A. R. Thorner, A. Nag, A. T. Heubeck, M. J. Buonopane, R. A. Redd, K. Bojarczuk, L. N. Lawton, P. Armand, S. J. Rodig, J. R. Fromm, G. Getz, and M. A. Shipp. 2019. 'Genomic analyses of flow-sorted Hodgkin Reed-Sternberg cells reveal complementary mechanisms of immune evasion', *Blood Adv*, 3: 4065-80.

Wu, S., Q. Zhang, F. Zhang, F. Meng, S. Liu, R. Zhou, Q. Wu, X. Li, L. Shen, J. Huang, J. Qin, S. Ouyang, Z. Xia, H. Song, X. H. Feng, J. Zou, and P. Xu. 2019. 'HER2 recruits AKT1 to disrupt STING signalling and suppress antiviral defence and antitumour immunity', *Nat Cell Biol*, 21: 1027-40.

Wuensch, S. A., R. H. Pierce, and I. N. Crispe. 2006. 'Local intrahepatic CD8+ T cell activation by a non-self-antigen results in full functional differentiation', *J Immunol*, 177: 1689-97.

Xing, Y., and K. A. Hogquist. 2012. 'T-cell tolerance: central and peripheral', *Cold Spring Harb Perspect Biol*, 4.

Young, L. S., L. F. Yap, and P. G. Murray. 2016. 'Epstein-Barr virus: more than 50 years old and still providing surprises', *Nat Rev Cancer*, 16: 789-802.

Zhou, X., S. Yu, D. M. Zhao, J. T. Harty, V. P. Badovinac, and H. H. Xue. 2010. 'Differentiation and persistence of memory CD8(+) T cells depend on T cell factor 1', *Immunity*, 33: 229-40.

Zimber-Strobl, U., L. Strobl, H. Hofelmayr, B. Kempkes, M. S. Staege, G. Laux, B. Christoph, A. Polack, and G. W. Bornkamm. 1999. 'EBNA2 and c-myc in B cell immortalization by Epstein-Barr virus and in the pathogenesis of Burkitt's lymphoma', *Curr Top Microbiol Immunol*, 246: 315-20; discussion 21.

Zuo, J., A. Currin, B. D. Griffin, C. Shannon-Lowe, W. A. Thomas, M. E. Ressing, E. J. Wiertz, and M. Rowe. 2009. 'The Epstein-Barr virus G-protein-coupled receptor contributes to immune evasion by targeting MHC class I molecules for degradation', *PLoS Pathog*, 5: e1000255.

Zuo, J., L. L. Quinn, J. Tamblyn, W. A. Thomas, R. Feederle, H. J. Delecluse, A. D. Hislop, and M. Rowe. 2011. 'The Epstein-Barr virus-encoded BILF1 protein modulates immune recognition of endogenously processed antigen by targeting major histocompatibility complex class I molecules trafficking on both the exocytic and endocytic pathways', *J Virol*, 85: 1604-14.